

IBO 2022 ARMENIA

FINAL REPORT



IBO
33rd 2022
ARMENIA

2023

**We would like to express our deep gratitude to the
Ministry of Education, Science, Culture and Sports of the Republic of Armenia,
International Biology Olympiad e.V.,
Team Telecom Armenia,
and Armenpress
for support.**



IBO 2022 Office

Yerevan State University

1 Alex Manoogian, Yerevan, 0025

ibo2022armenia@ysu.am

Published

January 2023

It was an honor for us to host the 33rd IBO in Yerevan, one of the oldest cities in the world.

The 21st century apparently is the century of Biology.

The development of technologies nowadays induces rapid development of Biology.

Fantastic efforts of the IBO community promote the career development of IBO participants who are future scientists in the area of life science.

We were extremely happy to be part of these efforts of introducing young students to the contemporary challenges of Biology.

Dr. Gayane Ghukasyan

CONTENTS

1. PREFACE	6
1.1 Facts and Figures	6
1.2 The History of NBO and IBO 2022	7
1.3 IBO 2022 Logo	7
2. IBO 2022 ORGANIZATION	8
2.1 The Organizing Committee	8
2.2 Funding and Budget	9
IBO 2022 PREPARATIONS	10
3. PARTICIPATION IN THE IBO 2022	16
3.1 Invitations and Participation Intents	16
3.2 The procedure of expressing the participation intent	17
3.3 Pre-registration	18
3.4 Payment	19
3.5 Team Data	19
3.6 Visa	20
4. IBO 2022 EXAMS	20
4.1 Practical Exams	22
4.2 The Assessment Program for Practical Exams	27
4.3 Theoretical Exams	27
4.4 Quality Assurance of Exams	28
5. IBO 2022 EVENTS AND VENUES	29
5.1 Program	29
5.2 Ceremonies	30
5.3 Excursions	39
6. INTERNATIONAL GROUP PROJECT 2022	62

6.1 IGP 2022 Organization	63
6.2 International Group Project Posters	74
7. CALCULATION OF EXAM RESULTS	91
7.1 NORMALISING RAW STUDENT EXAM SCORES AND CALCULATION OF FINAL STUDENT SCORE	91
7.2 SUMMARY STATISTICS OF STUDENT SCORES AT THE EXAMS	93
7.3 RELATIONSHIPS BETWEEN STUDENT PERFORMANCE IN THE DIFFERENT EXAMS	95
7.4 FINAL SCORES AND MEDAL DECISION	97
8. LOGISTICS AND INFRASTRUCTURE	104
8.1 Accommodation	104
8.2 Transport	105
9. VOLUNTEERS	107
10. MEDIA AND PR	110
11. RISK MANAGEMENT	120

1. PREFACE

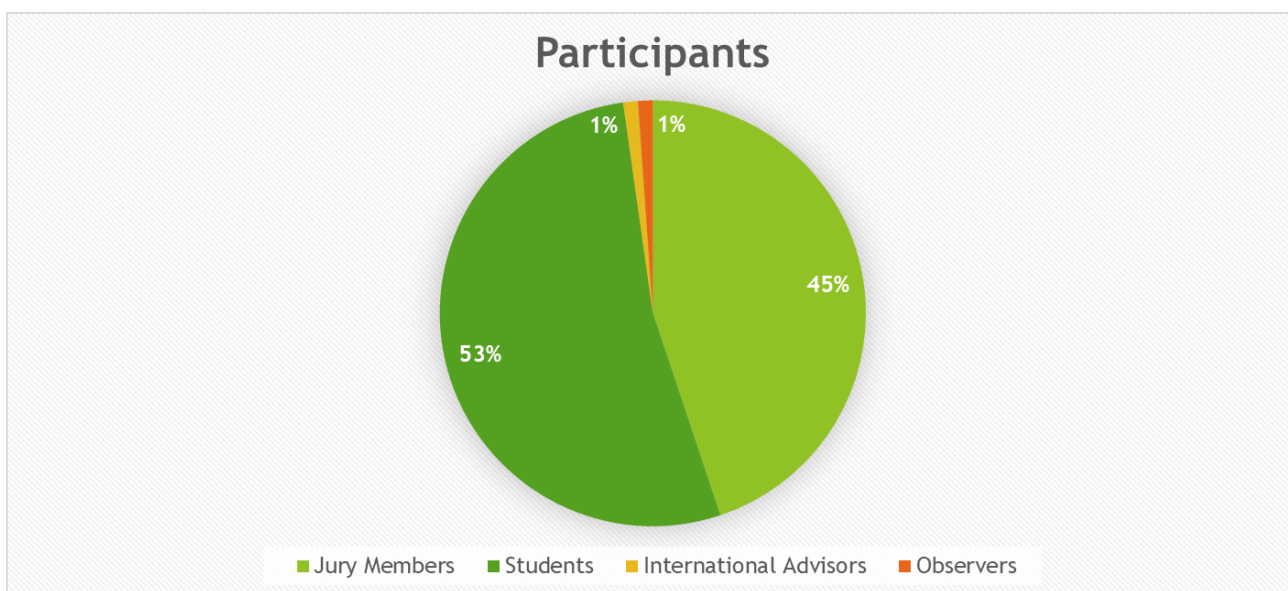
1.1 Facts and Figures

The 33rd International Biology Olympiad (IBO 2022) was held on July 10-18, 2022 in the capital of Armenia, Yerevan. The Olympiad was organized by **Yerevan State University**. The official authority of the IBO 2022 was the **Ministry of Education, Science, Culture and Sport of the Republic of Armenia**.

Participants from **62 member countries** and **3 observer countries** took part in the Olympiad. In total, **201** jury members, 5 observers, **237** students and **5** international advisors participated in the event.

This final report demonstrates the organization and implementation of the 33rd International Biology Olympiad held in Armenia.

The report includes “**IBO 2022 EXAMS**” zip folder as an appendix.



1.2 The History of NBO and IBO 2022

The National Biology Olympiad of Armenia was established in 1991. In 2008 Dr. Gayane Ghukasyan participated in the IBO in India as an observer. In 2009 Armenia became a member of the IBO. Since 2009, 38 Armenian students have participated in the IBO. During the IBO 2018 Tehran Olympiad, the IBO Association made the decision confirming that the Republic of Armenia would officially host the 33rd International Biology Olympiad on July 10-18, 2022.

1.3 IBO 2022 Logo

The IBO 2022 logo was created by Taron Simonyan in 2020.

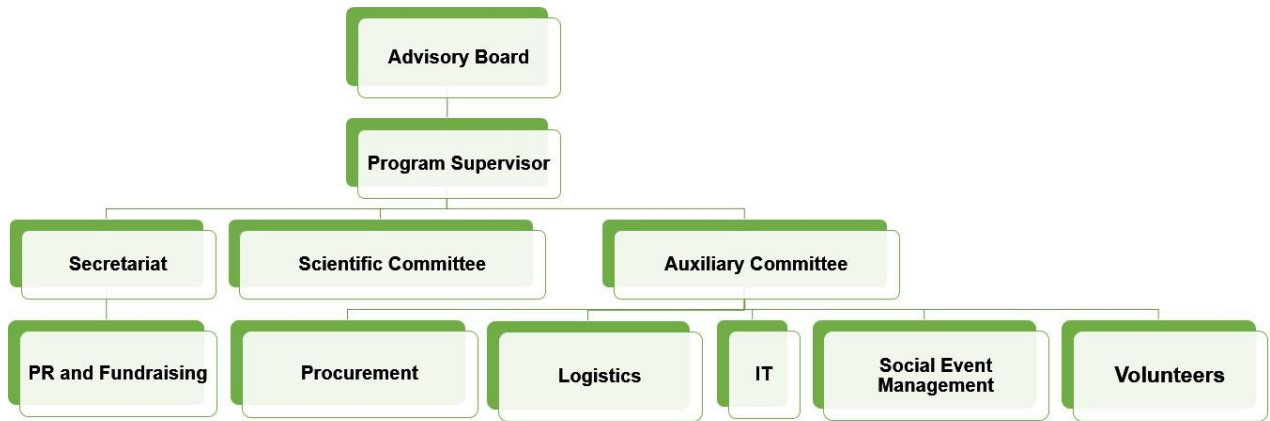
The stork is considered as the symbol of respect for parents. According to an old legend, the stork delivers food to its parents when they are no longer able to take care of themselves. Just like the storks, it is the responsibility of each generation to continue on the valuable scientific heritage of the ancestors. The color green symbolizes the eternity of life on Mother Earth.



IBO
33rd 2022
ARMENIA

2. IBO 2022 ORGANIZATION

2.1 The Organizing Committee



The IBO 2022 Organizing Committee was formed in 2020.

The IBO 2022 Office was founded in Yerevan State University.

The head of the organizing committee was the program supervisor Dr. Gayane Ghukasyan.

The Advisory Board of the IBO 2022 consisted of the representatives of the Ministry of Education, Science, Culture and Sport of the Republic of Armenia and Yerevan State University, 9 people in total. The head of the advisory board was RA Deputy Minister of Education, Science, Culture and Sports, Dr. Zhanna Andreasyan.

The organizing committee consisted of the scientific committee, the auxiliary committee and the secretariat.

The Scientific committee consisted of 14 people. The Scientific Committee developed 120 theoretical questions and 4 practical exams in total. 102 theoretical questions were presented to the subgroup for the discussion.

The Auxiliary committee consisted of 15 people. Some auxiliary committee staff was provided by Yerevan State University.

The Secretariat consisted of 6 people.

The Secretariat was formally established in 2020 in the IBO 2022 Office.

2.2 Funding and Budget

In total 1,200,000 USD was spent on the IBO 2022.

The amount includes:

- 333,000 USD - participation fee.
- 6736 USD (6217.35 CHF) - Oly-exams software
- 860,264 USD - donated by the Armenian Government



The IBO 2022 participation fee for each team (4 students + 2 jury members) was 2500 USD. The participation fee for each additional jury member and each observer was 2000 USD.

The technological partner of the Olympiad was the "Team Telecom Armenia" company, which provided the necessary technical solutions to ensure the running of the exams.

The information supporter of the Olympiad was "Armenpress" news agency.

The IBO Office bought the Oly-exams software (ExamTools and Google Translate & DeepL usage) for jury sessions of the IBO 2022. The total cost of the software was 6217.35 CHF (approx. 6736 USD).

IBO 2022 PREPARATIONS

To host the IBO 2022, Participants' bags and the following items were prepared by the auxiliary committee and given to the participants during the Olympiad.









White t-shirts were prepared for the participants.

Yellow t-shirts were prepared for the volunteers to be easily noted by the participants.



Lab coats with 4 different colors were prepared for the students of the 4 groups of the practicals.



3. PARTICIPATION IN THE IBO 2022

3.1 Invitations and Participation Intents

Firstly, the invitation letter was prepared by the IBO 2022 organizing committee and sent to the IBO Office to upload on the newly created registration portal. Although the IBO 2022 organizing committee had a user profile of the portal and a permission to use a variety of tools on the portal, the option to upload the invitation letter from our side was unavailable. The invitation letter was sent to the IBO Office and after being uploaded it was sent out on the 8th February, 2022.

On February 8, the IBO 2022 organizing committee sent the invitation to 76 countries and regions out of 78 IBO member countries and regions based on the data pool created on the portal. 2 members (Kazakhstan and Liechtenstein) were left because of incomplete data. The IBO 2022 organizing committee informed the IBO office about it and based on the available information provided by the IBO Office, the IBO 2022 organizing committee sent the invitation letter to Liechtenstein on February 11 and Kazakhstan on February 16.

The deadlines of all the stages were mentioned in the invitation letter.

The deadline to express the participation intent (informal information by all members whether their team will likely participate) was **1 March, 2022**.

On February 23 the IBO 2022 organizing committee used a portal tool to send reminders to those coordinators who have not responded yet.

63 members expressed their participation intent through the portal by March 1 and the IBO 2022 organizing committee decided to extend the deadline to March 10. In the meantime, the IBO 2022 organizing committee sent reminders through email as well. As a result, 6 more members expressed their intention to participate by the extended deadline. In total, 69 IBO members expressed their participation intent in the first stage.

Since only 1 invitation letter could be uploaded at the portal, the IBO 2022 organizing committee asked the IBO Office to upload the invitation letter prepared for the observers, and on March 10 the IBO 2022 organizing committee sent it to 11 countries that were interested to become observers according to the list formerly provided by the IBO Office. The following countries were interested to become observers: Afghanistan, Austria, Bosnia & Herzegovina, Botswana, Cambodia, El Salvador, France, Ghana, Kosovo, Kuwait, Macao.

The deadline for the observers to express their participation intent was **31 March 2022**.

4 countries (Afghanistan, Botswana, El Salvador and France) expressed their intention to participate as observers by March 31. In order for the observer countries to be able to submit their intent, it was necessary to set the global deadline for participation intent for March 31. This meant that members could also then submit participation intent until March 31 if they tried. This was a single setting in the system.

Later 10 members (Australia, Belarus, Canada, China, Colombia, Egypt, Hong Kong, Mexico, Turkmenistan, United States) and 2 observer countries (Botswana and El Salvador) withdrew to participate.

The Macedonian team completed all the stages but could not arrive in Armenia because of no convenient flights.

Between April-June, the IBO members Cyprus, Kyrgyzstan, Nigeria, Slovenia and Nepal and the observer country Bolivia expressed their will by email to participate in the IBO 2022. Later Nepal withdrew from participating. The IBO 2022 Organizing Committee set accelerated deadlines for these teams to complete all the steps as soon as possible.

3.2 The procedure of expressing the participation intent

After sending the invitation letter, the coordinators received an automatically generated email from the email address of the IBO registration portal (not from the email address of the IBO 2022 Armenia). The coordinators received an email which invited them to express the participation intent through the provided link of the IBO registration portal and presented the invitation letter attached. The coordinators had to follow the link to express their participation intent.

After expressing their participation intent the coordinators received an Invitation to the IBO Registration Portal. This was when they received their password for the newly created registration portal. The first problems the coordinators faced at this stage was that some coordinators had not noticed the password in this email and tried to log into the portal with their Member login credentials for the *ibo-info.org* website.

In addition, several coordinators contacted the IBO Office to replace their names because they were no longer in charge to express the team's participation intent. As everything was done by the portal and the invitations had been sent based on the data pool, this kind of requests usually took some time to figure out with the help of the IBO Office.

3.3 Pre-registration

After receiving their credentials to log into the portal, the coordinators had to complete the pre-registration by **March 31**. Pre-registration is the step when the coordinators definitely tell whether their teams will attend. The coordinators also indicate the number of participants (jury / students) and single rooms requested. At this stage coordinators confirm that they know that pre-registration constitutes a binding agreement with the host. Regardless of whether their team attends the IBO or not, any fees incurred or set by the host must be paid.

After indicating the number of participants and single rooms (there was no single room fee, the rooms were provided upon availability) an invoice with the all banking details was generated on the coordinator's portal account which they had to download.

At this stage the IBO 2022 organizing committee received lots of requests regarding the invoices, such as to change the addressee of the invoice (the invoices were automatically generated based on the coordinators' information in the data pool), to send 2 or more separate invoices to each funding organization of a team, etc. The IBO 2022 organizing committee tried to fulfill these requests through the portal whereas some of them had to be done manually.

The IBO 2022 organizing committee also received several requests to extend the deadline for pre-registration and therefore the deadline for the payment as well because of the uncertain situation of the pandemic and financial support in some countries and regions.

46 countries and regions, including the observers, completed the pre-registration before March 31, the initially set deadline.

The IBO 2022 organizing committee extended the deadline for pre-registration to April 7. Only 1 more team completed the pre-registration by then and the IBO 2022 organizing committee was asked by some teams to extend the deadline for some reasons, such as the uncertainty of their financial support, the stabilization of the pandemic situation etc.

Then the IBO 2022 organizing committee extended the pre-registration deadline to April 22 sending a series of reminders. 13 more teams completed the pre-registration this time. After April 22 the IBO 2022 organizing committee did not officially extend the pre-registration deadline but continued to receive requests from some teams that were already ready to complete the pre-registration.

2 more teams asked to open the pre-registration page by the end of April, 7 more teams in May and 1 team in June and the IBO 2022 organizing committee fulfilled their request.

2 new coordinators contacted the IBO 2022 organizing committee and informed that the old coordinators expressed the participation intent and received the credentials to log into the portal but were replaced later, that's why their team had not met up with the deadlines.

5 countries (4 regular and 1 observer) withdrew from participating although they had completed the pre-registration.

3.4 Payment

The deadline for the payment was initially set as **April 30**.

The IBO 2022 organizing committee sent reminders to the coordinators but only 22 teams paid the participation fee by this deadline. The IBO 2022 organizing committee extended the deadline to May 7. 18 more teams transferred the participation fee by this extended deadline. The IBO 2022 organizing committee was requested by some teams to extend the payment deadline for them for a number of reasons, such as until they would get financial support, until they would select their competitors to be approved for the finances, until they receive their visas etc. The IBO 2022 organizing committee agreed to extend the deadline for all the teams that had requested. As a result 18 countries transferred the fee by the end of May, 5 countries in June and 3 countries in July.

3.5 Team Data

The deadline for team data was initially set as **June 1**.

This is the stage when the coordinators fill in the personal details of each participant, such as the personal data, contact data, address data, consent and declaration forms, passport data, photo and details regarding educational, medical and dietary needs.

The IBO 2022 organizing committee constantly sent reminders about the team data to the coordinators however this deadline was missed as well mainly because of late national selection.

At this stage the IBO 2022 organizing committee faced a few trouble-causing situations such as the distribution of hotel rooms (because the IBO 2022 organizing committee didn't have the full list of the participants), the visa issuance of those countries that can receive visa only upon the formal invitation (but the IBO 2022 organizing committee did not have the names of

participants and their passport details for the invitation) and the preparations of printing the yearbooks (because of the incomplete list of participants and photos).

Since most participating teams had transferred the participation fee as of June, thus confirming their participation in the IBO 2022, the IBO 2022 organizing committee decided to wait for all those teams to submit the participants list and photos to include their names and photos in yearbooks. As a result, the IBO 2022 organizing committee received all this information in the beginning of July which caused the late printing of the yearbooks.

3.6 Visa

Among 65 participating countries and regions only 19 needed visas to enter Armenia.

11 countries were eligible to apply for E-VISA which is processed in 3 days.

8 countries could obtain the visa at the Embassies (Consulates) of the Republic of Armenia BY INVITATION ONLY. The individual invitation letters were to be submitted by the IBO 2022 organizing committee to the Ministry of Foreign Affairs of the Republic of Armenia and when approved the participants should visit the nearest Armenian Embassy/Consulate or send their passports there to get the visa. We informed those countries that for this procedure 1 month was required from our side after receiving the passport scans of the participants: up to 1 week to prepare all the documents within the university and up to 3 weeks to be approved by the Ministry. Unfortunately, some participants sent the required documents to the IBO 2022 organizing committee late, however, in the end, all the participants who applied for a visa, received the visa to come to Armenia.

4. IBO 2022 EXAMS

The IBO 2022 exams were conducted at The Sports and Concert Complex named after Karen Demirtchian.



320 special tables were purchased so that the theoretical and practical stages could be held as comfortably as possible for the participants.

320 brand new laptops were bought for the IBO 2022 exams.

4.1 Practical Exams

The topics of the Practical Exam of the IBO 2022 were:

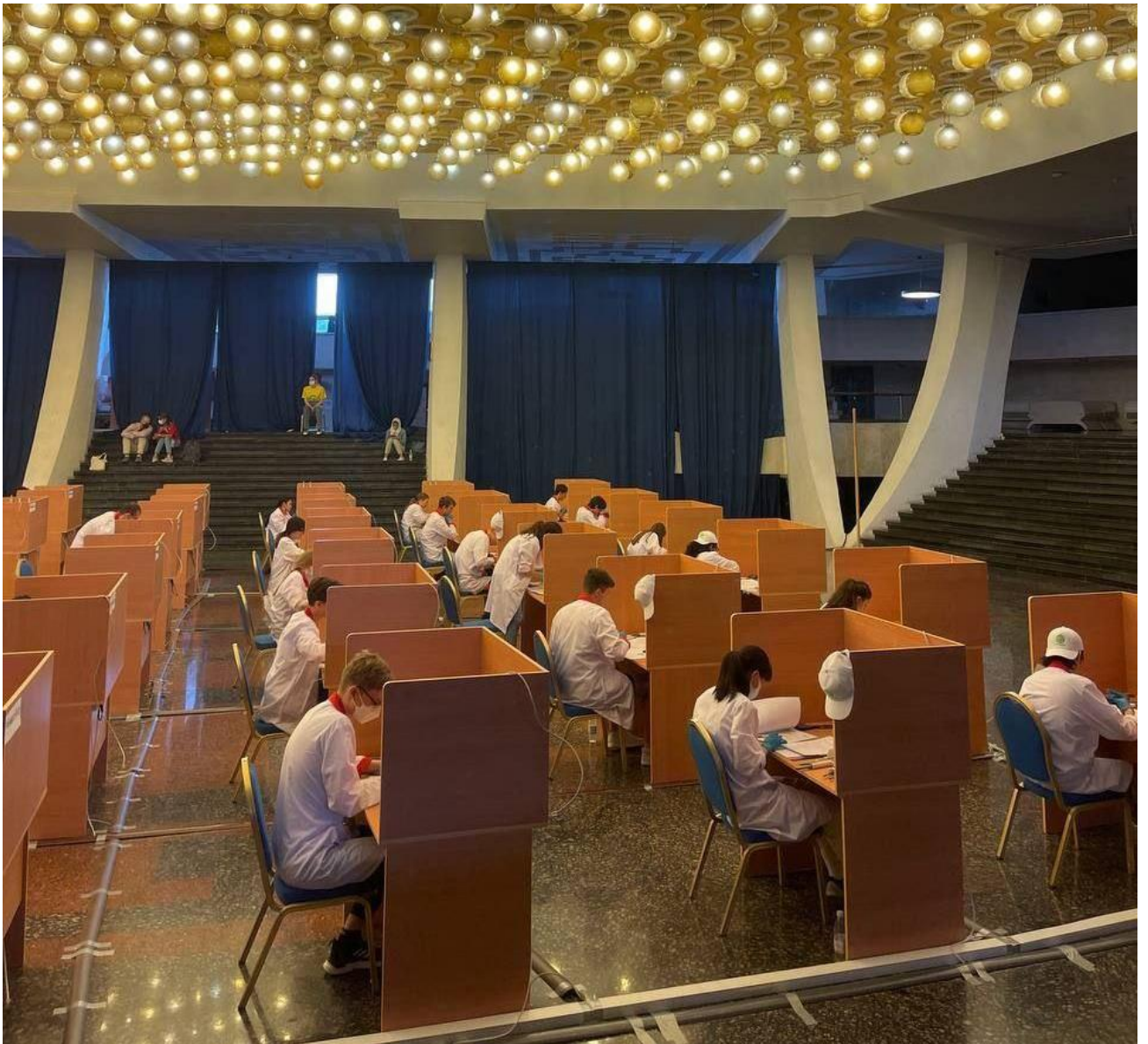
- **Animal Systematics and Anatomy**
- **Biochemistry**
- **Bioinformatics**
- **Plant Anatomy and Physiology**

During the practical exam, participants were given four experimental problems. Each practical task lasted 1.5 hours. The participants were divided into four groups, and each group performed the assigned tasks in order. There were 3 breaks. 2 of them lasted 20 minutes and 1 break lasted 1 hour.

The practical task of Bioinformatics was organized in a web application installed in laptops bought for the IBO 2022 exams.

The demo application of Bioinformatics was published on ibo2022.org official website beforehand.







Purchased items for Biochemistry

Name	Quantity
Spectrophotometer with opaque cuvette	81
Cuvettes	600
Pipette 5-50 μL	80
Pipette 20-200 μL	80
Pipette 100-1000 μL	80
Pipette tips – 100-1000 μl	200
Pipette tips – 5-200 μl	5000
Eppendorf tube holder	80
Empty Eppendorf tubes	700
Filter paper	1000
Gloves	320 pairs
Pen	80
Pencil	80
Eraser	80

Ruler	80
Marker pen	80
Clock (stopwatch)	80
Trash can	320
Calculator	80

Purchased items for Bioinformatics

Name	Quantity
Computer with Application running	80
Envelope with materials	320
Calculator	80
Pen	180

Purchased items for Plant Anatomy and Physiology

Name	Quantity
Bench lamp	80
Monocular microscope	80
Fresh spinach leaf (Spinacia)	320
Chilled solution labelled 1: "Isolation medium"	320
Solution labelled 2: "Reaction medium"	320
Glass beaker wrapped in foil (50 ml)	320
Mortar and pestle	320
Stopwatch	80
Sieve with cheesecloth	320
Fine glass capillary tubes	1600
Aluminum foil	320
Red filter	320
Green filter	320
Pasteur pipettes	640
Ice bath	80
Table for capillary tubes	80
Color scale	80
Glass rod	320
Scissors	320
Marker	80
Microscope slide	1300
Cover glass	1300

Tweezers	320
Scalpel	320
Razor blade	320
Inoculation loop to use as dissecting needle	320
Small dropper bottle of distilled water (labelled H ₂ O)	320
Small dropper bottle of HCl 25% solution (labelled HCl)	320
Small dropper bottle of phloroglucinol solution (labelled 3)	320
Small dropper bottle of glycerol (labelled 4)	320
Styrofoam rack with 4 pcs of Eppendorf tubes with plant stem samples labelled II to V	320
3 plants samples labelled B, C, and D in zip-lock bags	80
Microscope slide of an unknown plant labelled "I"	80
7 photos labelled A, E, F, G, H, I and J	80
Photo: Fig. 1 Types of stele in vascular plants	320

Purchased items for Zoology

Name	Quantity
Fish specimens for Part 1 only	240
Fish specimen of a supposed "new" species for Part 2 only	80
Photographs of fish for Part 2 only	240
Mask	320
Dissection tray	320
Magnifier with a double 3x and 10x lens	80
Tweezers	320
Scissors	320
Scalpel	320
Plastic gloves	320
A water bottle to keep fish moist	80
Paper tissue	320
Plastic bag for biological waste	320
Stationery (pen, pencil, pencil sharpener)	80
Red card	80

4.2 The Assessment Program for Practical Exams

A program was developed to check and assess the practical exams of Animal Systematics & Anatomy, Biochemistry and Plant Anatomy & Physiology.

The program worked on the basis of the FlexiCapture licensed software package of the ABBYY company.

The calculation part was done with Microsoft Excel.

FlexiCapture software enables recognition and conversion of handwritten and typed texts from pictures for further processing. In the IBO 2022 it was used to measure the results of practical work transferring the texts (mainly numbers) and X marks in the forms filled in by students into the Excel electronic editor, to perform calculations and evaluate the works.

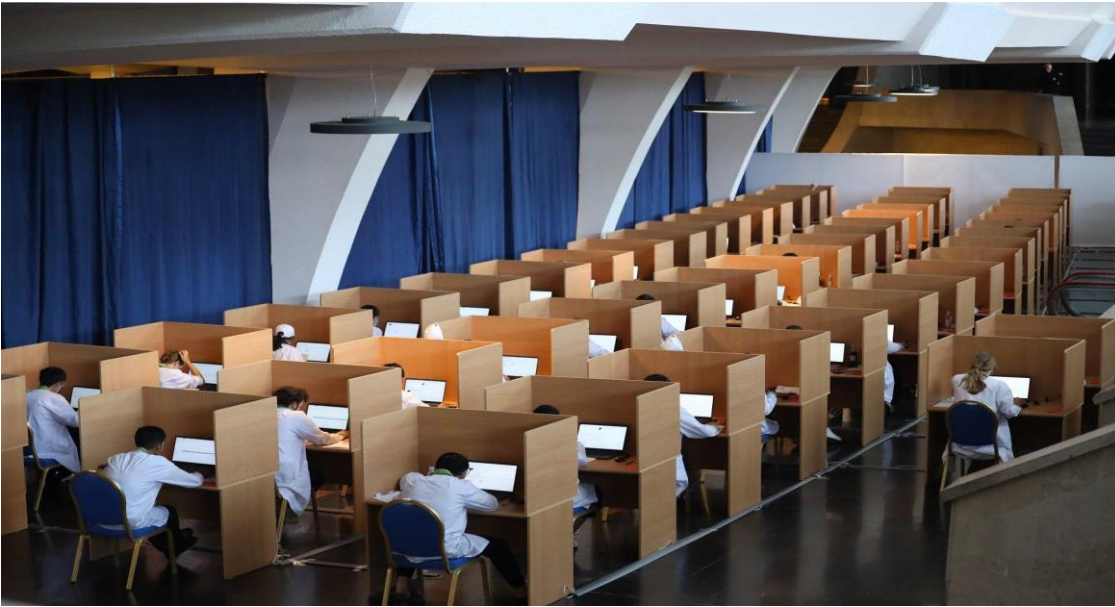
The completed ANSWER SHEETS were scanned, turned into pictures, which were processed with the program, receiving numerical values and marks. The latter were also transferred to the Excel spreadsheet to perform the necessary calculations.

4.3 Theoretical Exams

The theoretical exam contained **100 questions**.

The theoretical exam consisted of two parts: **part A** and **part B**, each lasting three hours.

The Classmarker web-based quiz maker was purchased for conducting the theoretical exam. The results were automatically generated after finishing the exam.



4.4 Quality Assurance of Exams

The quality of the IBO exams was discussed with the international advisors and sub-jury.

The subgroup consisted of 10 members: 5 international advisors and 5 sub-jury members.

The international advisors were Margaret Linford, Mary Oliver, Anindya Sinha and Poonpipope Kasemsap.

The sub-jury members were Jan Černý, José Matos, Saman Hosseinkhani, Takao Ishikawa, Tatsuhiko Noguchi (joined online), Katarina Jurikova (joined online).

The subgroup conducted its sessions at Ani Plaza Hotel on July 5-10, 2022.

The group of inspectors followed the implementation of the exams.

The head of the inspectors was Birthe Zimmermann.

5. IBO 2022 EVENTS AND VENUES

5.1 Program

JURY SCHEDULE

Day	Hour	Jury
10.07.22		Arrival of Participants Registration
	17:30-20:30	Opening Ceremony Welcome Dinner Venue: <i>Armenian Opera Theatre</i> Return to the Hotel
11.07.22	08:00-08:30	Breakfast
	09:00-11:00	Discussion of Practical Tasks Venue: <i>Ani Plaza Hotel</i>
	11:00-11:30	Coffee Break
	11:30-13:30	Translation of Practical Tasks
	13:30-14:30	Lunch
	14:30-16:30	Translation of Practical Tasks
	16:30-17:00	Coffee Break
	17:00-19:00	Translation of Practical Tasks
	19:00-20:00	Dinner
	20:00-22:00	Translation of Practical Tasks
12.07.22	08:00-08:30	Breakfast
	09:00-11:00	Discussion of Theoretical Questions 1
	11:00-11:30	Coffee Break
	11:30-13:30	Translation of Theoretical Questions 1
	13:30-14:30	Lunch
	14:30-16:30	Translation of Theoretical Questions 1
	16:30-17:00	Coffee Break
	17:00-19:00	Translation of Theoretical Questions 1
	19:00-20:00	Dinner
	20:00-22:00	Translation of Theoretical Questions 1
13.07.22	08:00-08:30	Breakfast
	09:00-11:00	Discussion of Theoretical Questions 2
	11:00-11:30	Coffee Break
	11:30-13:30	Translation of Theoretical Questions 2
	13:30-14:30	Lunch
	14:30-16:30	Translation of Theoretical Questions 2
	16:30-17:00	Coffee Break
	17:00-19:00	Translation of Theoretical Questions 2
	19:00-20:00	Dinner
	20:00-22:00	Translation of Theoretical Questions 2
	22:00-22:30	Coffee Break
	22:30-24:00	Downloading Translated Theoretical Tasks and Printing

Day	Hour	Jury
14.07.22	08:00-08:30	Breakfast
	09:00-09:15	Bus Transfer to Garni
	09:55-11:00	Excursion in Garni
	11:15-12:30	Excursion in Geghard
	12:30-13:30	Return to the Hotel
	13:30-14:30	Lunch
	14:30-15:00	Walk to Matenadaran (Institute of Ancient Manuscripts)
	15:00-17:00	Excursion in Matenadaran
	17:00-17:30	Return to the Hotel
	18:00-18:30	Dinner
15.07.22	19:30-20:00	Bus Transfer to Sport and Concert Complex
	20:00-23:00	After Party (Venue: <i>Sport and Concert Complex</i>)
	23:00-23:30	Return to the Hotel
	08:00-08:30	Breakfast
	09:00-14:30	General Assembly Meeting Venue: <i>Ani Plaza Hotel</i>
	11:00-11:30	Coffee Break
16.07.22	13:30-14:30	Lunch
	15:00-22:00	Results Review Venue: <i>Ani Plaza Hotel</i>
	16:30-17:00	Coffee Break
	19:00-20:00	Dinner
17.07.22	08:00-08:30	Breakfast
	09:00-18:00	IBO Educational Conference "The IBO Way to Excellence"
	11:00-11:30	Coffee Break
	13:30-14:30	Lunch
	16:30-17:00	Coffee Break
	18:30-19:00	Bus Transfer to the Restaurant
	19:00-23:00	Dinner out
	23:00-23:30	Return to the Hotel

Notes _____

Day	Hour	Jury
17.07.22	08:00-08:30	Breakfast
	08:30-09:00	Bus Transfer to Erebuni Historical & Archaeological Museum-Reserve
	09:00-11:30	Excursion in Erebuni
	11:30-12:00	Return to the Hotel
	12:00-13:30	Free Time
	13:30-14:30	Lunch
	14:30-15:00	Walk to Cafesjian Center for the Arts
	15:00-16:00	Excursion in Cafesjian Center for the Arts
	16:00-16:30	Return to the Hotel
	16:30-17:00	Coffee Break
18.07.22	17:00-17:30	Walk to Armenian Opera Theatre
	18:00-21:00	Closing / Award Ceremony Farewell Dinner Venue: <i>Armenian Opera Theatre</i> Return to the Hotel
		Breakfast
		Departure



COMPETITORS & JURY SCHEDULE

THE 33rd INTERNATIONAL BIOLOGY OLYMPIAD
 10-18 JULY 2022

Day	Hour	Competitors
10.07.22		Arrival of Participants Registration
	17:30-20:30	Opening Ceremony Welcome Dinner <i>Venue: Armenian Opera Theatre</i>
		Return to the Hotel
	22:00-06:00	Sleeping
11.07.22	08:00-08:30	Breakfast
	09:00-09:15	Bus Transfer to the Exam Venue
	09:45-11:00	Safety and Laboratory Instructions <i>Venue: Sport and Concert Complex</i>
		Return to the Hotel
	11:30-13:30	Free Time
	13:30-14:30	Lunch
	15:00-17:00	Excursion in Yerevan
	17:30-18:30	Dinner
	18:30-21:30	Free time
	21:30-22:00	Light Dinner
22:00-06:00	Sleeping	
12.07.22	06:30-07:00	Breakfast
	07:30-08:00	Bus Transfer to the Exam Venue
	09:00-17:00	Practical Exam <i>Venue: Sport and Concert Complex</i>
	12:30-13:30	Lunch
	17:00-17:30	The End of the Exam and Bus Transfer to the Hotel
	18:00-19:00	Dinner
	19:00-21:30	Free Time
	21:30-22:00	Light Dinner
	22:00-06:00	Sleeping
	13.07.22	08:00-08:30
08:45-09:00	Bus Transfer to Garni	
09:40-11:00	Excursion in Garni	
11:15-12:30	Excursion in Geghard	
12:30-13:30	Return to the Hotel	
13:30-14:30	Lunch	
14:30-15:00	Walk to Matenadaran (Institute of Ancient Manuscripts)	
15:00-17:00	Excursion in Matenadaran	
17:00-17:30	Return to the Hotel	
17:30-18:30	Dinner	
18:30-21:30	Free Time	
21:30-22:00	Light Dinner	
22:00-06:00	Sleeping	

Day	Hour	Competitors	
14.07.22	06:30-07:00	Breakfast	
	07:30-08:00	Bus Transfer to the Exam Venue	
	09:00-12:00	Theoretical Exam 1 <i>Venue: Sport and Concert Complex</i>	
	12:00-13:00	Lunch	
	13:00-16:00	Theoretical Exam 2	
	16:00-16:30	The End of the Exam and Bus Transfer to the Hotel	
	18:00-18:30	Dinner	
	19:30-20:00	Bus Transfer to Sport and Concert Complex	
		After Party <i>(Venue: Sport and Concert Complex)</i>	
	23:00-23:30	Return to the Hotel	
	23:30-07:30	Sleeping	
	15.07.22	08:00-08:30	Breakfast
		08:30-09:00	Bust Transfer to Erebuni Historical & Archaeological Museum-Reserve
09:00-11:30		Excursion in Erebuni	
12:00-13:30		Return to the Hotel Free Time	
13:30-14:30		Lunch	
14:45-15:00		Bus Transfer to Yerevan State University	
15:00-19:00		International Group Project Poster Session <i>(Venue: Yerevan State University)</i>	
19:00-19:15		Return to the Hotel	
19:30-20:30		Dinner	
20:30-22:00		Free Time	
22:00-06:00	Sleeping		
16.07.22	08:00-08:30	Breakfast	
	09:30-13:00	Walk to Cafesjian Center for the Arts Excursion in Cafesjian Center for the Arts	
	13:30-14:30	Lunch	
	15:00-15:30	Bus Transfer to Yerevan Park (Amusement & Theme Park)	
	15:30-21:30	Excursion in Yerevan Park	
	19:30-20:30	Dinner in Yerevan Park	
	21:30-22:00	Return to the Hotel	
	22:00-06:00	Sleeping	

Day	Hour	Competitors
17.07.22	08:00-08:30	Breakfast
	09:00-09:30	Walk to Vernissage Market
	09:30-11:30	Excursion in Vernissage
	11:30-12:00	Return to the Hotel
	12:00-13:30	Free Time
	13:30-14:30	Lunch
	14:30-17:00	Free Time
	17:00-17:30	Walk to Armenian Opera Theatre
	18:00-21:00	Closing / Award Ceremony Farewell Dinner <i>Venue: Armenian Opera Theatre</i>
	21:00	Return to the Hotel
	Sleeping	
18.07.22	09:00-11:30	Breakfast
	12:00-13:30	Departure

Notes _____

5.2 Ceremonies

The opening ceremony was held at Armenian National Academic Theatre of Opera and Ballet named after Alexander Spendiaryan with the participation of the Chief of Staff of the RA Prime Minister Dr. Arayik Harutyunyan, RA Minister of Education, Science, Culture and Sports Dr. Vahram Dumanyan, Rector of Yerevan State University Dr. Hovhannes Hovhannisyian. The IBO chairperson Dr. Ryoichi Matsuda made opening remarks.

During the opening ceremony, Mkhitar Heratsi, the 12th century Armenian physician and philosopher, via modern technologies greeted the young biologists of the 21st century and wished them success.

The speeches of the speakers were followed by a concert program organized by YSU Charles Aznavour Culture Center. The pop-symphonic orchestra of the Public Radio and Television of Armenia (artistic director: People's Artist of the Republic of Armenia Yervand Yerznkyan) and Sargis Bazhbeuk-Melikyan performed cultural performances.

Musical performances were followed by dance performances. "Mer Dar" dance was performed by the "Barekamutyun" dance ensemble (artistic director: RA People's Artist Norayr Mehrabyan), and the solo dance "Komitas" by Ani Haroyan.









The closing and award ceremony was held at Armenian National Academic Theatre of Opera and Ballet with the participation of Chief of Staff of the RA Prime Minister Dr. Arayik Harutyunyan, RA Deputy Minister of Education, Science, Culture and Sports Dr. Zhanna Andreasyan, Rector of Yerevan State University Dr. Hovhannes Hovhannisyan.

The event concluded with cultural performances. Musical performances were performed by the "YSU band" and "Little singers" choir (artistic director: RA honored educator Tigran Hekekyan).

The medals and group project awards were given to the participants. The trophy was officially transferred to the next host country UAE.











5.3 Excursions

During the pre-examination day, the students got acquainted with Yerevan, visited the **Victory Park** where the monumental statue of Mother Armenia (a female personification of Armenia) is located overlooking the capital city of Yerevan.





The participants went to UNESCO protected Garni Temple and Geghard Monastery.

Garni is known for the nearby classical temple. The Temple of Garni is a hellenistic period building in Armenia.



A souvenir (presented below) was distributed to the participants as a memento after the visit to



Geghard is a medieval monastery being partially carved out of the adjacent mountain, surrounded by cliffs.



Museum “Erebuni” is a museum of the history of the founding of Yerevan.

In the Erebuni fortress there is a cuneiform record inscribed on the stone slab which says: *“In the greatness of God Khaldi, Argishti, the son of King Menua, has built this impregnable fortress and called it Erebuni...”*





Matenadaran is a Research Institute of Ancient Manuscripts that has a permanent exhibition. Visiting Matenadaran gives the opportunity to get acquainted with the richest manuscript heritage of the Armenian people.

In Matenadaran a master class was held for the participants under the title "Application of Biological Methods in the Preservation of Armenian Manuscripts".











Cafesjian Center for the Arts is an art museum in Yerevan, Armenia. It is around the Yerevan Cascade which is a complex of massive stairs with fountains. The museum is dedicated to bringing the best of contemporary art to Armenia and presenting the best of Armenian culture to the world.







"Vernisage" is an open-air fair, where the participants got acquainted with the fusion of Armenian national traditions and the dominant taste in the modern world.





"Yerevan park" is a theme park with two dozen high-quality attractions, live shows, restaurant, merchandise shop and lovely characters who add that finishing touch to the fairy tale. The students visited the park after the exams, while the jury dined out at "Arqayadzor" restaurant complex.







After the exams, an outdoor entertainment event was held at the courtyard of The Sports and Concert Complex (the exam venue) where the students and jury members were reunited. The participants were taught and enjoyed Armenian traditional dances.







A souvenir (presented below) was distributed to the participants as a memento of The Sports and Concert Complex.



6. INTERNATIONAL GROUP PROJECT 2022

62 students from 31 teams participated in the International Group Project 2022 (IGP 2022). They selected a topic out of 5 suggested fields, and submitted their work as 17 different posters. The work was facilitated through former IBO participants from different countries (international facilitators). 15 facilitators from 8 countries worked with the students from June 12, 2022 to July 1, 2022. The work was conducted online.

Students had only 18 days to work together. This time shortage was due to late selection from individual teams of IBO 2022 participants, and some time needed for IGP 2022 registration and team allocation.

6.1 IGP 2022 Organization

On June 11, the IBO 2022 organizing committee organized a Zoom meeting with the facilitators and shared with them the information on IGP, how they are supposed to work, what are Do's and Don'ts, and what are the expected results. On June 12, the IBO 2022 organizing committee organized a similar info-meeting with the registered participants and informed them about group allocation based on the selection. On the same day, they connected with their facilitator and started to work on the project online.

The following fields were suggested to students for selection: Biomedicine, Molecular and Cell Biology, Bioinformatics and Artificial Intelligence, Across Species, Bionics and Biomimicry. They could select more than one topic in order to facilitate the organizational work of team allocation.

Molecular Cell Biology is the most selected topic (7 teams), along with Biomedicine (6 teams).

Topic	How many teams?
Biomedicine:	6
Molecular Cell Biology	7
Bioinformatics and AI	3
Bionics and Biomimicry	1
Across species	1

The jury members who evaluated the work were: Mary Oliver (UK), Maggy Linford (UK), Anindya (Rana) Sinha (India), Poonpipope Kasemsap (Thailand), José Matos (Portugal), Jan Černý (Czech Republic), Saman Hosseinkhani (Iran), Takao Ishikawa (Poland). Jury members evaluated the students according to 5 criteria, and gave a consensus score for each category. Six teams received an award: three teams-3rd prize, two teams-2nd prize, and one team-1st prize. The results are summarized in the table below.

Group	Facilitator	Name	Country	Medal	Topic	Poster Title	Research question / Creativity	Methodology	Discussion and conclusions	Presentation (on spot)	Question and answer (on spot)	Sum	Poster Prize
1	Shushan Toneyan (Armenia)	Michael, Purnama	Indonesia	Gold	Bioinformatics and AI	Evolution of the Fenna-Matthews-Olson (FMO) Complex	3	3	4	3	3	16	No
		Liam Audrey, Alleda	Philippines	Merit									
		Aravindh, Kuppusamy Velmurugan	Singapore	Bronze									
		Daviti Giorgadze	Georgia	Nothing									

2	Barbara, Buchalska (Poland)	Aleksandra Kowalczyk	Poland	Silver	Biome- dicine	Exposure of Mesenchymal Stem Cells to cerebrospinal fluid in Alzheimer's disease treatment	3	3	3	3	4	16	No
		Sebastian Krikke	Netherlands	Silver									
		Jorūnė Budriūnaitė	Lithuania	Bronze									
3	Lawnaldi, Sugiarto (Indonesia)	Tristan, van der Beek	The Netherlands	Bronze	Molecu- lar and Cell Biology	Nanobodies as Treatment Tools For Parkinson's Disease	5	4	3	5	5	22	3rd
		Basel Alkanjo	Syria	Silver									
4	Stevan Bodganov (North Macedonia)	Albert Rumle Bernsen	Denmark	Bronze	Bionics and Biomi- micry	Application of biomimicry-based materials to improve microclimate in Yerevan city center	5	5	5	3	4	22	3rd
		Szymon Bander	Poland	Silver									
		Karina Karimova	Russia	Gold									
5	Joan Nadia Laksmana (Indonesia)	Paul, Ugwu	Nigeria	Nothing	Biome- dicine	CAR T-cells treatment for Goodpasture's syndrome	3	3	3	4	3	16	No
		Jose Javier Quintana Rodríguez	Spain	Nothing									
		Zuzanna Żyra	Poland	Silver									
		Urh Šarlah	Slovenia	Nothing									
6	Anush Margaryan (Armenia)	Celine Xie	Denmark	Nothing	Across Species	THREE WAY SYMBIOSIS: Exploring a unique way Of Extreme Heat Tolerance	5	5	4	5	5	24	1st
		George, Lee	Singapore	Silver									
		ROHIT PANDA , PANDA	INDIA	Silver									
7	Nethmini, Rathnayake Nirasha (Sri Lanka)	Kriti Shahu	Nepal	N/A	Molecu- lar and Cell Biology	Novel method of identifying tumor status by using hyperpolarized	3	3	3	3	4	16	No
		Raven Foronda	Philippin es	Bronze									
		Abdullah Jaddaa	Syria	Silver									

		Mustafin Nazim	Russian Federation (IBO team)	Gold		substrates								
8	Jeremy Ng (Philippines)	Lawand Bayram	Syria	Merit	Molecular and Cell Biology	Preventing Breast Cancer Metastasis by Silencing the SNAP25 Protein	4	4	4	3	2	17	No	
		Giorgi Nebulishvili	Georgia	Nothing										
		Wijepala Abeysinghe												
		Thennakoon Mudiyansele												
		Praveen Charuka												
		Thennakoon	Sri Lanka	Nothing										
		Ema Suligoj	Slovenia	Bronze										
9	Jovana Stojcheska (North Macedonia)	Jagienka Mądrzak	Poland	Gold	Biomedicine	Mesenchymal stem cell-derived exosomes therapeutic role in diabetic cardiomyopathy	3	4	4	4	4	19	No	
		Moza Aldhanhani	United Arab Emirates	Nothing										
		Bobur Poudel	Nepal	N/A										
		Urban Bauk	Slovenia	Bronze										
10	Farrel, Marsetyo (Indonesia)	Adnan RIHAWI	Syria	Nothing	Molecular and Cell Biology	Controlled Expression of Telomerase	2	2	2	3	3	12	No	
		Mila Dimitrovska	The Republic of North Macedonia	N/A										
		Yerassyl Temirbekov	Kazakhstan	Silver										
		Karthik Pravin Ramachandran	Srilanka	Nothing										
11	Lilit Grigoryan (Armenia)	Owen Ong	Singapore	Gold	Molecular and Cell Biology	Therapy for Lactose Intolerance By CRISPR/dCas9-mediated Epigenome Editing	4	4	2	4	3	17	No	
		Harshan, Arulmoli	Sri Lanka	Bronze										
		Alikhan Zhumagaleyev	Kazakhstan	Silver										
		Yakov Korobitsyn	Russia	Gold										

12	Robert Yeghikyan (Armenia)	Min Seo, Koo	Singapore	Gold	Biome- dicine	Design of a Low-Cost Point-of-Care Test Kit for COVID-19 Cytokine Storm Susceptibility	4	5	4	5	4	22	3rd
		Joo Chan, Kim	South Korea	Silver									
		Semyon Shmakov	Russia	Gold									
013	Arman Simonyan (Armenia)	Povilas Šaučiuvienas	Lithuania	Silver	Bio- informatics and AI	A NOVEL PROPOSAL FOR INDUCING CONTROL-LABLE MAGNETO-TACTIC MOVEMENT IN THE CILIATE T. THERMO-HILA	4	4	5	5	5	23	2nd
		Dumitrescu Ștefan-Ionel	Romania	Bronze									
		Markuss Gustavs Kenins	Latvia	Bronze									
		RAYAN, RAHMAN	BANGLA DESH	Bronze									
14	Lilit Grigoryan (Armenia)	Joo Hyun, Hahm	South Korea	Silver	Molecu lar and Cell Biology	Tumor Supression through regulation of the BCL-3 Pathway	4	3	4	4	3	18	No
		FAYYAD, AHMMED	BANGLA DESH	Bronze									
		Nadav, Qvit	Israel	Silver									
		Nguyễn, Đỗ (Nguyen, Do)	Vietnam	Bronze									
15	Robert Yeghikyan (Armenia)	Yechan, Jeong	South Korea	Silver	Biome- dicine	No poster submitted							No
		Seraphim, Joliat	Liechtens tein	Merit									
		TAHSEEN SHAAN, LEON	BANGLA DESH	Bronze									
		Mindaugas Smetaninas	Lithuania	Bronze									
16	Tzang, Chih Chen (Taiwan)	Seoyeon, Jeon	South Korea	Bronze	Molecu- lar and Cell Biology	Applying Autophagy as a treatment for Huntington's	5	4	4	5	5	23	2nd
		Mane Kurghinyan	Armenia	Nothing									

		KHUNDKE R ISHRAQ, AHAMMAD	BANGLA DESH	Bronze		disease								
		Donato Elías Pellegrini	Argentin a	Silver										
17	Arman Simonyan (Armenia)	Nauris Priksans	Latvia	Silver	Bioinfo rmatics and AI	GENETIC BIOMARKERS OF PARKINSON'S DISEASE IDENTIFIED WITH MACHINE LEARNING METHODS	4	4	3	3	2	16	No	
		Ján Plachý	Slovakia	Silver										
		Syuzi Sahakyan	Armenia	Merit										
		Ottó Tatai	Hungary	Bronze										
18	Josue Francisco, Laszeski (Argentina)	Arman Hayrapetyan	Armenia	Bronze	Biome- dicine	Synthetic Fibrinogen as a treatment for Afibrino- genemia	3	3	4	3	3	16	No	
		Siluni Wickramath ilake	Sri Lanka	Nothing										
		Aikaterini, Karpouzi	Greece	Merit										
		Daniel Čičovský	Czech republic	Silver										

Jury members evaluated posters with the following five criteria, each 5 points maximum, and in total 25 points.

Research question / Creativity	Methodology	Discussion and conclusions	Presentation (on spot)	Question and answer (on spot)
--------------------------------	-------------	----------------------------	------------------------	-------------------------------

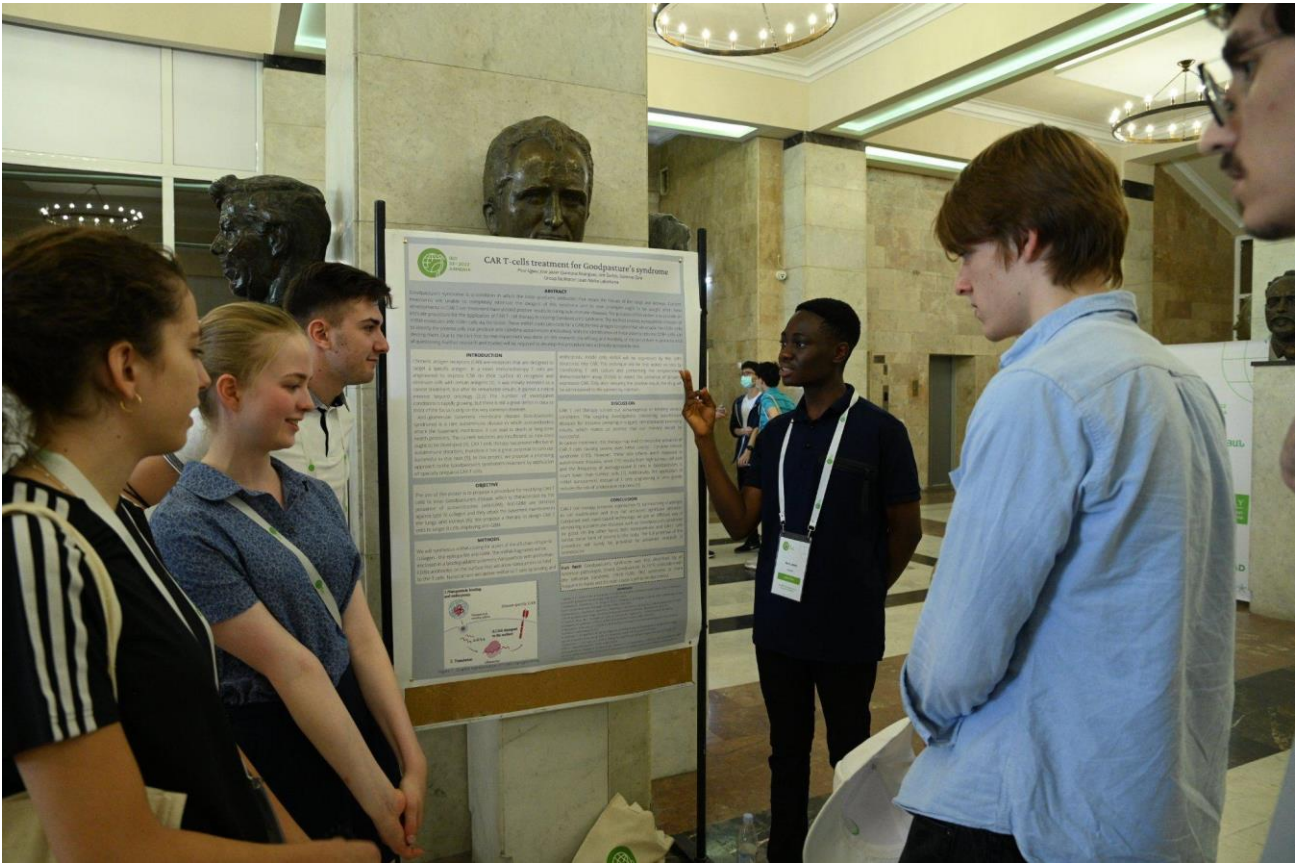
Jury members evaluated the first three criteria by reading pdf posters, and the last two on spot, at the poster presentation site. They gave their points not individually but as a consensus reached by all of them. The advantage of IGP is that it includes both theoretical and practical work, and it also includes teamwork skills, as well as public presentation, which are not tested during theory and practical tasks. So, it should be evaluated separately. It can have 10% value in total score, and Theory and Practical parts can have 45%+45%. Each team member will get the same score, as the other team members, as it will be impossible to judge the team members. The students will share the same score as the team received. The students who participated in the

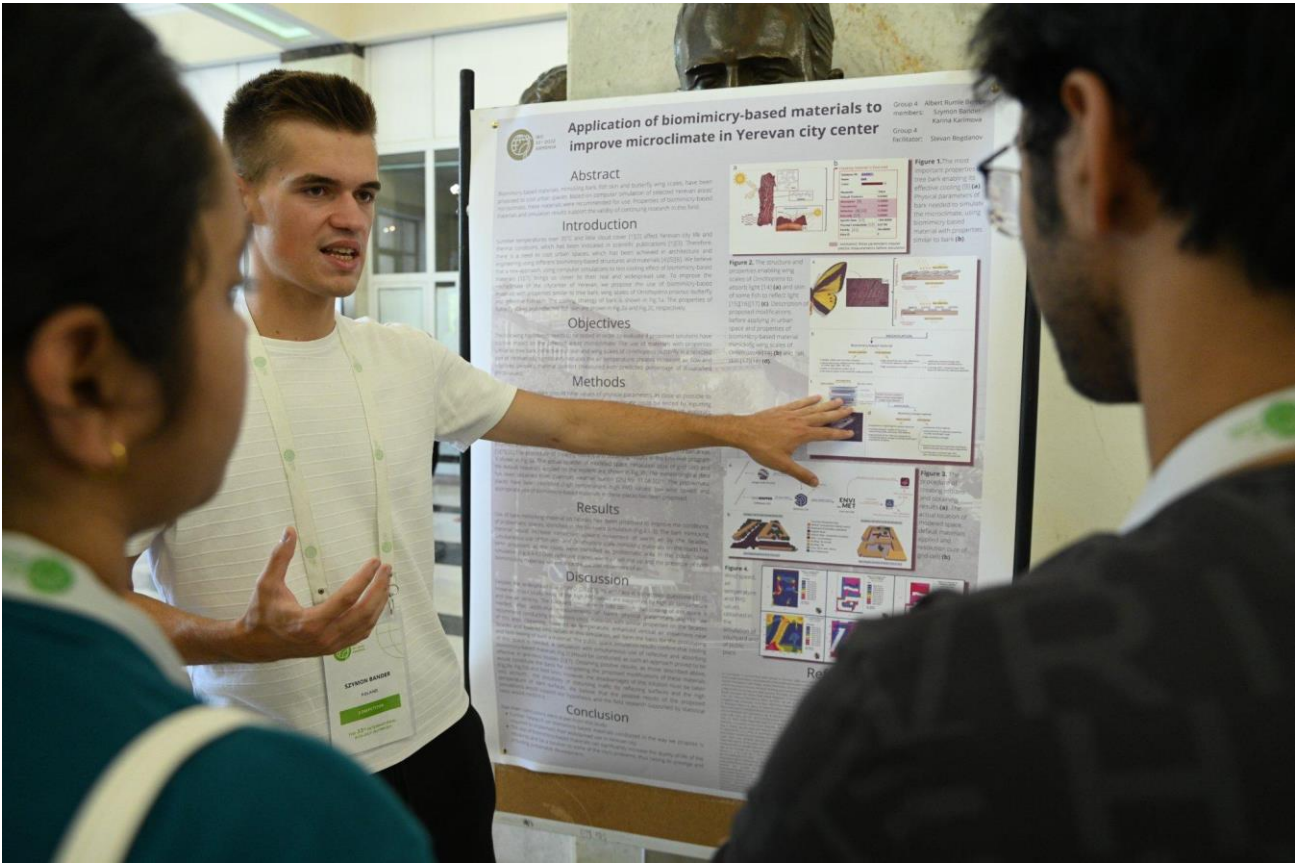
IGP 2022 have also participated in Theoretical and Practical exams of IBO2022, and some received medals. Their performance is summarized in the table above.

Initially 4 members per each group was allocated, however, some students did not participate as much as the others and dropped out from the group. The IBO 2022 organizing committee has asked the groups and facilitators to confirm the group member name only in the case they agree that all the students had sufficient contribution to be in the group. Hence, some groups had less than 4 members in the end.

An exhibition of posters of the international group project took place at YSU. A summary of the results of the group project was done.









An award and a certificate were given during the closing ceremony to the IGP winners.



A souvenir (presented below) was distributed to the participants as a memento of Yerevan State University.



6.2 International Group Project Posters



Evolution of the Fenna-Matthews-Olson (FMO) Complex

Kuppusamy Velmurugan Aravindh, Purnama Michael, Alleda Liam Audrey, Giorgadze Daviti
(main contributor) Group 1 [Facilitator: Shushan Toneyan]

1. Abstract

It was long hypothesised that quantum coherence dynamics are unlikely to take place in biological systems. Molecular collisions and radiation present in natural conditions are expected to prevent coherence from lasting for functionally meaningful durations.

However, in the past decade, several biological systems were found to demonstrate coherence dynamics. The FMO complex is one example of such a system. Found in green sulfur bacteria (GSB), the FMO complex is known to shuttle energy from the light-harvesting regions of the bacteria's photosynthetic apparatus to its reaction centre at near-perfect efficiencies. Whether this is a pre-requisite for photosynthetic apparatus to even develop or a trait that evolved because it enhanced photosynthetic efficiency remains a question.

To address this, we identify sequences homologous to the FMO complex in related species. Thereafter, we quantify the efficiency of coherence transfer promoted by the protein encoded by each of the sequences. By studying the evolutionary age of these sequences and defining a function that relates coherence transfer efficiency to fitness, we can plot a fitness-phenotype landscape. Using which, we can track the evolution of the FMO complex with regard to the ability to promote coherence transfer.

2. Introduction

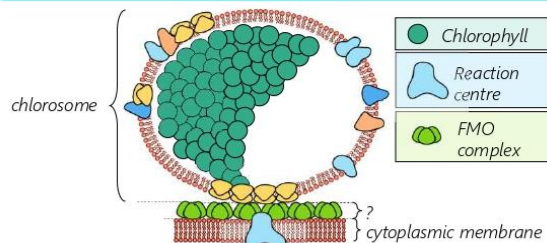


Fig: Photosynthetic Apparatus of Green Sulfur Bacteria

Observation Energy transfer from chlorosome to the reaction center is almost 100% efficient.

Theory The molecular structure of the FMO complex promotes coherence transfer – this could be an evolved trait.

Objective To determine if promoting coherence transfer is an evolved trait in the FMO complex of green sulfur bacteria.

3. Methods

- The most commonly studied FMO complex is derived from *Chlorobaculum tepidum*.
- Using *C. tepidum* as a starting point: select related species that have been present for different evolutionary times.
- Comparing these species with *C. tepidum* is akin to comparing ancestral species with *C. tepidum*.

A) Identify Species Related to *C. tepidum*

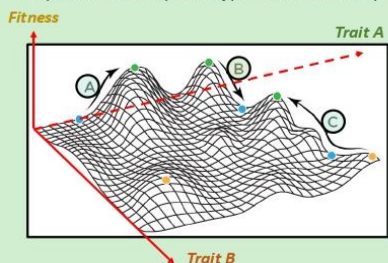
B) Find FMO-like Protein Sequences

- For each species homologous sequence, run the protein prediction algorithm BHAGEERATH-H to obtain a 3-dimensional model of the proteins of interest.

C) Predict FMO Molecular Structure

- C. tepidum*'s FMO complex is a trimer – the protein sequences of the monomers can be found in PDB (ID: 5H8Z_A, 6MEZ_B, 5H8Z_C)
- Run a protein BLAST to identify sequence homologies among the species identified.
- Plot a parsimonious phylogenetic tree for easier visualisation

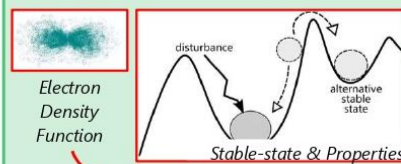
- Based on predicted protein structures from C) and coherence transfer efficiencies calculated in D), plot a relevant phenotype-fitness landscape



D) Build a Density Functional Theory Model

E) Plot Phenotype-Fitness Landscape

- Computational QM modelling** method to investigate electronic structure of systems
- Hohenberg-Kohn Theorem 1** Ground state energy E is unique functional of electron density $E = E[n(r)]$
- Hohenberg-Kohn Theorem 2** Electron density which minimizes functional energy is of a true ground state $E[n(r)] > E_0[n_0(r)]$



Gradient Descent; K-points Numerical Integration

- Determine coherence transfer efficiency

4. Discussion & Conclusions

- The precise effect a change in a key protein's conformation has on the survival and reproducibility of the organism is difficult to determine. Furthermore, we build the experimental design based on the assumption that the BHAGEERATH-H produces accurate predictions of FMO complex's molecular structure. These caveats can be addressed with 1) a case-controlled study of precisely how superior photosynthetic efficiency (more specifically, that of coherence transfer) might contribute to fitness, and 2) better 3-d models of protein structure, possibly by extracting them from living tissue and imaging them.
- The design proposed would serve as a foundational model for more robust studies, and contribute some preliminary knowledge to the field.

5. Key References

- Valleau S, Studer RA, Hase F, Kreisbeck C, Saer RG, Blankenship RE, Shakhnovich EI, Aspuru-Guzik A. Absence of Selection for Quantum Coherence in the Fenna-Matthews-Olson Complex: A Combined Evolutionary and Excitonic Study. ACS Cent Sci. 2017 Oct 25;3(10):1086-1095. doi: 10.1021/acscentsci.7b00269. Epub 2017 Aug 30. PMID: 29104925; PMCID: PMC5658757.
- Engel G, Calhoun T, Read E, et al. Evidence for wavelike energy transfer through quantum coherence in photosynthetic systems. Nature 446, 782-786 (2007). <https://doi.org/10.1038/nature05678>

Exposure of Mesenchymal Stem Cells to cerebrospinal fluid in Alzheimer's disease treatment

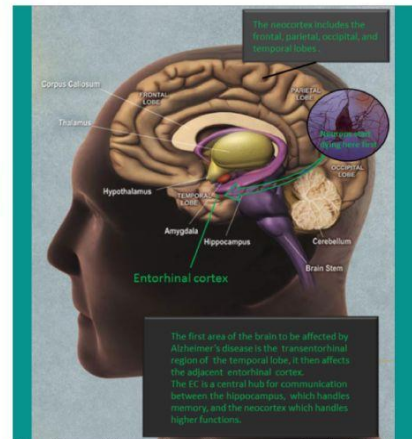
Group 2 (biomedicine): Jorūnė Budriūnaitė (Lithuania), Aleksandra Kowalczyk (Poland), Sebastian Krikke (Netherlands), Facilitator: Barbara Buchalska (Poland)

ABSTRACT

In this article we investigate whether treating mesenchymal stem cells used in an experimental treatment of Alzheimer's disease (AD) with cerebrospinal fluid or medium containing beta-amyloid- and tau proteins instead of with AD mouse brain homogenate will improve treatment outcome in transgenic APP/PS1 mice. The results of the treatment were assessed using memory tests and PET staining of beta-amyloid- and tau proteins.

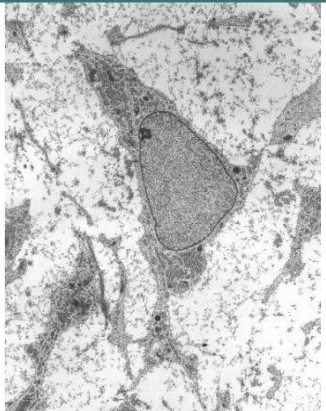
INTRODUCTION

Alzheimer's disease (AD) is a debilitating and universally fatal disease that affects large parts of the population (up to 30% of those aged 85 and older) and will cause an estimated disease burden of US\$ 9.1 trillion by 2050 [1][2]. It manifests itself in the form of gradually worsening cognitive deficits eventually resulting in almost complete loss of brain function and subsequent death. The causes and mechanism of AD are not fully understood but plaques consisting of beta-amyloid- and tau proteins are believed to be implicated. As of yet no effective treatments has been found to either cure AD or relieve its symptoms despite extensive efforts to do so [3; 4]. Recently Santamaria et al. (2021) have attempted to treat AD in model organisms (mice) by utilizing the paracrine activity of mesenchymal stem cells (MSCs). Though their efforts were successful, resulting in significant improvements of disease outcome, the methods used required the use of brain homogenate extracted from AD mice [5]. Due to ethical concerns it would be hard to replicate this therapy in humans so in this study we investigate the effectiveness of different substitutes for AD mouse brain homogenate.



The order in which AD affects different parts of the brain [10]

OBJECTIVES



Transmission electron micrograph of a mesenchymal stem cell displaying typical ultrastructural characteristics [9]

Currently there are no available treatments for AD, despite the active research. The objective of this poster is to suggest another treatment option for AD in transgenic mice, which, if successful, could be replicated in humans. Our suggested experiment seeks for a way in which a proven effective treatment in mice could be transformed so that it would be possible to test it out on humans, as human brain homogenate is not an ethical option for a trial.

Furthermore, we wish to research the effect that MSC's secretome has on a brain that is affected by AD, when MSC's are exposed to different substances and mixtures of substances in their growth medium. We also wish to discover more about the effects of exposing stem cells to different substrates before insertion into the mice.

DISCUSSION

MSCs are currently the most frequently studied of all stem cell types [3] because they are unique in terms of their paracrine anti-amyloid activity [4]. Studies have shown that MSC secretome treatment is much more efficient for AD mice if MSCs are in vitro exposed to brain homogenate of AD mice before their insertion to the treated mice [5]. However, we would not be able to apply this in human trials because of ethical issues which is why we propose using cerebrospinal fluid (CSF) instead. The content of AD patient's CSF is somewhat similar to that of their brain cells (e.g. tau protein) but there are differences, for instance an increased level of amyloid beta in brain and its decreased level in CSF [8]. That is the reason why one group in our experiment contains CSF enriched with amyloid beta.

We have planned five different groups so as to compare the efficiency of each treatment. It is hypothesized that MSCs exposed to CSF fluid would be less successful in improving AD mice memory than MSCs exposed to brain homogenate because the components of those substances are slightly different and that MSCs exposed to CSF fluid would be more successful in improving AD mice memory than MSCs exposed to medium enriched with amyloid beta and tau protein because the pathogenesis of AD cannot be restricted to those two components.

METHODS

In our experiment we are exposing MSCs to different substances so as to find the best possible treatment for Alzheimer's disease (AD) using their paracrine activity.

First MSCs are isolated from bone marrow of healthy donors (mice) and divided between five samples in which they are exposed in vitro to medium enriched with different substances: AD mouse brain homogenate, AD mouse cerebrospinal (CSF) fluid, AD mouse CSF fluid plus amyloid beta, amyloid beta and tau protein, and unmodified medium for 24 hours. Then the supernatant is collected and concentrated.

Transgenic APP/PS1 12-month-old male mice are divided into four groups and each group undergoes different intranasal treatment including daily inhalations with MSC secretome. After 30 days the effects are measured by memory test and positron emission tomography (PET) for amyloid beta and tau protein. Results of all groups are put together and compared.

The progression of the disease would be monitored by performing PET scans using Pittsburgh compound B. This method uses a radioactive analogue of thioflavin which binds to fibrillar A β forms, therefore visually assessing brain amyloidosis [6].

Since brain amyloidosis is not the only factor in degeneration, the memory of the mice would also be assessed. Since usually APP/PS1 mice develop impairments in reference memory first, then associative learning deficits associated with fear conditioning and finally passive avoidance deficits, tests for all of these deficits (the Morris water maze for reference memory testing, a fear conditioning test for associative learning and a passive avoidance test, where mice learn to avoid an unpleasant stimuli) should be done before and after the treatment and the results assessed [7].

REFERENCES

1. Breijyeh, Z., & Karaman, R. (2020). Comprehensive Review on Alzheimer's Disease: Causes and Treatment. *Molecules*, 25(24), 5789. <https://doi.org/10.3390/molecules25245789>
2. Rajan, K. B., Weuve, J., Barnes, L. L., McAninch, E. A., Wilson, R. S., & Evans, D. A. (2021). Population estimate of people with clinical Alzheimer's disease and mild cognitive impairment in the United States (2020–2060). *Alzheimer's & Dementia*, 17(12), 1966–1975. <https://doi.org/10.1002/alz.12362>
3. Duncan, T., Valenzuela, M. 'Alzheimer's disease, dementia, and stem cell therapy'. *Stem Cell Res & The.* 2017; 8:111
4. Fan X, Sun D, Tang X, Cai Y, Yin ZQ, Xu H. 'Stem-cell challenges in the treatment of Alzheimer's Disease: a long way from bench to bedside'. *Med Res Rev.* 2014;34:957–78.
5. Santamaria G, Brandi E, La Vitola P, Grandi F, Ferrara G, Pischiutta F, Vegliante G, Zanier E, R, Re F, Uccelli A, Forloni G, Kerlero de Rosbo N, Baldacci C. 'Intranasal delivery of mesenchymal stem cell secretome repairs the brain of Alzheimer's mice'. *Cell Death & Dif.* 2021; 28:203–218
6. Jack C R, Jr, Wiste H J, Vemuri, P, Weigand, S. D., Senjem, M. L., Zeng, G., Bernstein, M. A., Gunter, J. L., Pankratz, V. S., Aisen, P. S., Weiner, M. W., Petersen, R. C., Shaw, L. M., Trojanowski, J. Q., Knopman, D. S., & Alzheimer's Disease Neuroimaging Initiative (2010). Brain beta-amyloid measures and magnetic resonance imaging atrophy both predict time-to-progression from mild cognitive impairment to Alzheimer's disease. *Brain : a journal of neurology.* 133(11), 3336–3348
7. Webster Scott J., Bachtetter Adam D., Nelson Peter T., Schmitt Frederick A., Van Eldik Linda J. (2014) Using mice to model Alzheimer's dementia: an overview of the clinical disease and the preclinical behavioral changes in 10 mouse models. *Frontiers in Genetics*, 10, 3389/fgene.2014.00088 <https://www.frontiersin.org/article/10.3389/fgene.2014.00088>
8. Andreasen N, Hesse C, Davidsson P, Minthon L, Wallin A, Winblad B, Vanderstichele H, Vanmechelen E, Blennow K. 'Cerebrospinal fluid beta-amyloid(1-42) in Alzheimer disease: differences between early- and late-onset Alzheimer disease and stability during the course of disease'. *Arch Neurol.* 1999; 56(6):673-680
9. https://upload.wikimedia.org/wikipedia/commons/5/52/MSC_high_magnification.jpg
https://commons.wikimedia.org/wiki/File:Alzheimers_entorhinal_cortex.PNG

Created with BioRender Poster Builder

Nanobodies as Treatment Tools For Parkinson's Disease

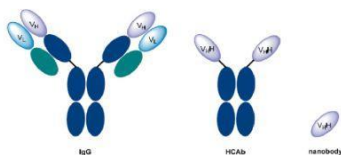


Abstract

Nanobodies are recombinant, single domain, variable fragments of camelid heavy chain-only antibodies. In recent years, more and more studies have been conducted in discovering their applications as efficient tools in diagnostics and disease therapy. Recent scientific research has approved the ability of these biomolecules to bind with β -amyloid proteins and prevent their further aggregation in Alzheimer's patients. In this poster, we highlight the possible capability of utilizing these nanobodies to inhibit the aggregation of alpha synuclein proteins, which are basically known to be pathologically related to the formation of lewy bodies in patients with Parkinson's disease.

Introduction

Unique functional heavy chain-only antibodies devoid of light chains are circulating in the blood of Camelidae, these antibodies recognize their antigen via one single domain known as VHH or Nanobody. High production yield in a broad variety of expression systems, minimal size, great stability, reversible refolding, outstanding solubility in aqueous solutions, and the ability to specifically recognize unique epitopes with subnanomolar affinity, have combined to make nanobodies a great class of biomolecules for research and various medical diagnostic and therapeutic applications. Parkinson's disease (PD) is the second most common neurodegenerative disease that affects populations worldwide. Indeed, many cellular hallmarks have been found to occur in PD patients, especially alpha synuclein aggregation and lewy bodies formation, the motor symptoms arise primarily from the loss of dopaminergic neurons in substantia nigra. Treatment of PD currently involves substituting dopamine, although many negative side effects had been recorded. In this poster we seek to design an experiment testing the potential effects of nanobodies to inhibit the aggregation of alpha synuclein proteins in PD patients, considering them as novel tools with many advantages for curing PD patients and reducing their symptoms.



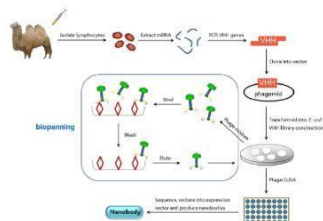
Schematic representation of conventional immunoglobulin (IgG), heavy chain-only antibodies (HCAbs) and nanobodies (VHH). VH, variable heavy; VL, variable light; VHH, VH of HCAbs

Objectives

The main objective is to propose a step by step experimental method for generating and utilizing nanobodies against alpha synuclein proteins to prevent their aggregation, which could help in treating PD patients.

METHODS

A camelid is immunized with the wild type alpha synuclein protein at regular intervals, after that, mRNA could be isolated from peripheral blood lymphocytes, VHH region in the isolated mRNAs is amplified by PCR and become ligated into a phagemid, which is a cloning vector that has both phage and plasmid properties. The phagemid is subsequently transformed into E.coli cells, then the phagemid is transformed into infective phages by the superinfection of phagemid bearing E.coli cells with helper phages. A VHH library contained within the phage community would be obtained. By phage display technique (Biopanning), certain phages that express wanted nanobodies could be gathered, and these phages are retrieved by ELISA. The final step is to deduce the nucleotide sequence of the VHH region from the selected phages. These specific sequences could be cloned into expression vectors to produce the desired nanobodies. The produced nanobodies can be injected intravenously in PD patients, they are known for their high permeability through various membranes and barriers, especially the blood brain barrier. Crossing the neurons' cellular membranes, they can bind specifically to alpha synuclein proteins and inhibit their polymerization into aggregates.



Overview of nanobody identification and production with biopanning for a phage display library. Hollow red diamonds in the figure denote antigens.

Discussion

Nanobodies acquire remarkable features that make them important candidates as next-generation tools for diagnostics and therapy. Particularly appealing is their ability to inhibit protein misfolding and aggregation especially in Alzheimer's disease. There is a great potential for nanobodies to become important therapeutics in the near future, displaying unprecedented efficacies in the treatment of diseases.

Alpha synuclein aggregation in PD patients is attributed majorly to the overexpression of the wild type protein, or the occurrence of 3 missense mutations that causes improper folding of the polypeptide and initiates its self-aggregation. Considering patients with the overexpression of the protein, nanobodies should be generated by immunizing the camelid with wild type alpha synuclein. On the other hand, treating patients that carry the missense mutations may require immunizing the camelids with the same mutant proteins. Further researches should focus on discovering specific epitopes on alpha synuclein that are highly correlated with the stability of the intact protein and the prevention of its self-aggregation.

CONCLUSION

The small size, strict monomeric state, robustness, and easy tailoring of these nanobodies distinguishes them from other antibody formats and small-molecule drugs, hence allowing their applications to extend toward different biological and medical researches. Using them as treatment tools for the Parkinson's disease still needs experimental approval. Its success would bring hope for those people that are suffering from neurodegenerative diseases all around the world.

References

- Poewe, W. et al. Parkinson disease. *Nat. Rev. Dis. Primers* 3, 17013 (2017)
- Almeida, Z. L., & Brito, R. M. (2020). Structure and aggregation mechanisms in amyloids. *Molecules*, 25(5), 1195.
- Liu, W., Song, H., Chen, Q., Yu, J., Xian, M., Nian, R., & Feng, D. (2018). Recent advances in the selection and identification of antigen-specific nanobodies. *Molecular immunology*, 96, 37-47.
- Sulzer, D., & Edwards, R. H. (2019). The physiological role of α -synuclein and its relationship to Parkinson's Disease. *Journal of neurochemistry*, 150(5), 475-486.
- Siontorou, C. G. (2013). Nanobodies as novel agents for disease diagnosis and therapy. *International journal of nanomedicine*, 8, 4215.
- Beitz, J. M. (2014). Parkinson's disease: a review. *Frontiers in Bioscience-Scholar*, 6(1), 65-74.
- Henderson, M. X., Trojanowski, J. Q., & Lee, V. M. Y. (2019). α -Synuclein pathology in Parkinson's disease and related α -synucleinopathies. *Neuroscience letters*, 709, 134316.

Application of biomimicry-based materials to improve microclimate in Yerevan city center

Group 4 Albert Rumle Bernsen
members: Szymon Bander
Karina Karimova
Group 4
facilitator: Stevan Bogdanov

Abstract

Biomimicry based materials, mimicking bark, fish skin and butterfly wing scales, have been proposed to cool urban spaces. Based on computer simulation of selected Yerevan areas' microclimate, these materials were recommended for use. Properties of biomimicry-based materials and simulation results support the validity of continuing research in this field.

Introduction

Summer temperatures over 35°C and little cloud cover [1][2] affect Yerevan city life and thermal conditions, which has been indicated in scientific publications [1][3]. Therefore, there is a need to cool urban spaces, which has been achieved in architecture and engineering using different biomimicry-based structures and materials [4][5][6]. We believe that a new approach, using computer simulations to test cooling effect of biomimicry based materials [5][7], brings us closer to their real and widespread use. To improve the microclimate of the citycenter of Yerevan, we propose the use of biomimicry-based materials with properties similar to tree bark, wing scales of *Ornithoptera priamus* butterfly and reflective fish skin. The cooling strategy of bark is shown in Fig.1a. The properties of butterfly scales and reflective fish skin are shown in Fig.2a and Fig.2c, respectively.

Objectives

The following hypothesis needs to be tested in order to evaluate if proposed solutions have positive impact on the selected areas' microclimate: The use of materials with properties similar to tree bark, reflective fish skin and wing scales of *Ornithoptera* butterfly in a selected part of Yerevan city significantly reduces the air temperature, creates increased air flow and improves people's thermal comfort (measured with predicted percentage of dissatisfied (PPD) values).

Methods

Material mimicking bark should have values of physical parameters as close as possible to those found in nature. It's influence on urban microclimate could be tested by inputting data into software, as presented in Fig.1b. The proposed modifications of materials mimicking wing scales of *Ornithoptera* and mimicking reflective fish skin, are shown in Fig.2b and Fig.2d, respectively. These modifications are necessary before applying them in urban space. Two microclimatic simulations of 24h period were carried out on a chosen backyard and a public place in the city center of Yerevan. Simulations were conducted in the software Envi-met, a well-described tool [19] used in the latest microclimatic research in urban areas [5][7][20]. The procedure of creating models and obtaining results in the Envi-met program is shown in Fig.3a. The actual location of modeled space, resolution (size of grid cell) and the default materials applied on the models are shown in Fig.3b. The meteorological data has been obtained from Zvartnots weather station [25] for 31.08.2021. The problematic places have been identified (high temperature, high PPD values, low wind speed) and appropriate use of biomimicry-based materials in these places has been proposed.

Results

Use of bark mimicking material on facades has been proposed to improve the conditions of problematic spaces, identified in the backyard simulation (Fig.4.1-3). The bark-mimicking material would increase convective upward movement of warm air by the facades. Simultaneous use of fish skin- and *Ornithoptera* scale-mimicking materials on the roads has been proposed, as the roads were identified as problematic area in the public space simulation (Fig.4.4-6.) Over reflective places, warm air will rise up and the presence of both biomimicking materials will enhance the parallel movement of air.

Discussion

Despite the widespread use of PPD [26][27], its accuracy is sometimes questioned [28]. However, in our study, most of the high PPD values are supported by high air temperature and low air velocity. The backyard simulation results confirm that cooling of this space is needed. After additional measurements of bark's physical parameters (Fig.1b), we recommend conducting simulations using materials with similar properties on the facades of this area. Obtaining lowered air temperature, enhanced vertical air movement near facades and lowered PPD values in this simulation, will form the basis for the prototyping and field testing of such a material. The public space simulation results confirm that cooling of this space is needed. A simulation with simultaneous use of reflective and absorbing biomimicry-based materials (Fig.2) should be conducted, as such an approach proved to be effective in previous studies [5][7]. Obtaining positive results, as those described above, would constitute the basis for completing the proposed modifications of these materials (Fig.2b; Fig.2d) and field tests. However, the disadvantages of this solution must be taken into account: the possibility of disturbing traffic by reflecting surfaces and the high temperature of dark surfaces. We believe that the positive results of the proposed simulations would support our hypothesis, and the field research supported by statistical tests would confirm it.

Conclusion

Two main conclusions were drawn from this study:

- Further research on biomimicry-based materials conducted in the way we propose is required to implement their widespread use in Yerevan city.
- The use of biomimicry-based materials can significantly increase the quality of life of the residents and be a solution to some of the city's problems, thus raising its prestige and providing sustainable development.

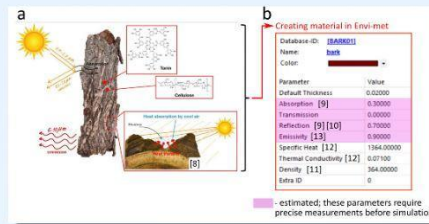


Figure 1. The most important properties of tree bark enabling its effective cooling [9] (a). Physical parameters of bark needed to simulate the microclimate, using biomimicry based material with properties similar to bark (b).

Figure 2. The structure and properties enabling wing scales of *Ornithoptera* to absorb light [14] (a) and skin of some fish to reflect light [15][16][17] (c). Description of proposed modifications before applying in urban space and properties of biomimicry-based material mimicking wing scales of *Ornithoptera* [14] (b) and fish skin [17][18] (d).

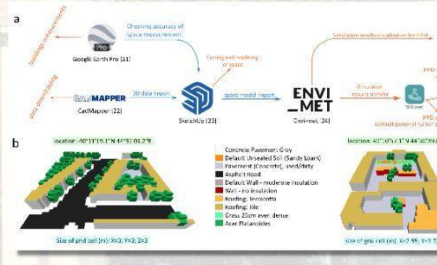
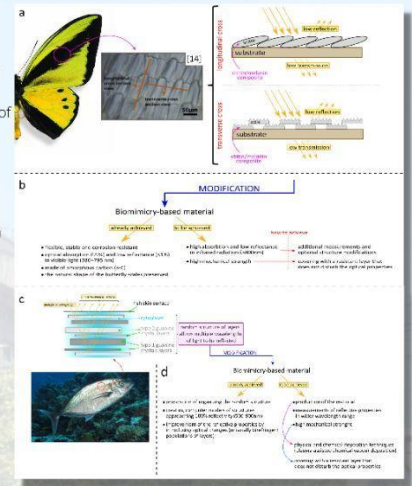


Figure 3. The procedure of creating models and obtaining results (a). The actual location of modeled space, default materials applied and resolution (size of grid cell) (b).

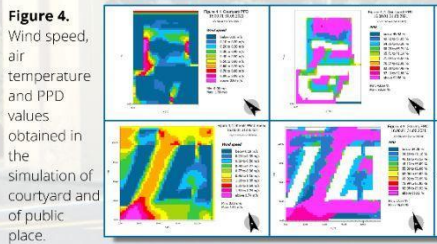


Figure 4. Wind speed, air temperature and PPD values obtained in the simulation of courtyard and of public place.

References

1. Georgiana A. Sarmentier, wind climate in Vojvodina valley and systems. Clim Dyn 48, 1827–1848 (2017). <https://doi.org/10.1007/s00382-016-0912-7>
2. <https://www.meteorological.gov.am/>
3. <https://www.meteorological.gov.am/>
4. <https://www.meteorological.gov.am/>
5. <https://www.meteorological.gov.am/>
6. <https://www.meteorological.gov.am/>
7. <https://www.meteorological.gov.am/>
8. <https://www.meteorological.gov.am/>
9. <https://www.meteorological.gov.am/>
10. <https://www.meteorological.gov.am/>
11. <https://www.meteorological.gov.am/>
12. <https://www.meteorological.gov.am/>
13. <https://www.meteorological.gov.am/>
14. <https://www.meteorological.gov.am/>
15. <https://www.meteorological.gov.am/>
16. <https://www.meteorological.gov.am/>
17. <https://www.meteorological.gov.am/>
18. <https://www.meteorological.gov.am/>
19. <https://www.meteorological.gov.am/>
20. <https://www.meteorological.gov.am/>
21. <https://www.meteorological.gov.am/>
22. <https://www.meteorological.gov.am/>
23. <https://www.meteorological.gov.am/>
24. <https://www.meteorological.gov.am/>
25. <https://www.meteorological.gov.am/>
26. <https://www.meteorological.gov.am/>
27. <https://www.meteorological.gov.am/>
28. <https://www.meteorological.gov.am/>

CAR T-cells treatment for Goodpasture's syndrome

Paul Ugwu, Jose Javier Quintana Rodriguez, Urh Šarlah, Zuzanna Żyra
Group facilitator: Joan Nadia Laksmana

ABSTRACT

Goodpasture's syndrome is a condition in which the body produces antibodies that attack the tissues of the lungs and kidneys. Current treatments are unable to completely eliminate the dangers of this syndrome and so new strategies ought to be sought after. New developments in CAR T-cell treatment have yielded positive results in curing auto immune diseases. The purpose of this poster is to provide an intricate procedure for the application of CAR T- cell therapy in treating Goodpasture's syndrome. The method involves nanoparticle infusion of mRNA molecules into CD8+ cells via the blood. These mRNA molecules code for a CAR(chimeric antigen receptor) that will enable the CD8+ cells to identify the plasma cells that produce anti-GBM(the autoimmune antibodies). With the identification of these plasma cells the CD8+ cells can destroy them. Due to the fact that no real experiment was done on this research, the efficacy and feasibility of this procedure is prone to a lot of questioning. Further research and studies will be required to develop this procedure into a clinically acceptable one.

INTRODUCTION

Chimeric antigen receptors (CAR) are receptors that are designed to target a specific antigen. In a novel immunotherapy T cells are engineered to express CAR on their surface to recognize and eliminate cells with certain antigens [1]. It was initially intended as a cancer treatment, but after its remarkable results, it gained a clinical interest beyond oncology [2,3] The number of investigated conditions is rapidly growing, but there is still a great deficit in data as most of the focus is only on the very common diseases.

Anti-glomerular basement membrane disease (Goodpasture's syndrome) is a rare autoimmune disease in which autoantibodies attack the basement membrane. It can lead to death or long-term health problems. The current solutions are insufficient, so new ones ought to be developed [4]. CAR T cells therapy has proved effective in autoimmune disorders, therefore it has a great potential to turn out successful in this case [5]. In this project, we propose a promising approach to the Goodpasture's syndrome's treatment by application of specially prepared CAR-T cells.

OBJECTIVE

The aim of this poster is to propose a procedure for modifying CAR T cells to treat Goodpasture's disease, which is characterized by the presence of autoantibodies (anti-GBM). Anti-GBM are directed against type IV collagen and they attack the basement membrane in the lungs and kidneys [6]. We propose a therapy to design CAR T cells to target B cells displaying anti-GBM.

METHODS

We will synthesize mRNA coding for a part of the $\alpha 3$ chain of type IV collagen - the epitope for anti-GBM. The mRNA fragments will be enclosed in a biodegradable polymeric nanoparticle with antihuman CD8 α antibodies on the surface that will allow nanocarriers to bind to the T cells. Nanocarriers will deliver mRNA to T cells by binding and

endocytosis. Inside cells mRNA will be expressed by the cell's structures into CAR. This technique will be first tested ex vivo by transfecting T cells culture and performing the enzyme-linked immunosorbent assay (ELISA) to detect the presence of properly expressed CAR. Only after ensuring the positive result, the drug will be administered to the patients by injection.

DISCUSSION

CAR T cell therapy turned out advantageous in treating various conditions. The ongoing investigations concerning autoimmune diseases for instance pemphigus vulgaris demonstrated promising results, which makes us positive that our therapy would be successful.

In cancer treatment, this therapy may lead to excessive activation of CAR T cells causing severe, even lethal toxicity - Cytokine release syndrome (CRS). However, these side effects aren't expected in autoimmune diseases, since CRS results from high tumour cell load and the frequency of autoaggressive B cells in Goodpasture's is much lower than tumour cells [7]. Additionally, the application of mRNA nanocarriers instead of T cells engineering in vitro greatly reduces the risk of undesirable reactions [8].

CONCLUSION

CAR-T cell therapy presents approaches to surmounting challenges in cell modification and thus has attracted significant attention. Combined with nano-based technology, we get an efficient way of eliminating autoimmune diseases such as Goodpasture's syndrome for good. On the other hand, both nanoparticles and CAR-T cells exhibit some form of toxicity in the body. The full potential of this procedure will surely be provided by advanced research in biomedicine.

Fun fact! Goodpasture's syndrome was first described by an American pathologist, Ernest Goodpasture, in 1919, coincident with the Influenza pandemic (1918-1920). This syndrome is more frequent in males and it's main cause is yet to be discovered.

REFERENCES

- Siddiqi, H. F., Staser, K. W., & Nambudiri, V. E. (2018). Research techniques made simple: CAR T-cell therapy. *Journal of Investigative Dermatology*, 138(12), 2501-2504.
- Mohanty, R., Chowdhury, C. R., Arega, S., Sen, P., Ganguly, P., & Ganguly, N. (2019). CAR T cell therapy: A new era for cancer treatment. *Oncology reports*, 42(6), 2183-2195.
- Zmievskaia, E., Valiullina, A., Ganeva, I., Petukhov, A., Rizvanov, A., & Bulatov, E. (2021). Application of CAR-T cell therapy beyond oncology: autoimmune diseases and viral infections. *Biomedicine*, 9(1), 59.
- Greco, A., Rizzo, M. I., De Virgilio, A., Gallo, A., Fusconi, M., Pagliuca, G., ... & De Vincentis, M. (2015). Goodpasture's syndrome: a clinical update. *Autoimmunity reviews*, 14(3), 246-253.
- Musette, P., & Bouaziz, J. D. (2018). B cell modulation strategies in autoimmune diseases: new concepts. *Frontiers in immunology*, 9, 622.
- Hellmark, T., & Segelmark, M. (2014). Diagnosis and classification of Goodpasture's disease (anti-GBM). *Journal of autoimmunity*, 48-49, 108-112. <https://doi.org/10.1016/j.jaut.2014.01.024>
- Elbrecht, C. T., & Payne, A. S. (2017). Setting the target for pemphigus vulgaris therapy. *JCI insight*, 2(5), e92021. <https://doi.org/10.1172/jci.insight.92021>
- Parayath, N. N., Stephan, S. B., Koehne, A.L., Nelson, P. S., & Stephan, M. T. (2020). In vitro-transcribed antigen receptor mRNA nanocarriers for transient expression in circulating T cells in vivo. *Nature communications*, 11(1), 1-17.

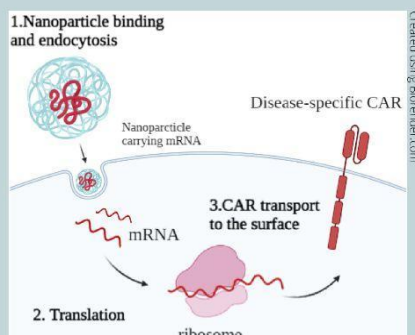


Figure 1. Graphic representation of T cells reprogramming



IBO
33rd 2022
ARMENIA

THREE WAY SYMBIOSIS

Exploring a unique way Of Extreme Heat Tolerance

Facilitator: Anush Margaryan
Members: Rohit Panda (India)
Celine Xie (Denmark)
George Lee (Singapore)

ABSTRACT

Fungi are able to manipulate the phenotypic plasticity of their host plants. Recently, viruses have been found to play a role in this symbiosis, thus creating a 3-way relationship. This relationship between viruses, fungi and plants have been found to increase heat tolerance of all 3 species in the relationship by upregulating expression of certain fungal proteins. In this project, we aim to find out the specific roles of proteins, upregulated in fungi and plants, under heat stress, by knocking out certain genes in the fungi or plants to determine the effect on the thermotolerance.

INTRODUCTION

Climate change is slowly becoming the largest threat humanity faces. Rising temperatures lead to more frequent droughts, wildfires, and invasive pest outbreaks, leading to the loss of plant species. This problem motivated us to discover and explore how some organisms show novel characteristics to exhibit extreme heat tolerance and thrive at temperatures as high as 70 degrees. One of its kind, fungal symbiosis has been shown to contribute greatly to plants' ability to survive stressful conditions, even being one of the main reasons plants were able to colonise terrestrial conditions.

METHODOLOGY

Sample preparation for RNA extraction

To determine the differences in gene expression caused by *C. protuberata* infected with CThTV under heat stress, we will compare the transcriptomes of the host plants. As noted in a previous study [2], there was a difference in the rate of fungal colonisation for dicots and monocots. Hence, we will be using *Solanum lycopersicon* and a monocot *Dichantheium lanuginosum* as host plants.

Extraction of RNA transcripts from plants

We will extract the total RNA from the plants to compare gene expression. In total, there should be 16 RNA samples to analyse since there are 4 factors to vary: type of plant, presence of endophyte, presence of heat-stress, and type of plant tissue. To extract the RNA transcripts from the roots and leaves samples, the samples will be frozen and homogenised, then mixed with Plant RNA Reagent (Life Technologies) to be extracted and purified. [1]

METHODOLOGY (CONT.)

Subtracted cDNA library construction


In order to identify the function of various RNA transcripts, subtracted cDNA libraries were constructed [4]. A cDNA library is constructed by using reverse transcriptase to convert the RNA transcripts into complementary DNA, and the DNA is inserted into plasmids to be stored as a collection. Subtractive hybridisation allows for comparison between 2 types of RNA, so the library would only contain cDNA corresponding to mRNA expressed in tissue type and not the other. [5]

For each library, the cDNA from a plant sample under heat stress was the "tester" and the cDNA from the corresponding plant sample without heat stress was the "driver", so the resulting subtracted cDNA library will only consist of endophyte-induced expressed sequence tags.

Identification of mRNA function and quantification of expression levels

We will sequence the plasmids in all cDNA libraries. [5] The sequences can then be matched with online databases for DNA sequences using BLASTX, to identify the proteins that the DNA sequences would express.

To specifically quantify the changes in expression of genes, real-time quantitative reverse-transcriptase polymerase chain reaction (qRT-PCR) is conducted on the total RNA for each constructed cDNA library. [5]

Figure 1  Panic grass (*Dichantheium lanuginosum*) found growing at 46.5°C in Yellowstone National Park. This unusual thermotolerance was further investigated to find the symbiotic endophyte. (Source: Montana State University)

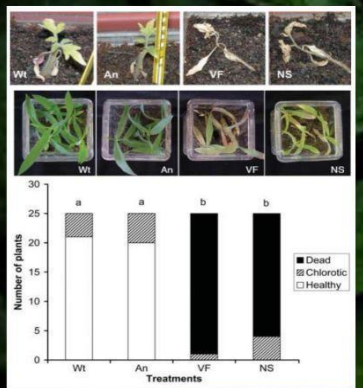


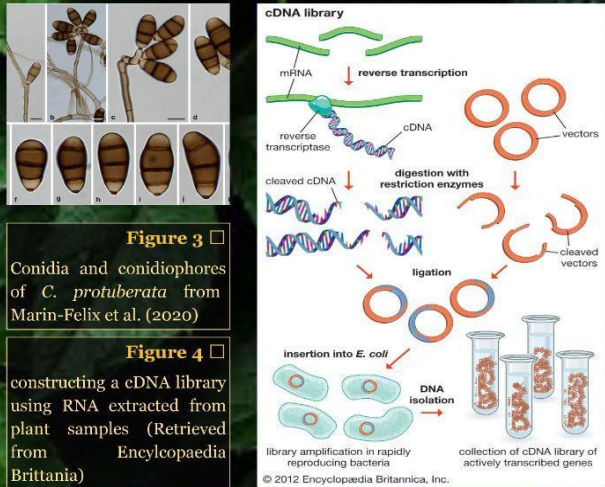
Figure 4  constructing a cDNA library using RNA extracted from plant samples (Retrieved from Encyclopaedia Britannica)


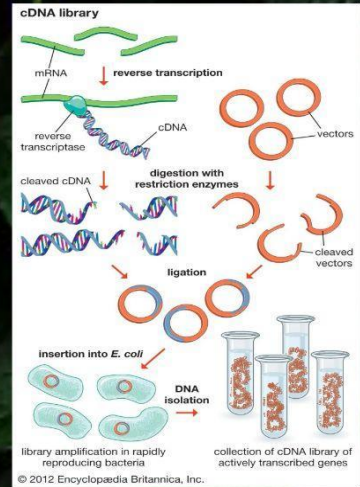
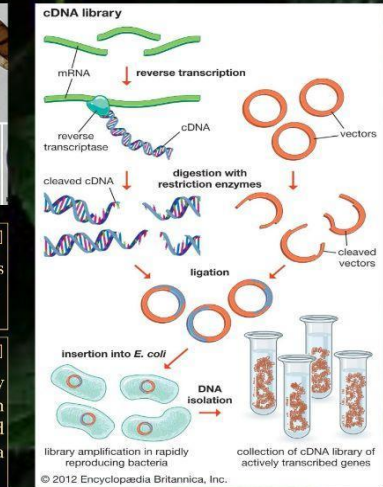
Figure 3  Conidia and conidiophores of *C. protuberata* from Marin-Felix et al. (2020)

Figure 4  constructing a cDNA library using RNA extracted from plant samples (Retrieved from Encyclopaedia Britannica)



DISCUSSION

Our proposed experiment should be able to quantify the changes in gene expression in endophyte-colonised monocot and dicot host plants under heat stress by comparing the transcriptomes via cDNA libraries. This will provide more insight into this unique 3 way symbiosis and could be applied in studying current food crops. The information learned could be useful for engineering of more heat-resistant crops, which is highly relevant given the trajectory of global warming

REFERENCES

[1] Youkang, R., Almeida, A. M., Yoo, S., Anbu, T., Hill, C., & Speck, C. D. (2003). A method for extracting high quality RNA from diverse plants for next generation sequencing and gene expression analysis. *Applications in Plant Sciences*, 1(6), 330-370. <https://doi.org/10.3732/app.1300070>

[2] Margriet Lutz M., Rodman, R. K., Rodriguez, E. J., & Rosenthal, M. J. (2007). A virus in a fungus in a plant: Three-way symbiosis required for thermal tolerance. *Science*, 305(5811), 511-515. <https://doi.org/10.1126/science.1139207>

[3] Robinson, R. K., Sheehan, K. E., Stout, R. G., Rodriguez, E. J., & Hovson, J. M. (2002). Thermotolerance generated by plant/fungal symbiosis. *Science*, 298(5596), 1381-1383. <https://doi.org/10.1126/science.1079625>

[4] Merry, M. R., Owerly, J., He, J., Tang, Y., & Rosenthal, M. J. (2002). Testing apart a three-way symbiosis: Transcriptome analysis of *Chlorostoma* protoplasts in response to viral infection and heat stress. *Biochemical and Biophysical Research Communications*, 40(2), 225-230. <https://doi.org/10.1006/bbrc.2000.07024>

[5] Sambrook, J. E. (2001). *Production of a subtracted cDNA library*. *Current Protocols in Molecular Biology*, 3(10). <https://doi.org/10.1002/0471422727.m0203005>

Novel method of identifying tumor status by using hyperpolarized substrates



Group 7 members: Kriti Shahu - Raven Foronda - Abdullah Jaddaa - Mustafin Nazim
Group facilitator: Nethmini Nirasha

Abstract

Cancer stays nearly the most actively discussed problem in Life Sciences. The discovery of imaging biomarkers that are early indicators of long-term treatment response in cancer should improve patient survival and accelerate the development of new drugs. One novel approach is connected with MRI imaging; this method is based on a phenomena of Nuclear Magnetic Resonance (i.e. NMR) which characterized by low signal-to-noise ratio and also only some highly abundant molecules could be visualized in this method such as fatty acids and water (1H NMR-signal). This situation could be improved by using hyperpolarized substrates, it was clear that the development of hyperpolarization techniques offers the possibility of gaining information about the real-time in vivo kinetics of the metabolic transformations. Today different approaches to hyperpolarization were developed. (Dr. Kirill V. Kovtunov et al, 2018).

Introduction

Hydrogenative-PHIP (h-PHIP) results from the addition of hydrogen, enriched in the para-isomer, to unsaturated substrates, catalyzed by organometallic complexes. Therefore, h-PHIP polarized molecules contain two protons, that derive from the pairwise addition of hydrogen to the unsaturated precursor. (Reineri et al, 2021)

Fig.1 demonstrates how hyperpolarized substrates could be prepared.

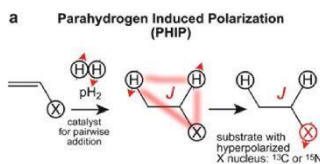


Fig. 1

Tumor cells are known to have different metabolic abnormalities that allow investigators to use it as a marker to distinguish between normal tissues and transformed cells. Cancer cells may reprogram their metabolic phenotypes to adapt to microenvironmental changes and the results of these reprogramming give a selective advantage to cancer cells under the unfavorable environment. It is typical for most dense tumors to show strong hypoxic microenvironment that enhances anaerobic oxidation and inhibits oxidative phosphorylation although in the presence of oxygen (Pseudohypoxia); hence increases the production of lactate, pyruvate and H+ through glycolysis in a process known as the "Warburg effect". (Chao Wang et al, 2021). In addition, the neighboring normal tissue may influence cancer metabolism. Note that tumours from different tissue origins driven by the same oncogene may have different metabolic patterns in accordance with the type of the cancer. (Gabriele Grassmann et al, 2021).

Objectives

Treatment response has traditionally been assessed by measuring changes in tumor size; increasingly, functional and molecular information is also being used to assess treatment response as these parameters often respond earlier than size measurements alone. For example, uptake of the glucose analog 18F-labeled 2-fluoro-2-deoxy-D-glucose (FDG) can be imaged noninvasively by PET and is now used as a marker of disease progression for some clinical indications. However, not all tumors demonstrate avid FDG uptake; therefore, the development of new biomarkers for detecting treatment response is required. We consider that hyperpolarized molecules would be one of the most effective and informative ways to identify a status of the tumor. We also hypothesized that due to appearance of a strong difference in microenvironment of tumor cells we can differentiate between tumor and necrotic tissue (Fig.2).

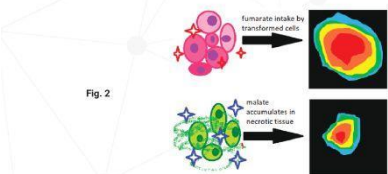


Fig. 2

We aim to provide a safe and effective method for new drugs screening and further in diagnosis. It could also be used to analyze the role of the target molecule in tumor metabolism. Therefore, in this study, we selected [1,4-13C] fumarate as a target bio-tracer. We also discussed the advantages and disadvantages of this treatment and possible side effects.

Materials and Methods

Hyperpolarized molecules of fumarate were obtained by PHIP method. Reaction was held in organic solvent and after that extraction followed into basic solution (NaOH:H2O); physiological pH was maintained in base solution. fMRI was held to visualize fumarate and malate distribution across tumor tissue.

Discussion

Why do we use fumarate?

Other metabolites of Krebs cycle could be used but only fumarate has shown selective accumulation and is easily can be hyperpolarized by both d-DNP and PHIP method. Using catalyst, the acetylene dicarboxylate precursor readily forms maleate, i.e., the cis-isomer of the butenedioic acid. Since maleate is a toxic compound, in the context of PHIP applications, only complete hydrogenation to succinate leads to a useful metabolite (Ripka et al, 2018).

Fumarate (trans-butenedioic acid) is a metabolite that cells convert into malate or succinate. The use of PHIP hyperpolarized fumarate to report on fumarase activity was the subject of intense scrutiny. That enzyme is responsible for the interconversion of fumarate and malate and is localized exclusively within the cells cytoplasm and mitochondria. Fumarate enters the cells through the sodium dependent dicarboxylate acid transporters and the fumarate-malate metabolic transformation is observed.

It was shown, recently, that fumarate can be obtained from the pairwise hydrogenation of an acetylene dicarboxylate (ADC) precursor in water, using a ruthenium-based catalyst [RuCp*(MeCN)3]PF6 to achieve the necessary trans-hydrogenation, with a minor formation of the fully hydrogenated succinate product (Guthertz et al, 2018).



Fig.3 Reaction scheme showing the chemical addition of para-enriched hydrogen to an unsaturated [1-13C]acetylene dicarboxylate precursor to yield [1-13C]fumarate.

Source or para-hydrogen

A mixture or 50:50 mixture of ortho- and parahydrogen can be made in the laboratory by passing it over an iron(III) oxide catalyst at liquid nitrogen temperature 77 K or by storing hydrogen at 77 K for 2-3 hours in the presence of activated charcoal. In the absence of a catalyst, gas phase parahydrogen takes days to relax to normal hydrogen at room temperature while it takes hours to do so in organic solvents. Other optimization techniques are being developed now.

Malic acid accumulation

Malic acid accumulated in a region of necrosis due to emitted fumarase enzyme from damaged cells' mitochondrion. This information is approved and highly supported by Fig.4 and Fig.5. (Gallagher et al, 2009).

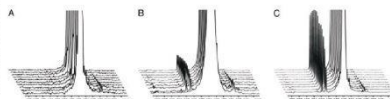


Fig.4 13C spectra acquired over a period of 1 min after injection of hyperpolarized [1,4-13C2] fumarate into suspensions of intact murine lymphoma cells (~5 x 10^7 cells) or lysed cells; these are representative spectra from the data shown in Fig. 2. For clarity, only every third spectrum is shown and each series has been scaled to the maximum fumarate signal. (A) Untreated cells. (B) Cells 16 h after etoposide treatment. (C) Lysed cells. The truncated signal from the hyperpolarized [1,4-13C2] fumarate is at 175.4 ppm, the signal from [1-13C]malate at ~181.6 ppm, and the signal from [4-13C]malate at ~180.6 ppm.

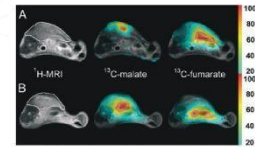


Fig.5 Representative transverse images from untreated (A) and etoposide-treated (B) mice with s.c.-implanted lymphoma tumors. The 1H image shows the anatomical location of the tumor, outlined in white. Adjacent to this are false-color CSIs superimposed on the 1H image, which demonstrate the spatial distribution of the total hyperpolarized 13C malate and 13C fumarate signals. The color scale indicates the relative signal intensity compared with the maximum intensity in each image. To reduce the effects of noise, voxels with signal intensities <20% of the maximum signal intensity were removed from the image. Although the images have been scaled to their respective maxima, the maximum malate signal intensity in each experiment is ~10-25% of the maximum fumarate signal.

Conclusion

Hyperpolarized substrates represent a convenient and non-invasive method of receiving an information of tumor status and a perspective method that could be applied in screening of new drugs. This novel method allows to investigate tumor response in a subtler way than most others. Finally, we admit that this new tool has its own disadvantages.

• Pros

- 1) High resolution of this method is demonstrated due to about 10-fold signal amplification.
- 2) Absolutely non-invasive, all the molecules used are isotopic analogues or even demonstrate no differences between biomolecules except spin indicating about 100% biocompatibility.
- 3) Great variety of applied substrates.
- 4) Importantly, this technique does not involve ionizing radiation and exploits endogenous molecules, some of which are already appeared into humans.

• Cons

- 1) Short longevity of applied substrates.
- 2) Need to use minor-isotopic-enriched reagents in synthesis of biomolecules or drugs precursors.

REFERENCES

- Dr. Kirill V. Kovtunov et al. Hyperpolarized NMR Spectroscopy: d-DNP, PHIP, and SABRE Techniques (2018) accessed from <https://doi.org/10.1002/asia.201800551>

- Reineri, F., Cavallari, E., Carrera, C. et al. Hydrogenative-PHIP polarized metabolites for biological studies. Magn Reson Mater Phys 34, 25-47 (2021) accessed from <https://doi.org/10.1007/s10334-020-00904-x>

- Chao Wang and Daya Luo. The metabolic adaptation mechanism of metastatic organotropism. (2021) 10:30. accessed from <https://doi.org/10.1186/s40164-021-00223-4>

- Grassmann, G.; Mondal, A.; Leithner, K. Flexibility and Adaptation of Cancer Cells in a Heterogeneous Metabolic Microenvironment. Int. J. Mol. Sci. 2021, 22, 1476 accessed from <https://doi.org/10.3390/ijms22031476>

- Ripka B, Eills J, Kour H, Leutzsch M, Levitt MH, Munnemann K (2018). Hyperpolarized fumarate via parahydrogen. Chem Comm, 54:12246-12249, accessed from <https://doi.org/10.1039/C8CC06636A>

- Guthertz A, Leutzsch M, Wolf LM, Gupta P, Rummelt SM, Goddard R, Farès C, Thiel W, Furstner A (2018). Half-sandwich ruthenium carbene complexes link trans-hydrogenation and gem-hydrogenation of internal alkynes. J. Am. Chem. Soc. 2018, 140, 8, 3156-3169 accessed from <https://doi.org/10.1021/jacs.8b00665>

- Ferdia A, Gallagher et al. Production of hyperpolarized [1,4-13C2]malate from [1,4-13C2]fumarate is a marker of cell necrosis and treatment response in tumors. 2009 Nov 24;106(47):19801-6 accessed from <https://doi.org/10.1073/pnas.0911447106>

Abstract

Preventing the metastasis is important in order to increase the life expectancy of breast cancer patients. Silencing the SNAP25 protein, one of the SNARE proteins, would inhibit migration of extracellular proteins and membrane fusion. Translation of SNAP25 could be inhibited by injecting double stranded RNA with the same sequence as mRNA transcript for SNAP25.

Introduction

Breast cancer is cancer that develops from breast tissues and it is the most common cancer among women in most countries. An estimated 2.3 million females were diagnosed with breast cancer in 2020, accounting for approximately 24.5% of all cancer cases worldwide. In stage IV breast cancer, also known as metastatic breast cancer, the cancer is spread to the other organs in the body including the lungs, liver, brain, and most commonly bone. Unless controlled, it is highly likely to cause severe complications and finally lead to death. The study explores controlling cell migration that is crucial in metastasis by silencing integrins through RNA interference (RNAi), which has presented high degrees of efficiency and specificity; hence, metastasis can be prevented, increasing the life expectancy of the patients.

Methodology

Integrin count at the cell membrane is reduced by injecting siRNA, that has the same nucleotide sequence as an mRNA of SNAP25 protein. Cells would recognize it as a viral RNA and, therefore, start inhibiting mRNA with exact same sequence, leading to reduced concentration of the protein. SNAP25 is crucial for cell migration, since it is one of the SNARE proteins and plays a huge role in membrane fusion (Fig. 4).

Membrane fusion is essential for Cancer metastasis. Silencing or inhibiting any of the SNARE proteins would disrupt four-helix bundle formation (Fig.4) and membrane fusion would no longer occur, therefore, because of the essential integrins no longer being present at the cell front, movement of the tumor cells decrease, significantly reducing the Metastasis of the cancer.

Why SNAP25?

While there were variety of proteins to choose from, we decided on SNAP25 and here is why: Even though, delivery method of the siRNA is a tissue specific injection and, therefore, chances of it spreading in blood and even bypassing the liver unharmed are low, it is imperative to ensure, that non-cancerous cells would not be harmed by this method, especially when patient already has immunodeficiency caused by other treatments, like chemotherapy. NCBI has tested and published the concentration of SNARE proteins in different tissues of healthy patients[7]. While others are somewhat equally distributed, SNAP25 is mainly only found in Brain (RPKM = 400-500) and only insignificant amounts of it are present in other organs (RPKM = 1-3), meanwhile SNAP25 is one of the most recognized overproduced proteins in breast cancer, along with VAMP3, VAMP4, SNAP23, SYNTAXINI, etc.[4, 8]. Accordingly, siRNA will disrupt membrane fusion in breast cancer cells, but won't be harmful to others, in case it somehow gets in.

Silencing with siRNA

In general, there are several ways of silencing, inhibiting proteins, such as injecting antibodies. However, the study utilized siRNA for couple of reasons:

- 1) Different kinds of cancer use Different kinds of SNARE proteins and developing or finding antibodies for each is more difficult, than identifying the nucleotide sequence of mRNA already found in the cell, making this method applicable to wider range of diseases;
- 2) Stopping the translation of the protein, rather than inhibiting it after its production is better in terms of limiting the energy usage, especially in tumor cells, in which ATP production is a problem on its own, since it fully relies on glycolysis and lactic acid fermentation, even in aerobic conditions.

Silencing with siRNA is a well researched method which exploits cell defense against viruses. Upon entering the cell the siRNA is cleaved by dicer (an enzyme that cleaves RNA) and loaded onto Ago-2 Argonaute. The protein-RNA complex would bind to the mRNA transcripts for the SNAP-25 protein, inhibiting the translation (Fig. 5).

Preventing Breast Cancer Metastasis by Silencing the SNAP25 Protein

Objectives

- Introducing a successful method to prevent breast cancer metastasis via RNA interference.
- Choosing the breast cancer specific SNARE protein.
- Constructing siRNA with already known nucleotide sequence of mRNA of SNAP25 protein.
- Transferring siRNA using tissue specific injection, to avoid spreading it in blood.
- Silencing SNARE protein with siRNA and as a result, disrupting membrane fusion.
- Reducing membrane fusion to inhibit cell migration and stop breast cancer metastasis.

Fig. 1 : Stimulation of VEGFR1 expression in normal microvascular endothelial cells

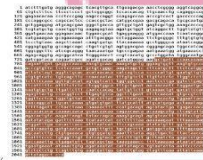
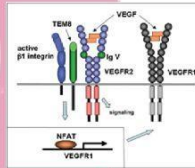


Fig. 2 : Sequence used to manufacture siRNA (derived from mRNA of SNAP25)

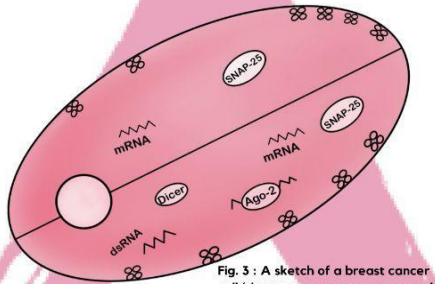


Fig. 3 : A sketch of a breast cancer cell (the top part represents normal cell, the bottom a transfected one)

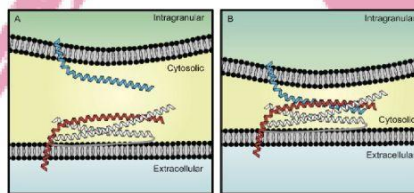


Fig. 4 : Four helix bundle formation. Proteins: Blue - VAMP, Red - Syntaxin, White(x2) - SNAPs

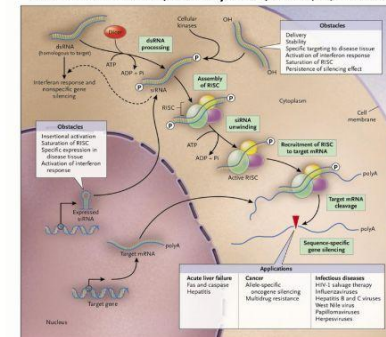


Fig. 5 : RNA interference pathway

The production of siRNA

siRNA would be produced in vitro. The cDNA transcript for the SNAP25 protein (Fig.2) would be ligated into a vector for bacteriophage ϕ 6 and put into bacteria which would produce the two strands separately and the transcripts would later on join.

Delivery

siRNA would be conjugated to a VEGFR antibody and would be injected into the cancerous tissue. VEGFR is a vascular endothelial growth factor receptor. Upon ligand binding it would be endocytosed into the cell and the resulting vesicle would be degraded. The siRNA would be released into the cytosol

Discussion

To prove that our idea was reasonable and somewhat possible we searched for experiments regarding these topics. We were able to find an article named: "Silencing of VAMP3 inhibits cell migration and integrin-mediated adhesion"[3], in which they talk about silencing VAMP3 protein of pancreatic cancer cells in Vitro using siRNA to slow down Membrane fusion and, therefore, disrupt the regulation of B1 integrin on cell surface. Experiment was a huge success, here is a small excerpt: "Indeed, silencing of VAMP3 effectively reduced the amount of B1 at the cell surface. In contrast, immunoblotting analysis showed that the levels of total cellular B1 were not altered in the VAMP3 knockdown cells. The reduction of cell surface B1 but not total cellular B1 suggested, that VAMP3 knockdown disrupted the trafficking of B1 integrin to the plasma membrane. The decreased motility of VAMP3 knockdown cells probably resulted from reduced delivery of B1 integrin to the cell surface."

Conclusion

In conclusion, we think, that silencing the SNAP25 protein is an option to stop breast cancer metastasis without harming other cells and could be used along with other treatments. Tissue specificity of SNAP25 (almost only present in brain) gives us the safe protein to target and it being overproduced during breast cancer makes it effective against tumor cells. Stopping metastasis would prevent a disease from spreading into other organs and will significantly increase the life expectancy of stage IV cancer patients. We decided to inhibit the production of SNAP25 to specifically target the most common cancer among women, but methodology of the treatment could be used against other illnesses after slight alterations. For any chosen protein, nucleotide sequence of the siRNA can be gathered from mRNA already found in the cell. Selection of receptors on the membrane of the tumor cell should also be taken into consideration.

References

- [1] Aalto AP, Sarin LP, van Dijk AA, Saarna M, Poranen MM, Arumäe U, Bamford DH. Large-scale production of dsRNA and siRNA pools for RNA interference utilizing bacteriophage ϕ 6 RNA-dependent RNA polymerase. RNA. 2007 Mar;13(3):422-9. doi: 10.1261/ma.348307. Epub 2007 Jan 19. PMID: 17237359; PMCID: PMC1800515.
- [2] Meister G, Tuschli T. Mechanisms of gene silencing by double-stranded RNA. Nature. 2004 Sep 16;431(7053):343-9. doi: 10.1038/nature02873. PMID: 15372041
- [3] Luftman, K., Hasan, N., Day, P., Hardee, D., & Hu, C. (2009). Silencing of VAMP inhibits cell migration and integrin-mediated adhesion. *Biochemical and Biophysical Research Communications*, 380(1), 65–70. doi:10.1016/j.bbrc.2009.01.036
- [4] Targeting SNARE-Mediated Vesicle Transport to Block Invasiveness of Cancer Cell Invasion Geyra Gorshain, Olivia Grafinger and Marc G. Cappolino
- [5] Mansoori B, Sandooghian Shotorbani S, Baradaran B. RNA interference and its role in cancer therapy. *Adv Pharm Bull*. 2014;4(4):313-321. doi:10.5681/apb.2014.046
- [6] Lei S, Zheng R, Zhang S, Wang S, Chen R, Sun K, Zeng H, Zhou J, Wei W. Global patterns of breast cancer incidence and mortality: A population-based cancer registry data analysis from 2000 to 2020. *Cancer Commun (Lond)*. 2021 Nov;4(11):1183-1194. doi: 10.1002/cac.2.12207. Epub 2021 Aug 16. PMID: 34399040; PMCID: PMC8262656.
- [7] National Center for Biotechnology Information. (2022, May 22). SNAP25 synaptosome associated protein 25 [Homo sapiens (human)]. NCBI. <https://www.ncbi.nlm.nih.gov/gen?Db=gene&Cmd=DetailsSearch&Term=616>
- [8] Protein Atlas. (n.d.). Expression of SNAP25 in cancer - Summary - The Human Protein Atlas. The Human Protein Atlas. <https://www.proteinatlas.org/ENSG00000132839-SNAP25/pathology>
- [9] Gorshain, G., Grafinger, O., & Cappolino, M. G. (2021). Targeting SNARE-Mediated Vesicle Transport to Block Invasiveness of Cancer Cell Invasion. *Frontiers in Oncology*, 11. <https://doi.org/10.3389/fonc.2021.679955>

Authors

Poster made by: Group 8
Ema Sulajaj
Gjergj Nebulishvili
Proveen Thennakoon
Lowand Bayram
Facilitator:
Jeremy Ace Ng



MESENCHYMAL STEM CELL-DERIVED EXOSOMES THERAPEUTIC ROLE IN DIABETIC CARDIOMYOPATHY

Moza Aldhanhani



Jagienka Mądrzak



Bobur Poudel



Urban Bauk



Facilitator: Jovana Stojcheska (North Macedonia)



ABSTRACT

Diabetes is a health condition that affects sugar levels in your blood, thus causing numerous problems in the cardiovascular system. Exosomes are showing promise as a method of treating those problems. Our project intends to study their effectiveness using mice. We will isolate exosomes produced by mesenchymal stem cells using the most effective method developed, however more effective ones will no doubt be developed in the future. Future research would need to be done to evaluate applicability of our results to humans and the exact contents of those exosomes.

OBJECTIVES

- Define exosomes including mesenchymal stem cell-derived exosomes and their function.
- Explain how MSC-derived exosomes can be isolated, stored and preserved.
- Demonstrate how exosomes can be used in diabetic cardiomyopathy treatment.
- Assess methods/mechanisms involved in the treatment of diabetic cardiomyopathy.
- Discuss how further research can be applied to improve the use of exosomes in treating cardiovascular complications of diabetes.

INTRODUCTION

All cells, prokaryotes and eukaryotes, release extracellular vesicles (EVs) as part of their normal physiology and during acquired abnormalities. Exosomes are EVs with a size range of ~40 to 160 nm in diameter with an endosomal origin. Depending on the cell of origin, exosomes can contain many constituents of a cell, such as a fluid lipid bilayer, surface proteins/receptors, mRNAs, microRNA (miRNA), specific set of proteins, transcription factors, and other substances. Interestingly, exosomes released into the circulation and bodily fluids are the major mediators of cell-cell communications, which are involved in the regulation of various biological processes of their target cells via regulation of certain gene expressions.

Mesenchymal stem cells (MSCs) constitute a heterogeneous subset of stromal regenerative cells and could be harvested easily from several types of adult tissues. MSCs are considered a promising therapy tool in cardiovascular diseases (CVDs) as numerous preclinical studies of ischemic and nonischemic cardiomyopathy employing MSC-based therapy have demonstrated that the properties of reducing fibrosis, stimulating angiogenesis, and cardiomyogenesis have led to improvements in the structure and function of remodeled ventricles. However the low engraftment, immune rejection and tumorigenic potential limit the clinical application of stem cell transplantation therapy. Increasing evidence suggested that exosomes generated from stem cells exerted similarly protective and reparative properties with cellular counterparts of stem cell transplantation in repairing therapies.

Heart failure occurring in patients with diabetes and without hypertension and coronary artery disease, also referred to as diabetic cardiomyopathy, is a common complication of diabetes. Numerous mediators/factors (e.g., oxidative stress, cardiac inflammation, insufficient myocardial angiogenesis, lipid accumulation, cardiac fibrosis, and cell death) have been identified as its contributors. In our study we want to investigate the potential therapeutic effects of MSC-derived exosomes in preventing diabetic cardiomyopathy in STZ-induced diabetes mice model. Refer to Figure 1.

DISCUSSION

Diabetes is a chronic condition that is always affecting a noticeable chunk of the world population. The importance of this research lies in providing a new way to mitigate the effects this condition has on the cardiovascular system. Exosome based therapy has the potential to provide the same therapeutic effects of cell-based therapy without some of its immunological and tumorigenic complications.

However, one major barrier to the usage of exosome therapy will certainly be the production and isolation of said exosomes. The exact mechanism involved in the therapeutic effects of MSC-derived exosomes is beyond the scope of this project and can be explored by future research. The most beneficial cell culture environment for the production of the most effective exosomes by MSCs is also yet to be revealed. Perhaps co-culturing of MSCs with cardiomyocytes is one of the most promising approaches that will improve the efficacy of exosomes. There are different methods of exosome isolation, each with its own strengths and weaknesses, therefore we chose the one that fits our needs best. The field of exosome isolation has made remarkable progress in past years so it is safe to say that this will become less of a problem in the future, whether by invention of completely new methods of isolation or combination of already known ones. Our research proposal contains certain limitations. One of which is our usage of size-based isolation methods for exosomes. Due to heterogeneity of exosomes no existing isolation method yields a perfect solution and there are bound to be certain contaminants within the solution. Similarly, we can't differentiate between different types of exosomes, so our MSC-derived exosomes could be contaminated by other types of exosomes.

METHODS

The required mesenchymal stem cells (MSCs) can be isolated from the bone marrow and inoculated into the hollow fiber bioreactor for 3D culture. Instead of preparing the culture in 2D flasks, using the 3D has increased exosome production and more effectiveness. Exosomes are heterogeneous in size, content, function and source making isolation difficult. Size-exclusion chromatography (SEC) has been described as the best method for separating exosomes from most proteins, simultaneously recovering morphologically and functionally intact exosomes from plasma¹⁰.

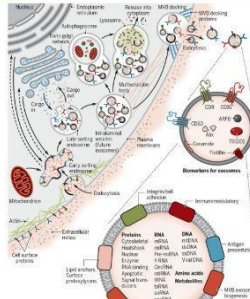


Figure 1. Biogenesis and identification of exosomes

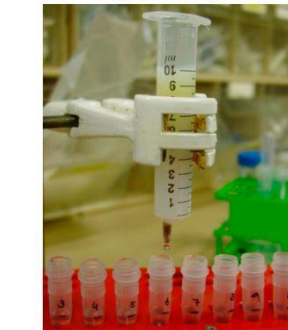
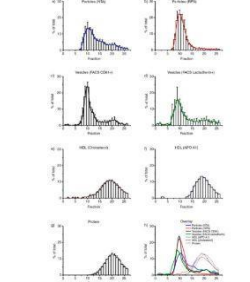


Figure 2. Size-exclusion Chromatography by Boing and colleagues¹²

CONCLUSION

To expand and improve our methods of treatment for diabetes-induced cardiac complications we are proposing a study on the effectiveness of MSC-derived exosomes in treating and mitigating diabetic cardiomyopathy. We intend to use mice for our research because of their biological similarity to us and ease of use in laboratories. The effect a treatment has on mice is often predictive of the effect it will have on humans, but not always. To see whether our results are applicable, future research would need to explore the response of the human body to MSC-derived exosomes. If that research confirms their effectiveness on humans we will have another powerful tool in combating cardiovascular consequences of diabetes worldwide.

Exosomal preparations from SEC methodology have low levels of contaminants and co-precipitates, leading to a relatively homogenous final exosome isolation.

The exosomes investigated in the study can be acquired by SEC by performing as described by Boing and colleagues. Succinctly, we can stack 12 mL of Sepharose CL-2B (Sigma Aldrich, St. Louis, MO, USA) in a 20-mL syringe (BD Plasticpak™, San Jose, CA) and we can wash and equilibrate with PBS (Oxoid). Then, we load two mL of plasma onto the column and start fraction collection (0.5 mL per fraction and a total of 20 fractions were collected) immediately using PBS as an elution buffer.

To investigate diabetic cardiomyopathy, we will use the STZ-Induced Diabetic Model. Mice (6-8 weeks old, FVB/N) will be prepared to induce type 1 diabetes in a mouse model by daily intraperitoneal injection of STZ (Sigma-Aldrich) at a dose of 50 µg/g dissolved in a citrate buffer (0.1 mol/L Na citrate, pH 4.5) for 5 days.

Throughout the 3 month study period, starting from 9 days after the last STZ injection, doses of 40 µg of MSC-derived exosomes will be administered to mice via intravenous injection at 7 day intervals, and the control group will be injected with an exosome-free buffer, following the same administration pattern.

After 3 months we will perform M-mode echocardiography to measure cardiac contractile parameters in vivo. Next we will measure the isolated heart function using the Langendorff perfusion apparatus to investigate rates of contraction and relaxation. Given that chronic hyperglycemia can result in adverse cardiac remodeling such as cardiomyocyte hypertrophy, apoptosis, fibrosis, and reductions in microvessel densities, which contribute to ventricular dysfunction, we will perform histological analysis of mice subjected to exosomal injections and the control group. We will measure the extent of myocardial apoptosis, fibrosis (using collagen I/III levels as markers), cardiomyocytes size and the number of microvessels. Refer to Figure 2.

EXPECTED RESULTS

A recent study showed that administration of MSC-derived exosomes in an I/R mouse model increased the ATP level, reduced oxidative stress, and improved cardiomyocyte survival. This indicates that the intravenous transplantation of MSC-derived exosomes might have an anti-apoptotic effect on cardiomyocytes in STZ-treated mice through a miRNA-mediated mechanism. It is believed that they should also replicate the pro-angiogenic effect of their parent cells, as well as act as anti-fibrotic factors thanks to miRNA that regulates the deposition of extracellular matrix proteins. We expect the collected data will indicate that MSC-derived exosomes could prevent diabetes-caused cardiac injury (i.e., hypertrophy, apoptosis, fibrosis, and microvascular rarefaction) in STZ-treated mice model, thereby improving myocardial contractile function in comparison with the control group.

References:

1. Zhang, Y., et al. The origin, function, and therapeutic application of exosomes. *Frontiers in Cell and Developmental Biology* 2021 | 9:632737.
2. Wang, W., et al. Exosome-derived miRNAs and their potential role in cardiovascular disease. *Journal of Cellular Biochemistry* 2021 | 122:1138-1146.
3. Kaur, H., et al. Exosomes: A Novel Therapeutic Approach for Diabetes Mellitus. *Journal of Cellular Biochemistry* 2021 | 122:1138-1146.
4. Zhang, Y., et al. Exosomes: A Novel Therapeutic Approach for Diabetes Mellitus. *Journal of Cellular Biochemistry* 2021 | 122:1138-1146.
5. Zhang, Y., et al. Exosomes: A Novel Therapeutic Approach for Diabetes Mellitus. *Journal of Cellular Biochemistry* 2021 | 122:1138-1146.
6. Zhang, Y., et al. Exosomes: A Novel Therapeutic Approach for Diabetes Mellitus. *Journal of Cellular Biochemistry* 2021 | 122:1138-1146.
7. Zhang, Y., et al. Exosomes: A Novel Therapeutic Approach for Diabetes Mellitus. *Journal of Cellular Biochemistry* 2021 | 122:1138-1146.
8. Zhang, Y., et al. Exosomes: A Novel Therapeutic Approach for Diabetes Mellitus. *Journal of Cellular Biochemistry* 2021 | 122:1138-1146.
9. Zhang, Y., et al. Exosomes: A Novel Therapeutic Approach for Diabetes Mellitus. *Journal of Cellular Biochemistry* 2021 | 122:1138-1146.
10. Zhang, Y., et al. Exosomes: A Novel Therapeutic Approach for Diabetes Mellitus. *Journal of Cellular Biochemistry* 2021 | 122:1138-1146.
11. Zhang, Y., et al. Exosomes: A Novel Therapeutic Approach for Diabetes Mellitus. *Journal of Cellular Biochemistry* 2021 | 122:1138-1146.
12. Zhang, Y., et al. Exosomes: A Novel Therapeutic Approach for Diabetes Mellitus. *Journal of Cellular Biochemistry* 2021 | 122:1138-1146.

CONTROLLED EXPRESSION OF TELOMERASE

BY: MILA DIMITROVSKA, ADNAN RIHAWI, YERASSYL TEMIRBEKOV, KARTHIK PRAVIN RAMANCHANDRAN

Facilitator : Farrel Alfaza

TELOMEROPATHY OR TELOMERE BIOLOGY DISORDER (TBD)

- There are two types of telomeropathies: secondary and primary.
- Primary telomeropathies involve mutations in main telomere-maintenance genes.
 - Secondary telomeropathies usually involve mutations and defects in DNA repair machinery. DNA damage in the region of telomerases is not repaired correctly and they may become shorter.

TELOMERE-MAINTENANCE AGENTS:

- TRF1 and TRF2 recognize duplex TTAGGG repeats
- POT1 recognizes single stranded TTAGGG overhangs
- TIN2, TPP1, and RAP1 interconnect shelterin proteins
- Telomeric repeat-containing RNA (TERRA) - telomerase regulation
- Telomerase: Telomerase reverse transcriptase (TERT) and telomerase RNA component
- Poly(A)-specific ribonuclease (PARN)
- Regulator of telomere elongation helicase 1 (RTEL1)
- Telomere maintenance component 1 (CTC1)
- Telomerase Cajal body protein 1 (TCAB1)

Mutations in any of these components lead to shortened telomeres (accelerated shortening), or short telomeres can be inherited.

SYMPTOMS:

- Cytopenia
- BMF
- MDS/AML
- No immune response
- Skin cancer
- Glaucoma/cataract
- Lacrimal duct stenosis
- Head and neck cancer
- Interstitial lung disease
- Liver cirrhosis
- Avascular necrosis
- Osteoporosis

Current TBD treatments are aimed to reduce symptoms and increase life quality of patient, but ultimately all of them are not dealing with main problem - short telomeres.

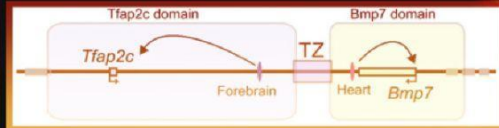
If telomerase itself is not affected by mutation and TBD is caused by another telomere-maintenance proteins mutation, it can be possible to maintain normal telomere length by increasing the expression levels of telomerase.

Constitutively high expression levels of telomerase gene can be also dangerous to the organisms since short telomeres play role in cancer prevention and long telomeres are usually associated with high cancer risk.

In order to avoid this kind of complications in the treatment we propose drug-controlled enhancer-insulator system that can be inserted upstream the telomerase gene (TERT and TERC). TERC is transcribed by RNA pol 2 and has its own promoter region (unlike other ncRNAs).

METHOD: CONTROLLED SILENCER

Synthetic Topological Insulator with TetO for Chromatin-engineering (STITCH) - is a DNA region that can inhibit interaction of gene and its enhancer when inserted between them. Main part of insulator model was taken from mouse *Tfap2c-Bmp7* locus with following structure:

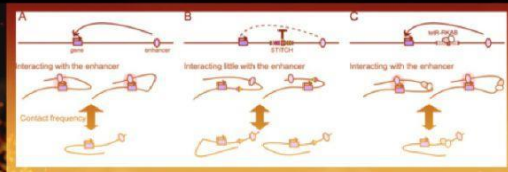


Where TZ separates actions of two enhancers: forebrain and heart. TZ itself consists of directed CTCF-binding sites (CTCF - CCCTC-binding factor - zinc finger protein).

This silencer shows decrease in expression when inserted between human promoter and enhancers, showed on the example of MYC gene.

In order to make it drug-controlled tetO with tetR-KRAB systems was used. tetO is tetracycline operator inserted in silencer region. tetR binds to it when tetracycline (or its analogs like doxycycline - DOX). tetR-KRAB is fused gene.

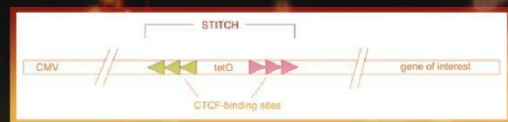
KRAB is able to induce heterochromatin formation around tetO and turn silencer off - increasing expression of controlled gene. Overall expression is sensitive to tetracycline or doxycycline.



tetR-KRAB was inserted via piggyBac transposon.

We can insert strong enhancer - CMV - human cytomegalovirus enhancer - natural mammalian promoter with high transcriptional activity. Boshart M, Weber F, Jahn O, Dorech H, Sief K, Fleckenstein B, Schaffner W, 1985: A Very strong enhancer is located upstream of an immediate early gene of human cytomegalovirus. Cell 41:521-530. DOI: [https://doi.org/10.1016/S0092-8674\(85\)80025-8](https://doi.org/10.1016/S0092-8674(85)80025-8), PMID: 2985280

Resulting structure:



Abstract

Lactose intolerance occurs in two-thirds of adult humans and can cause bloating, diarrhoea and abdominal cramps due to an inability to digest lactose. It is characterised by a fall in expression of lactase-phlorizin hydrolase (LPH), an enzyme that breaks down lactose, after weaning in infants. The primary treatment for lactose intolerance involves lactase pills before meals, which are not always accessible or affordable. Studies suggest that age-based methylation of the LCT gene (encoding for LPH) may be responsible for the fall in LPH production [1]. DNA methylation at CpG sites is known to decrease expression of genes by preventing binding of transcription factors and thus expression of genes.

Objective: We propose the use of CRISPR/dCas9-mediated demethylation of LCT to restore their expression, allowing for LPH production in adults and increased tolerance to lactose.

Introduction

CRISPR/dCas9 Demethylation

Normally, Cas9 acts as an endonuclease and creates double-stranded breaks in DNA. Cas9 selects its targets by binding to a guide RNA (gRNA) complementary to a segment of genomic DNA upstream of a PAM sequence (NGG). The CRISPR/dCas9 system uses a mutated form of Cas9 that is unable to cleave DNA but can still bind to its gRNA target.

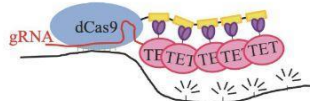


Fig. 1 Multiple TET1 domains are directed to the appropriate gene by dCas9, resulting in demethylation [2].

dCas9 is then fused to the SunTag system, which acts as a scaffold to attach several demethylation domains from the TET1 protein. Thus, the dCas9 system (as described in [2]) is able to target a specific region of DNA and perform localised demethylation using the TET1 domains.

Methodology - Experimental Design

Mouse model of adult-onset lactose intolerance

Mice, like other mammals, display lactose intolerance as adults. A comparison of epigenetic markers between C57BL/6Ncr1 mice and humans found that both had age-based increases in methylation at intron 2 of LCT [1]. LCT intron 2 is evolutionarily conserved and its deletion lowered LPH expression significantly, suggesting that it plays an important regulatory role [1] and is a suitable target.

Selecting appropriate gRNAs

Using the methylation data from [1], we can apply available programs like ChopChop [3] to design suitable gRNAs. Factors to consider include proximity to the methylation site and off-target binding.

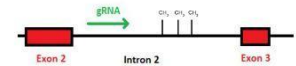


Fig. 2 gRNA for intron 2 of LCT gene will be used for targeted demethylation

Which cells do we target?

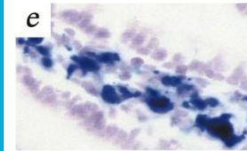


Fig. 3 Lamina propria cells expressing lactase with long term effects [4].

LPH is normally produced by enterocytes in the brush border of the intestine, which have a very short turnover time. Epigenetic modification of these short-lived cells would hence be unlikely to have a lasting impact on LPH production. Instead, we target long-lived intestinal cells like those in the lamina propria, where upregulation of LPH production can have a lasting impact [3].

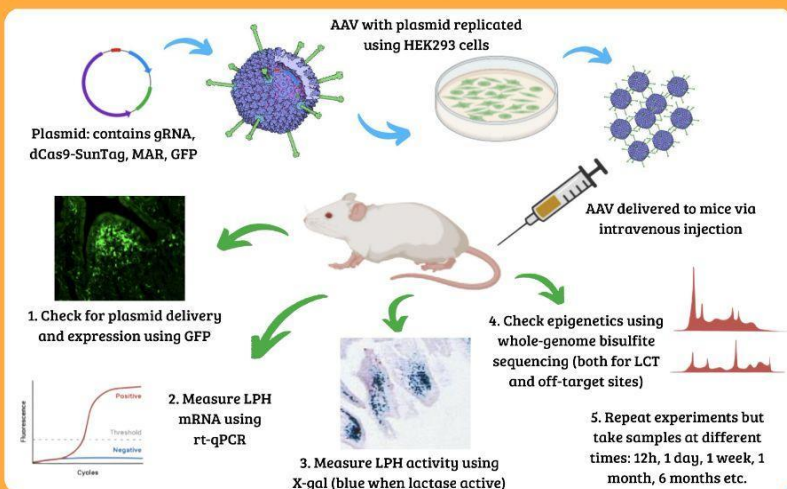
Preventing remethylation by Dnmt proteins

LCT could be remethylated by Dnmt proteins (similar to [5]), which maintain DNA methylation patterns. Hence, long-term expression of our CRISPR/dCas9 system is needed to maintain the unmethylated status of LCT. We thus introduce our system to the target cells in the form of a plasmid, which has a constitutive promoter for the gRNA and CRISPR/dCas9 system as well as a matrix-associated region that allows for long-term retention of the plasmid and expression of the dCas9 system.

Adeno-associated Viruses

Adeno-associated viruses (AAV) are attractive vectors for gene transfer because they lack viral genes, do not replicate after delivering their payload and can transduce most cells [6]. We selected type 2 AAVs as they were shown to be the most effective at delivering genes to intestinal cells. [7] AAVs can be produced using the 'triple transfection' technique, where the desired plasmid is inserted into an AAV along with two other plasmids that allow for independent replication. The viruses are replicated in HEK293 cells and extracted for use. [8]

Methodology - Experiments



Conclusion

In conclusion, our experiment assesses the viability of epigenetic modification as a gene therapy for lactose intolerance in mouse models. Given that our gRNA targets a well-conserved region between mice and humans, this method can easily be adapted for human use, offering a long-term solution to lactose intolerance.

References

- [1] Labrie, V., Buake, O. J., Oh, E., Jevremovic, R., Prok, C., Gostinas, O., Molecka, A., Petreiti, R., Zerbib, A., Adamonis, K., Jankauska, E., Koceravicius, K., Gerdavicius, J., Neir, A., Zhang, A., Zerbib, S., Oh, C., Shihang, Y., Kapustin, L., Petrovic, A. (2018). Lactase non-persistence is directed by DNA variation-dependent epigenetic aging. *Nat Struct Mol Biol* (2018). <https://www.nature.com/articles/s41594-018-0117-1>
- [2] Morris, S., Hu, T. & Henkel, I. (2018). Editing of DNA Methylation Using dCas9-Pegged Repet and ssPv-TET1 Catalytic Domain Fusion. *Methods Mol Biol* (2018). <https://pubmed.ncbi.nlm.nih.gov/29261349/>
- [3] Lebars, K., Monogon, T. G., Kruse, M., Torres-Cervantes, Y. M., Tjeldnes, H., & Volen, E. *CHOPCHOP v3: expanding the CRISPR web toolbox beyond genome editing*. *Nucleic Acids Research* (2019).
- [4] Dairing M. J., Xu R., Young D., Kaplan M. D., Sherwin R. S. & Leone P. (1998). Peroral gene therapy of lactose intolerance using an adeno-associated virus vector. *Nature Medicine* (1998). <https://pubmed.ncbi.nlm.nih.gov/971716/>
- [5] Hashimoto, K., Yano, K., Kawabuchi, K., Tsujimoto, K., Hamaguchi, H., Tamaki, T., Nagata, Y., Nakano, H., Hara, S., Honda, I., Yamada, T., & Okawa, Y. (2020). Targeted DNA demethylation of the P53 promoter by CRISPR/dCas9-mediated epigenome editing. *Scientific Reports* (2020). <https://www.nature.com/articles/s41598-020-61035-6/>
- [6] Moonshen, P. E. & Scammiari, R. J. (2000). Adeno-associated virus vectors for gene therapy: more pros than cons? *Mol Med Today* (2000).
- [7] Palgok S., Moh C., Porvankar S., Herlihy J. D., Campbell-Thompson M., Byrne R. J. & Valentine J. K. (2008). Gene delivery to intestinal epithelial cells in vivo with recombinant adeno-associated virus types 1, 2 and 5. *Dis Dis Sci* (2008).
- [8] Nature Research. *Vigore Biosciences*. (n.d.) Three is the magic number in gene therapy production. <https://www.nature.com/articles/616273-018-0007-6>



Design of a Low-Cost Point-of-Care Test Kit for COVID-19 Cytokine Storm Susceptibility

Topic: Biomedicine

Group 12:
Koo Min Seo
Kim Joo Chan
Chioma Blessing Obidigbo

Group facilitator: Robert Yeghikyan

Abstract

Since the outbreak of the SARS-CoV-2 virus in December 2019 from Wuhan, China, it has since become a global health threat whose pathological effects are still being explored. Infection in COVID-19 patients has been linked to "cytokine storms", an event whereby the overstimulated immune system results in excessive production of pro-inflammatory cytokines. This can lead to damaging effects such as acute respiratory distress syndrome (ARDS), which results in high mortality. In our project, we propose the design of an affordable and accurate test kit using an SNP-LAMP assay to detect COVID-19 cytokine susceptibility to pre-empt the onset of cytokine storms by seeking immediate medical attention upon infection.

Introduction

Cytokine storms are a physiological reaction in which the innate immune system causes an uncontrolled and excessive release of pro-inflammatory signaling molecules called cytokines. The rate of mortality from cytokine storms is high, making up a large proportion of 6.34 million COVID-19 deaths to date. During the outbreak of SARS-CoV-1 and MERS-CoV, cytokine storms were identified as a key cause for lung and organ failure.

The provision of point-of-care test kits that can be used by untrained individuals would encourage timely administration of medical treatment and can act as a breakthrough in reducing mortality and improving medical response.

Genetic background of cytokine storm susceptibility

Although the mechanism leading to cytokine storm remains unknown, considering the interferon signaling pathway, variants in cytokine genes such as IL1B, IL1R1, IL1RN, IL6, IL17A, FCGR2A, and TNF could be related to cytokine storms.

Objectives

To design a safe, affordable and accessible point-of-care test kit to test for susceptibility to cytokine storm after COVID-19 infection



Methods

1

Design Principles

- Individuals' COVID-19 cytokine storm susceptibility relies heavily on several SNP variations. The Test Kit is designed to detect six (or more) of the most relevant SNPs so that individuals can predict their COVID-19 Susceptibility at home.
- The epithelial cells of the mouth are removed with a swab and placed in a liquid bottle (tube) to extract DNA. After extraction, DNA is added to the reaction solution by dropping one drop of the DNA solution into each tube.
- When the reaction mixture is put in hot water, DNA amplification occurs, and the possibility of cytokine storms can be predicted depending on the number of tubes in which fluorescence is observed after the reaction is completed.

2

SNP-LAMP

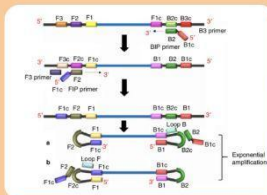


Figure. Loop-Mediated Isothermal Amplification (LAMP) mechanism

In LAMP, a strand-displacing DNA polymerase initiates the synthesis and loop structures form to facilitate subsequent rounds of amplification

SNP-LAMP

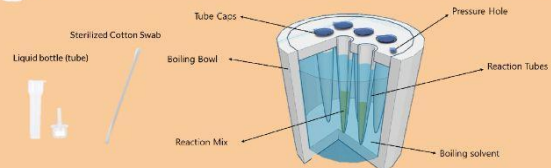
- Used to detect single nucleotide polymorphisms (SNP)
- Mutation point designed to be at 3' end corresponding to the B2 primer
- Extra mismatched nucleotide enhances specificity to every target nucleotide site

Metal indicator **calcein** changes color as $[Mg^{2+}]$ decreases during progression of amplification



3

Test Kit Design



1. The Reaction Mix contains an appropriate amount of the LAMP primer, reaction buffer and reaction enzymes.
2. The liquid/vaporized boiling solvent isn't toxic. It diffuses through the Pressure hole.
3. The boiling bowl transmits the heat of boiling water (close to 100 degrees) to the boiling solvent, which has a boiling temperature of 65 degrees Celcius. This maintains the temperature of Reaction Tubes at 65 degrees Celcius, the optimal condition for LAMP reaction.

Discussion

1

Advantages to Alternatives

~60 min
VS PCR 2-4 hours



Negligible equipment cost
VS PCR USD50k



Accurate &
reliable



2

Importance of Testing for Susceptibility

Cytokine storm is a leading cause of death due to COVID-19, as it often leads to multiple organ dysfunction syndrome (MODS).

Early identification of cytokine storm susceptibility enables patients to seek timely treatment such as immunomodulators, corticosteroids and cytokine antagonists to prevent progression and reduce mortality.

Conclusion

Predicting cytokine storms earlier in the disease course can help with timely and effective administration of treatment. Our project takes advantage of the genetic biomarkers of a cytokine storm and the principles of SNP-LAMP to design a safe and easy-to-use test kit for general use by the public.

Key References

- [1] Varona, M., & Anderson, J. L. (2021). Advances in Mutation Detection Using Loop-Mediated Isothermal Amplification. *ACS Omega*, 6(5), 3463–3469. <https://doi.org/10.1021/acsomega.0c06093>
- [2] Fricke-Galindo, I., & Falfán-Valencia, R. (2021). Genetics Insight for COVID-19 Susceptibility and Severity: A Review. *Frontiers in Immunology*, 12. <https://doi.org/10.3389/fimmu.2021.622176>



A NOVEL PROPOSAL FOR INDUCING CONTROLLABLE MAGNETOTACTIC MOVEMENT IN THE CILIATE *T. THERMOPHILA*

Authors: M. G. KĒNIŠ, P. ŠAUCIUVIENAS, R. RAHMAN, ŠT. DUMITRESCU

Keywords: Bioinformatics, Computer Vision, Magnetosomes, Gene Manipulation, Magnetothermia

ABSTRACT

We propose a method for the control of movement using magnetic fields by inserting the *Magnetospirillum* magnetosome gene island (MAI) into the ciliate *Tetrahymena thermophila*, utilizing both bioinformatics techniques and proposing methodology. A novel algorithm was developed: palindrome identification from an amino acid sequence; in addition, DNA alignment software was used extensively in writing the proposal. These experiments shall serve as proof of principle and identify possible problems and requirements for this to be carried out on leukocytes, which could be utilized in cancer therapy, as is discussed.

INTRODUCTION & OBJECTIVES

Magnetosomes are unique intracellular structures found in magnetotactic bacteria (MTB) that consists of inorganic ferromagnetic crystal: magnetite (Fe_3O_4) or greigite (Fe_3S_4), surrounded by a protein-based membrane with special structures (1, 2, 4).

Typically, magnetosomes are linked in short chains - oligomagnetosomes or in longer ones - polymagnetosomes (4). Magnetosome membrane proteins act as mechanoreceptors (3) that detect small movements of internal inorganic crystals, caused by small variations in external magnetic field. Magnetosomes may be involved in bacterial movement - directly, if a polymagnetosome acts as an internal chord that directs the displacement (3), or indirectly, if the process serves as a promoter for a signaling pathway that causes the flagellum's rotation, and, therefore, oriented movement (3, 5).

Observations show that the magnetosomes' activity is positively correlated with pH, sodium or potassium ion concentrations and with the modulus of exterior magnetic induction, since it acts as a natural ferromagnet (2). Usually, in the Northern Hemisphere, free MTBs deviate towards the north magnetic pole and to the south in Southern Hemisphere, meaning that the magnetosome's internal magnet's polarity is determined by the ecological conditions, rather than by genetic predeterminism (2).

Spirillum is the most common bacterial morphology for MTBs, however some MTBs (individual or colonial) are organized as cocci or bacilli (1). One of the most researched clades of MTBs in articles is the genus *Magnetospirillum* (1), but there are also magnetotactic bacteria in Phylum Desulfobacterota.

The ciliate *Tetrahymena Thermophila* in the phylum Ciliophora displays nuclear dimorphism, containing both a diploid micronucleus (MIC) and a highly polyploid macronucleus (MAC) (6). Sexual reproduction occurs by conjugation and recombination of DNA from the MICs, leaving just one diploid set of DNA in the MIC, from which the MAC is then created (7, 8). In addition, the chromosomes are fragmented at specific sites containing a highly conserved element called the chromosome breakage sequence forming chromosomes with telomeres near the breakage site; this occurs only during MAC differentiation and not during vegetative growth (9, 10).

GENE MANIPULATION & TRANSFER

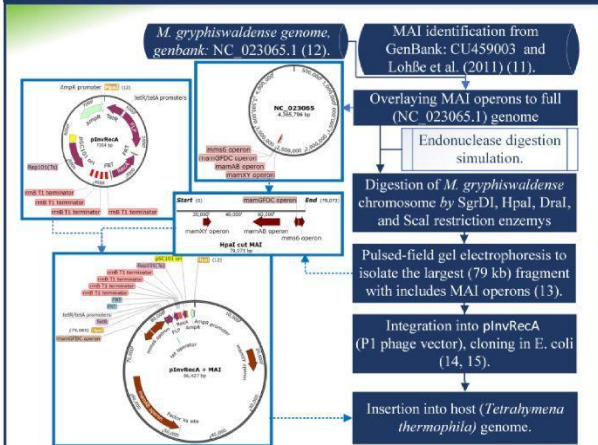


Figure 1. Flowchart genetic manipulation for production of magnetotactic eukaryote (11, 12, 13, 14, 15).

METHODS & THOUGHT EXPERIMENTS

Magnetotactic movements are unoriented movements in a medium with magnetic activity. Cells with magnetosomes move rapidly, since common MTBs may swim twice as fast as rapid swimmers like *E. coli* (1).

Take a control group from a population of the eukaryotic organisms of interest (*T. thermophila*), and split them into two equal groups (A) and (B), placed in different culture media. Expose group (A) to a magnetic field and group (B) to a medium with crystals of NaCl. Groups (C) and (D) correspond to (A) and (B), but they contain transgenic eukaryotes. Keep the four cultures in identical temperature and pressure conditions and after 30 minutes of activity, evaluate temperature differences (16).

We expect groups C and D should result in statistically significant higher temperatures, since higher magnetotactic activity correlates with molecular movement rate, resulting in higher final temperature. Also, a valid test should express a higher temperature in culture (C) than (D), since magnetosomes react better to ferromagnetic than diamagnetic stimulation. A test that exhibits all these conditions would be considered positive, otherwise, it is considered negative.

We propose to utilize Machine Learning algorithms (AI) that deal with image recognition to be able to analyze the synchronicity of movement as showcased in Figure 2 (17).

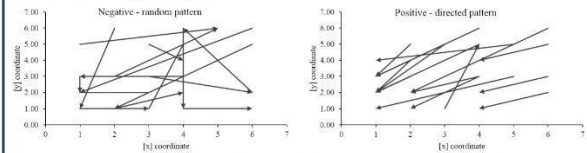


Figure 2. Basic movement models for random and directed patterns

In addition, for the task of finding suitable restriction enzymes, we developed software to identify restriction enzymes whose sites may appear in an exon due to silent mutations; it may be accessed here: <https://github.com/Sauciu1/Silent-mutation-enzyme-failure-prevention>. Should there be silent mutations, it may be necessary to re-sequence the genetic code, as it results in digestion of the insert sequence.

DISCUSSIONS & CONCLUSION

Magnetosomes have potential in diverse applications, such as, immunomagnetic separation, targeted drug delivery, enzyme immobilization, bioremediation and magnetic hyperthermia among many others (18). However, several limitations restrict applicability of the study and its possible implications.

Most MTBs require a hard to maintain anaerobic or microaerophilic environment for optimal yield (19, 20). As a growth medium, though chocolate blood agar may appear to contain suitable substrate, i.e. heme iron, it is not commonly used.

A major limitation is that *M. gryphiswaldense* possesses three distinct stop codons (TAG, TAA, and TGA), while *T. thermophila* employs only the TGA codon, consequently, depending on mRNA fragments transcription, their translation could result in non-functional proteins, failing to form functional magnetosomes (21).

By using this experiment as a model and studying how the gene expression and biosynthesis of the magnetosome may be maintained in this ciliate, we can approach the integration of the magnetosome genes into more complex eukaryotes, such as mice and humans. We can look at the possibility of magnetosome integration in certain leukocytes that normally respond to cancer cells, e.g., the natural killer or natural killer T cells, to enhance their cancer targeting and attacking abilities through specific magnetic hyperthermia (22).

BIBLIOGRAPHY

- [1] Yan, L., Zhang, S., Chen, P., Liu, H., Yin, H., & Li, H. (2012). Microbiological Research, 167(9), 507-519; [2] Yan, L., & Xing, W. (2018), 357-386; [3] Acosta-Avalos, D., Leilo, P., Abreu, F., & Bazylinski, D. A. (2018). Reference Module in Biomedical Sciences; [4] Bazylinski, D. (2001). Encyclopedia of Materials: Science and Technology, 441-447; [5] Clark, D. P., & Pazzernik, N. J. (2016). Biotechnology, 219-248; [6] Eisen, J. A., Coyne, R. S., Wu, M., Wu, D., Thiagarajan, M., Wortman, J. R., Badger, J. H., Ren, Q., Amodeo, P., Jones, K. M., Talon, L. J., Detler, A. L., Salzberg, S. L., Shiva, J. C., Hays, B. J., Majors, W. H., Farzad, M., Carlton, J. M., Smith, R. K., Orias, E. (2006). PLoS Biology, 4(9), e286; [7] Cervantes, M. D., Hamilton, E. P., Xiong, J., Lawson, M. J., Yuan, D., Hadjithomas, M., Miao, W., & Orias, E. (2013). PLoS Biology, 11(3), e1001518; [8] Wahab, S., Saetonne, A., Nabeel-Shah, S., Dannah, N., & Fillingham, J. (2020). Frontiers in Cell and Developmental Biology, 8; [9] Fan, Q. (2000). Nucleic Acids Research, 28(4), 895-900; [10] Yu, G. L., & Blackburn, E. H. (1991). Cell, 67(4), 823-832; [11] Lohße, A., Ullrich, S., Katzmann, E., Borg, S., Wanner, G., Richter, M., Voigt, B., Schweder, T., & Schlier, D. (2011a). PLoS ONE, 6(10); [12] Wang, X., Wang, Q., Zhang, W., Wang, Y., Li, L., Wen, T., Zhang, T., Zhang, Y., Xu, J., Hu, J., Li, S., Liu, L., Liu, J., Jiang, W., Tian, J., Li, Y., Schäfer, D., Wang, L., & Li, J. (2018). Genome Announcements, 2(2); [13] Lopez-Carvalho, L., Martínez-Benitez, M. B., Herrera Iñárriz, J. A., & Flores Soto, E. (2019). Analytical Biochemistry, 573, 17-29; [14] Bajpai, B. (2013). Advances in Biotechnology, 1-10; [15] GSI Biotech LLC. (2020, September 29). Plasmid Maps and Sequences. plnVRecA-SnapGene; [16] Murase, K., Takata, H., Takeuchi, Y., & Saito, S. (2013). Physica Medica, 29(6), 624-630; [17] Danuser, G. (2011b). Cell, 147(5), 973-978; [18] Alphonandery, E. (2014). Frontiers in Bioengineering and Biotechnology, 2; [19] Ali, I., Peng, C., Khan, Z. M., & Naz, I. (2017). Journal of Basic Microbiology, 57(8), 643-652; [20] Yang, J., Li, S., Huang, X., Tang, T., Jiang, W., Zhang, T., & Li, Y. (2013). Frontiers in Microbiology, 4; [21] Horowitz, S., & Gorovskiy, M. A. (1985). Proceedings of the National Academy of Sciences, 82(9), 2452-2455; [22] Alphonandery, E., Guyot, F., & Chebbi, J. (2012). International Journal of Pharmaceutics, 434(1-2), 444-452; **plasmid and gene sequence images were constructed using SnapGene software.

Abstract

B-Cell Lymphoma 3 (BCL-3) is a protein involved in a pathway that regulates Nuclear Factor Kappa-B (NF-κB), a transcription factor that is prevalent in cell proliferation regulation. Misregulation of BCL-3 has been found to cause a variety of cancers, including several lymphomas as well as solid tumors. It was found that BCL-3 is regulated by phosphorylation and ubiquitination. Pre-clinical experimental approaches, such as regulation of BCL-3 phosphorylation through kinase expression control are suggested to have potentials as novel cancer treatment.

Objective

The aim of the project is to repress tumor growth through regulation of the BCL-3 pathway, specifically targeted on the phosphorylation of BCL-3.

Cell Proliferation and Cancer

Cancer is a condition in which cells in the body grow and reproduce uncontrollably. It damages surrounding healthy tissue and often spreads to other parts of the body. Cancer claimed nearly 10 million lives in 2020, approximately 1 in 6 deaths worldwide. Misregulation of cell proliferation is reported to result in cancer development.

BCL-3 NF-κB Gene Regulation Pathway

BCL-3 acts as a regulator of NF-κB by forming a transcription factor complex [1]. Major pathways are (Figure 1):

- Stabilization of repressive NF-κB p50 homodimers through inhibition of ubiquitination.
- Removal of repressive NF-κB p50 homodimers situated on DNA, allowing NF-κB heterodimers (p65/p50) to activate transcription.
- Direct activation of NF-κB target gene transcription through p50 homodimers association.

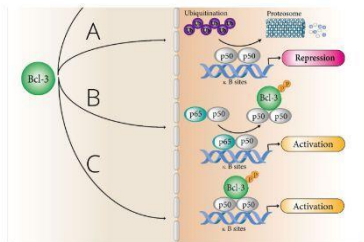


Figure 1: BCL-3 pathways

References:

- Maldonado V, et al. Mol Cancer. 2011 Dec 23;10:152.
- Liu H, et al (2022). Front. Immunol. 13:847699.
- Zhao Y, et al. Biochem Biophys Res Commun. 2005 Sep 30;335(3):865-73.
- Kovalenko A, et al. Nature. 2003 Aug 14;424(6950):801-5.
- Palmer S, et al. Immunol Res. 2008;42(1-3):210-8.
- Xia L, et al. Onco Targets Ther. 2018 Apr 11;11:2063-2073.
- Frederick, et al. (2022). Cells, 11(5), 821.

Methods

Phosphorylation of BCL-3 is controlled through several approaches.

Inducing phosphorylation

Overexpression of GSK3 is expected to phosphorylate BCL-3 on sites S394 and S398, resulting in the protein's degradation.

Inhibiting phosphorylation

Inhibition of key kinases such as, Akt, ERK2, and IKK which are necessary for BCL-3 phosphorylation, is expected to reduce BCL-3 activation, hindering cancer growth as a result.

In addition, another possible approach to inhibit phosphorylation is through the let-7 family of miRNA which regulates the Akt pathway [7].

Analyzing the effects

The level of phosphorylation and ubiquitination are examined to inspect the effectiveness of the methods listed above. The analyses are performed through *in vitro* protein assay such as western blotting and deubiquitination assay [3, 4]. Tumor cell culture and examination *in vitro* is also necessary to observe a shift in cell growth.

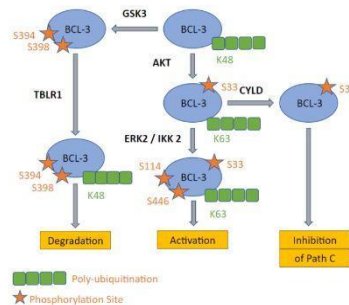


Figure 2: Modifications of BCL-3



Figure 3: BCL-3 protein structure

Results

Palmer, *et al* demonstrated that BCL-3 is one of the major regulators of NF-κB [5]. Liu, *et al* showed that BCL-3 activates NF-κB by forming a complex with a p50 homodimer.

NF-κB is a transcription factor for genes involved in cell proliferation and cell death, and it was found to be extensively involved in cancer development and progression [6].

Application

Shown are possible future applications:

Basic Research

Elucidating further how modifications of BCL-3, NF-κB and related proteins can affect cancer. Research into regulating those modifications BCL-3 would lead to revealing unknown BCL-3 mechanisms.

Therapeutic

Identifying molecules that inhibit phosphorylation of BCL-3 with high specificity, as well as developing a molecule to obstruct the creation of BCL-3 - p50 homodimer complexes, should suppress tumor growth.

Discussion

The BCL-3 - NF-κB pathway is a critical and promising candidate as a target for developing novel treatments for various cancers.

Herein, we have demonstrated that regulating NF-κB activity by BCL-3 phosphorylation is a promising approach to control cancer.

Analyzing the role of other processes within the cell and how they are affected by the modification can further reveal its role in cell function.

Further research regarding possible side-effects and the processes involved in the role of these modifications would make the process more efficient and may eventually result in an effective treatment for cancer.

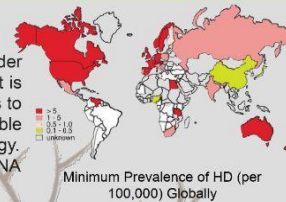
Applying Autophagy as a treatment for Huntington's disease

Group 16: Seoyeon Jeon, Mane Kurghinyan, Khundker Ishraq Ahammad, Donato Elias Pellegrini
Facilitator: Jerry Tzang



Abstract

Huntington's disease (HD) is a fatal autosomal dominant genetic disorder that causes the progressive breakdown of nerve cells in the brain. It is caused by the aggregation of mutated Htt protein. The aim of this study is to upregulate the degradation of the soluble and already aggregated insoluble forms of mHtt by Chaperone-Mediated and Ubiquitin-mediated Autophagy. Adeno-associated viruses(AAV), can be used as vectors containing mRNA coding the proteins that are involved in autophagy regulation.



Introduction

Huntington's disease

Neurodegenerative disorders encompass a wide range of conditions. One of such diseases is **Huntington's disease (HD)**, that, based on a meta-analysis, affects approximately 2.71 per 100,000 [1]. HD is a genetic autosomal dominant neurodegenerative disease caused by the expansion of a CAG repeat in the huntingtin (HTT) gene. This triplet expansion encodes a polyglutamine stretch (polyQ) in the N-terminus of the high molecular weight (348-kDa) and ubiquitously expressed Huntingtin protein (Htt). Normal individuals have between 6 and 35 CAG triplets, while expansions longer than 40 repeats lead to HD [2](Figure 1). There's currently no cure for Huntington's disease. Medicine can help reduce some of the symptoms caused by Huntington's disease, but they don't stop or slow down this lethal condition.

Autophagy

In order to maintain cellular homeostasis, cells have developed elaborate quality-control mechanisms for proteins and organelles. One of this systems include the degradation pathways, called globally "autophagy". Autophagy can diversify in many types such as **Chaperon-mediated (CMA)** and **Ubiquitin-mediated autophagy (UMA)** of protein aggregates (aggrephagy)[3].

Objectives

The aim of this study is to induce the activity of autophagy in neural brain cells, which is a highly conserved mechanism of lysosomal-mediated protein degradation, for targeting Huntingtin aggregates.

Methodology

For soluble mHtt : Chaperone-Mediated Autophagy

Chaperone-mediated autophagy (CMA) is lysosomal pathway primarily characterized by its selective nature of protein degradation, which is mediated by chaperon **HSC70** (heat shock cognate 71 kDa) and lysosome-associated membrane protein **LAMP-2A**. The HSC70 binds to mutated Htt then the complex binds to the LAMP-2A in the lysosomal membrane and enters the lumen.

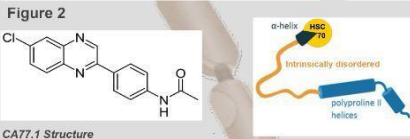
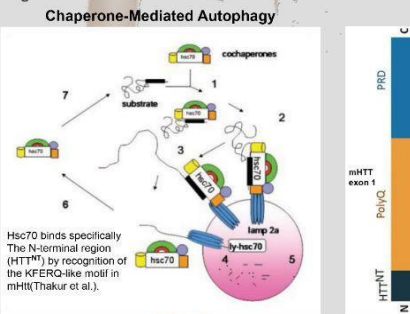
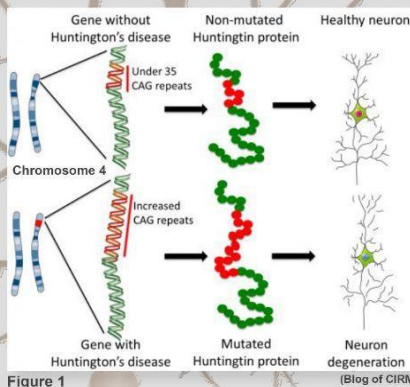
HSC70

HSC70 is a unique protein that mediates CMA. HSC70 binds unfolded/misfolded proteins that have an exposed KFERQ amino acid sequence motif and transports them to the lysosome. The HSC70/KFERQ-client protein complex interacts and binds to the cytosolic tail of the monomer form of LAMP-2A [4].

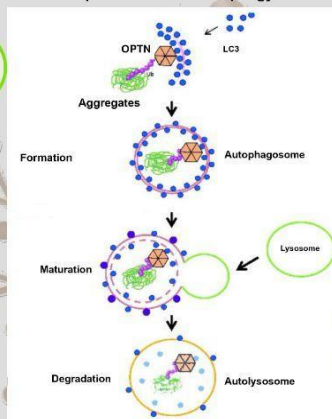
LAMP 2A

LAMP 2A selectively translocates protein to lysosome. A conformational change of LAMP-2A transfers HSC70 to a lysosomal form(lys-Hsc70), which pulls the client protein into the lysosome for degradation(Figure 2). The transcription of LAMP 2A can be activated by compound CA77.1. CA77.1 can penetrate the blood-brain barrier (BBB) and promote the synthesis of LAMP 2A when applied orally[5].

Formation of Htt protein



Ubiquitin-mediated Autophagy



For insoluble mHtt :

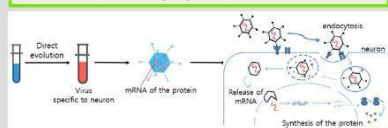
Ubiquitin-mediated Autophagy

Optineurin

Optineurin (OPTN) is a receptor that has an ubiquitin binding domain region (UbBD) that recognizes polyUbK63 signals. OPTN interacts with **inclusion bodies (IB)** formed by mHtt, that can **not** be degraded by the CMA pathway [6]. OPTN transfer IB to autophagosomes by directly binding with ATG8s through the LC-interacting region(LIR). The dynein/dynactin complex transports mature autophagosome near the lysosomes and form autolysosomes through the SNARE complex. After the fusion, lysosomal proteases degrade the IB [7](Figure 3).

AAV as a way of promotion

The specificity of HSC70 to mHtt can be increased by using synthetic dimer (QBP1) that targets both polyQ sequence of mHtt and HSC70[8]. The production of HSC70 and the dimer can be **kicked-off** in the brain by **injecting Adeno-associated viruses(AAV)**, vector containing mRNA coding the proteins. Mutated AAV can be used to target the BBB and transfer mRNA into the brain[9]. The production of OPTN can be promoted in the brain by increasing the concentration of OPTN mRNA. Mutated AAV containing OPTN mRNA can be used for the purpose.



Discussion

In primary stages of HD, CA77.1 can be applied orally to increase LAMP 2A transcription and thereby increasing CMA with less risk of immune response. If CA77.1 treatment fails, then viral transduction neuron specific AAV with the mRNA sequence of a dimer that has domains of both HSC70 and mHtt can be used [9]. However, in later stages of HD when insoluble IBs form, mRNA of OPTN can be inserted through AAV transduction to degrade polyQ aggregates. These methods are specific to mHtt, so wild-type HTT has low chance of being degraded. But AAV transduction methods can't be used if the patient has been treated by this method before. In that case, a different viral vector should be used. Moreover, since this only focuses on mHtt degradation, methods such as gene editing are needed for more permanent solution.

Conclusion

Upregulating the production of the proteins involved in the autophagy systems discussed above, can be a way to enhance aggrephagy and delay disease progression. However, the interaction between two methods isn't investigated yet, so the risk of side effects must be considered.

References

- Pringsheim, T., Wiltshire, K., Day, L., Dykeman, J., Steeves, T., & Jette, N. (2012). The incidence and prevalence of Huntington's disease: A systematic review and meta-analysis. *Dice*, 1, F. (2007).
- Bates, G., Dorsey, R., Cusella, J. et al. Huntington disease. *Nat Rev Dis Primers* 1, 15005 (2015).
- Dice, J. F. (2007). Chaperone-Mediated Autophagy. *Autophagy*, 3(4), 295-299. doi:10.4161/aut.4144
- Kaushik, S., & Cuervo, A. M. (2018). The coming of age of chaperone-mediated autophagy. *Nature Reviews Molecular Cell Biology*, 19(6), 365-381. doi:10.1038/s41580-018-0001-8
- Anguliano, J., Garner, TP, Mahalingam M, Das BC, Gavathiotis E, Cuervo AM (June 2013). "Chemical modulation of chaperone-mediated autophagy by retinoic acid derivatives". *Nature Chemical Biology* 9 (6): 374-82. doi:10.1038/nchembio.1230. PMID: 24017119. PMID 23584676.
- Wen-Chuan Shen, Hwei-Ying Li, Guang-Chao Chen, Yijiang Chen & Pang-hsien Tu (2016). Mutations in the ubiquitin-binding domain of OPTN/optineurin interfere with autophagy-mediated degradation of misfolded proteins by a dominant-negative mechanism. *Autophagy*, 11.4, 685-700
- Hyungsun Park, Ju-Hee Kang and Seungju Lee. Autophagy in Neurodegenerative Diseases: A Hunter for Aggregates (2020)
- Barber, H. (2022). Neuron-specific virus overcomes barriers to brain-related gene therapy. *Spectrum*. doi:10.53053/KPM3598
- Bauer, Peter O, Goswami Anand, Wong, Hon Kit, Okuno, Misako, Kurosawa, Masaru, Yamada, Mizuki, Miyazaki, Haruko, Matsumoto, Gen, Kino, Yoshihiro, Nagai, Yoshitaka (2010). Harnessing chaperone-mediated autophagy for the selective degradation of mutant huntingtin protein. *Autophagy*, 28(3), 256-263. doi:10.1038/nbt.1608

Abstract

Although neurodegeneration in Parkinson's disease is yet to be fully understood, considerable evidence suggests that genetic factors can influence susceptibility to the disease.

In this project, we will try to examine which genes are associated with the disease. Modern AI methods (mainly machine learning) let us find genes that are linked to Parkinson's disease. This empowers us to predict whether someone is prone to the illness by examining their genome and comparing the genes.

Introduction

Parkinson's disease (PD) is the second most common neurodegenerative disease [1]. PD is characterized by the loss of dopaminergic neurons in the substantia nigra with the development of Lewy bodies containing α -synuclein. The clinical features of PD include tremors, rigidity, bradykinesia and cognitive impairment.

There are four biomarkers to identify PD: clinical, imaging, biochemical and genetic. A few methods are designed to identify genes and noncoding elements such as long noncoding RNAs. In current PD genetics nomenclature, 18 specific chromosomal regions termed PARK (from Parkinson) and numbered in chronological order of their identification (PARK1, PARK2, PARK3, etc) are found to be associated with the disease [4]. Several mutations are considered to cause dominant PD. Scientists have found new genes responsible for recessive or X-linked PD [5]. In our study we will discuss the genetic biomarkers of PD, different methods and computer tools for identifying them.

Methods

Machine learning algorithms, are widely used in various studies to identify the genes associated with various diseases.

In machine learning and statistics, feature selection is the method of selecting a subset of relevant features. There are several types of feature selection (Perturbation based selection, Hilbert-Schmidt selection, etc.). Classification methods are also diverse (SVM, Random forest, Adaboost, etc.).

New PD-linked genes or PD risk factors can be identified by gene mapping. Gene mapping in human diseases is localization of genes [4]. These methods include linkage analysis and genome-wide association studies. The gene underlying any heritable form of human disease can be mapped and identified by linkage analysis. The first step in classical linkage analysis is to hypothesize the mode of inheritance of the disease on the basis of a constructed pedigree. Linkage analysis is based on the tendency of a disease-causing sequence to remain unchanged, and markers at specified loci to be inherited together (linked).

The advent of recent sequencing technology, most notably next-generation sequencing (whole genome or exome) facilitates gene identification. In GWAS (Genome-wide association studies), the identification of genetic risk factors for the development of PD is achieved by analysing as many as 500 000 different single-nucleotide polymorphisms (SNPs) [4]. If certain variants are more frequent in the PD patients, they are considered to be associated with the disease. Many scientists used different methods in their work. For example, Radivojac presented an approach to predict the disease related genes based on

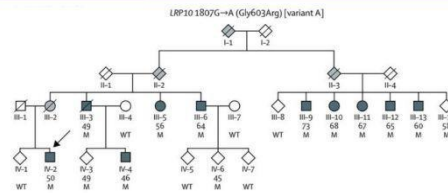


Figure 1. Pedigree of one family with PD, on which genome-wide linkage analysis was done, [6]

Gene	Year	Additional clinical features besides Parkinsonism
<i>SNCA</i>	1997	Cognitive, behavioral, and autonomic dysfunction, myoclonus
<i>LRRK2</i>	2004	Few, variable. Possibly only milder non-motor disturbances
<i>EIF4G1</i>	2011	Probably not pathogenic
<i>VPS35</i>	2011	Cognitive and behavioral changes (?)
<i>DNAJC13</i>	2013	None
<i>CHCHD2</i>	2015	None. Two carriers with tremor only
<i>TMEM230</i>	2016	One large family only
<i>RIC3</i>	2016	One family only

Table 1. Monogenic causes for autosomal dominant PD, [5]

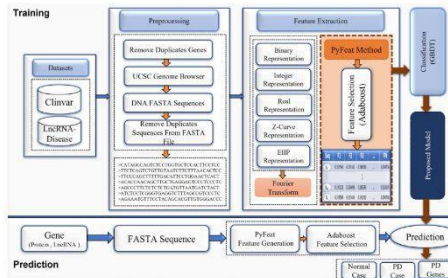


Figure 2. The proposed prediction system for identifying protein and lncRNA genes associated with PD, using the PyFeat method, [3]

Gene	Year	Atypical clinical features
<i>PARK2 (Parkin)</i>	1998	None
<i>DJ-1</i>	2003	None. Psychiatric features, dystonia (in some patients)
<i>PINK1</i>	2004	None. Cognitive/psychiatric symptoms (in some patients)
<i>FBXO7</i>	2008	Spasticity, equinovarus deformity (in some patients)
<i>22q11.2del</i>	2013	Intellectual disability
<i>SYNJ1</i>	2013	Dystonia, cognitive decline, seizures
<i>RAB39B</i>	2014	Severe intellectual disability, X-linked mode of inheritance
<i>DNAJC6</i>	2015	Intellectual disability, other neurological features
<i>PODXL</i>	2016	None. One family only. To be confirmed in independent studies
<i>VPS13C</i>	2016	Severe cognitive dysfunction, tetraplegia
<i>PTRHD1</i>	2017	Severe cognitive dysfunction, muscular weakness

Table 2. Monogenic causes for autosomal recessive or X-linked PD or atypical juvenile Parkinsonism, [5]

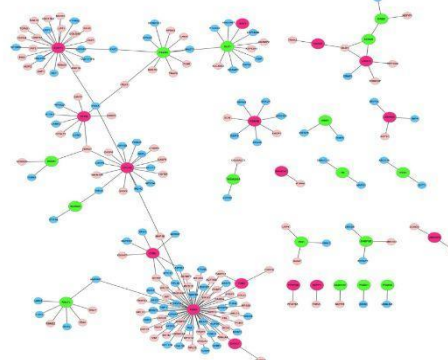


Figure 3. The protein-protein interaction of upregulated (green) and downregulated (red) genes in substantia nigra of patients with PD, [7]

the protein-protein interaction (PPI) network [3].

First, they presented feature vectors in three ways: disease-protein relationship, protein sequence, and protein function information. Second, the used information gene to rank features. Finally, in the classification step, they applied the support vector machine (SVM) classifier as a supervised technique with two layers for predicting genes related to the disease. There is also a new proposed system that can analyze two separate datasets: proteins and lncRNAs. Figure 2 shows a novel framework of the proposed prediction system comprising four steps, which is called PyFeat method [3].

A significant method is hierarchical clustering, an unsupervised clustering based machine learning technique. The general application of this method is generation of dendrograms showing similarity between the expression patterns of potentially PD-linked genes based on transcriptomics data used as an input. The benefit of hierarchical clustering is that it allows for comparison of supposed PD-linked genes with genes of known linkage with PD or other genes of pathogenic character, which is critical in generating a board understanding of genetic interaction.

Discussion

With these above mentioned methods scientists have discovered several genes and risk factors that can cause different variants of PD. Mutations in DNAJC13, CHCHD2, TMEM230 and RIC3 have been reported as new causes for monogenic dominant PD [5]. Compared to monogenic dominant PD and to the well established recessive early-onset PD genes PARK2, DJ1, and PINK1, the newly identified recessive forms appear more complex. Table 2 summarizes currently known and putative genes for recessive and X-linked PD.

All of above mentioned methods can be used to identify biomarkers of PD in different studies, but in result of our research we found out that the PyFeat method is the most accurate, because it analyses not only the proteins, but also lncRNAs and microRNAs.

Conclusion

To summarize, there are many genes affecting PD, but only 5-10% of that genes have been characterized and validated [3]. Other genetic factors causing PD are yet to be identified by the joint efforts of geneticist and clinicians working with PD.

Applying machine learning methods to study PD has enabled considerable advances in the field. Hence the development of more sophisticated algorithms and system-wide pathway analysis will help to better understand and characterize the biology of Parkinson's disease.

References

- Azadeh, Hoda & Abdollah Zadeh, Azadeh & Moradan, Atefeh & Salehshahzade, Zahra. (2021). Study of Genes Associated With Parkinson Disease Using Feature Selection.
- Gan-Or, Zion, Dhan, P. A., & Rouleau, G. A. (2015). Genetic perspective on the role of the autophagy-lysosome pathway in Parkinson disease. *Autophagy*, 11(9), 1443-1457. <https://doi.org/10.1080/15488627.2015.1067364>
- Hefny, M., El-Ghannagy, S., Mekky, H., Elmogy, M., & Soliman, H. (2022). Predicting Parkinson disease related genes based on PyFeat and gradient boosted decision tree. *Scientific Reports*, 12(1), 10004. <https://doi.org/10.1038/s41598-022-14127-9>
- Helen, C., & Westenberg, A. (2012). Genetics of Parkinson's disease. *Cold Spring Harbor Perspectives in Medicine*, 2(1), a008888. <https://doi.org/10.1101/cshperspect.a008888>
- Paschmann, A. (2017). New genes causing hereditary Parkinson's disease or parkinsonism. *Current Neurology and Neuroscience Reports*, 17(9). <https://doi.org/10.1007/s11910-017-0780-8>
- Quaderi, M., Mandemakers, W., Grochowska, M. M., Mariani, R., Graf, H., Fabrizio, E., Gresswell, G. L., Bonifati, V. (2019). LRP10 genetic variants in familial Parkinson's disease and dementia with Lewy bodies: a genome-wide linkage and sequencing study. *Lancet Neurology*, 17(7), 597-608. [https://doi.org/10.1016/s1473-4421\(19\)30179-0](https://doi.org/10.1016/s1473-4421(19)30179-0)
- Wang, L., & Wang, Z. (2020). Integrative analysis of mRNA expression profiling in Parkinson's Disease. *Medical Science Monitor: International Medical Journal of Experimental and Clinical Research*, 26. <https://doi.org/10.12659/msm.920846>



IBO
33rd 2022
ARMENIA

Synthetic Fibrinogen as a treatment for Afibrinogenemia

IGP Group 18: Biomedicine

Group members: Arman Hayrapetyan
Siluni Wickramathilake
Aikaterini Karpouzi
Daniel Čičovský

Group Facilitator: Josue Francisco Laszeski

Abstract

Fibrinogen is a blood plasma glycoprotein, which is synthesized by the liver. The conversion of fibrinogen to fibrin is catalysed by thrombin and plays a key role in clot formation. Fibrinogen replacement therapy is used to treat bleeding episodes in patients with congenital and acquired fibrinogen deficiency. This study suggests to synthesize fibrinogen by three types of colonies of genetically modified yeast, one for each subunit of fibrinogen. Methods that we use in this research are gene editing, cultivation, centrifugation of cultures, protein purification and in-vitro protein assembly.

Introduction

Fibrinogen (fig. 1) is a 340 kDa protein synthesized primarily by hepatocytes. Fibrinogen plays a key role in normal hemostasis by promoting blood clot formation, platelet aggregation, and fibrinolysis (fig. 2). Hereditary defects of fibrinogen can affect either the quantity (hypofibrinogenemia and afibrinogenemia) or the quality (dysfibrinogenemia) of circulating fibrinogen. Fibrinogen replacement therapy is currently indicated as prophylaxis and therapy of hemorrhage in congenital and acquired fibrinogen deficiency. [1]

It is the commonly used treatment for bleeding episodes in patients with afibrinogenemia and includes plasma-derived fibrinogen concentrate, cryoprecipitate and fresh frozen plasma (FFP). But thrombotic complications have been reported in patients with afibrinogenemia following replacement therapy, including ischemic foot lesions, ischemic stroke, renal and ovarian vein thrombosis, deep venous thrombosis, development of anaphylactic reactions and pulmonary embolism. [1]

Objective

Our objective is to propose a method for artificially producing fibrinogen in order to provide a more reliable treatment for the described diseases.

Methods

Using three separate Polymerase Chain Reactions (PCR), the cDNA from genes responsible for the production of the three non identical polypeptide chains that compose fibrinogen are replicated. Through the process of reverse transcription occurs the double-stranded DNA molecule on which the sequence that occurs by the action of a restriction enzyme, such as Eco-RI, is then attached. Using the same restriction enzyme, the plasmid becomes linear, which allows the desired gene to be inserted, and is then embolized on a petri dish with yeast, such as *Saccharomyces cerevisiae* (fig. 3). These plasmids contain a selectable marker, usually an antibiotic resistance gene, so the antibiotics act as a filter to select only the bacteria containing the plasmid DNA (fig. 4). Then, these are placed into a bioreactor and cultivated, so as to produce the desired strands, that can be connected through artificial glycosylation to form fibrinogen [2].

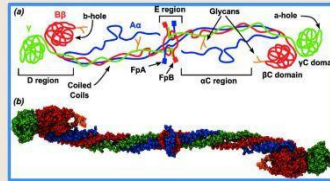


Fig 1. Fibrinogen molecule. Schematic representation and 3D model from Köhler et al [2015].

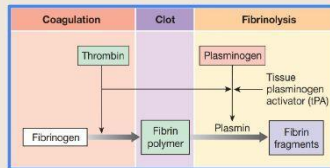


Fig 2. Scheme of coagulation, clotting and fibrinolysis. From Silverton [2019].

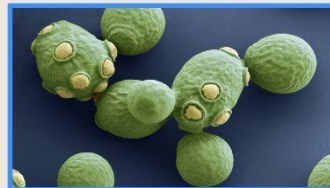


Fig 3. Yeast colored SEM. Species: *Saccharomyces cerevisiae*. From Scott [2022].

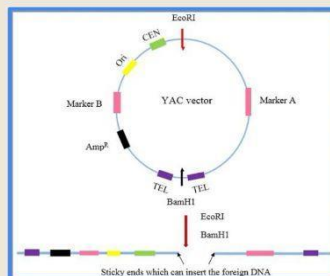


Fig 4. Yeast Artificial Chromosomes (YAC). All necessary parts included. From Murray and Szostak [2022].

Discussion

The main advantage of this method is that cultivation of the yeast is much easier than artificial biosynthesis of giant organic molecules like fibrinogen. It resembles the usage of recombinant bacteria to produce insulin. Many species of yeast are used as model organisms, so scientists know a lot about their biology and biochemistry. In our project, yeast could be similarly utilised to replace bacteria, because it is a eukaryotic cell and can do eukaryotic post translational protein modifications [3]. However, these modifications are different from human ones and it can cause immune reaction [3]. Solution of the problem can be given by modern genetical engineering methods.

One of question connected to this topic is protein composition. Fibrinogen is made of the three subunits and it is not sure that the yeast cell can compose the whole protein from these subunits. It can be solved as in the case of insulin. We can have three types of colonies (one for α subunit, one for β subunit and one for γ subunit) and the whole protein would be in-vitro assembled after the extraction.

Another problem could be that the synthesized fibrinogen could negatively affect metabolism of the yeast. Thus, this aspect must be addressed in posterior research.

Conclusion

Usage of fibrinogen synthesized by genetically modified yeast could be in the future effective and cheap treatment for people with the fibrinogen deficiency. Techniques similar to this have a plethora of applications, and can make treatments more accessible, as the broad usage of recombinant proteins for diabetes has proven [4]. Before it will be used it will need a lot of work of many scientists. We hope that this research will inspire someone to think more about this topic, so as to achieve an improvement in healthcare overall.

References

1. Franchini, M. & Lippi, G. Fibrinogen replacement therapy: a critical review of the literature. *Blood Transfus* 10, 23–27 (2012).
2. Gellissen, G. et al. Heterologous protein production in yeast. *Antonie van Leeuwenhoek* 62, 79–93 (1992).
3. Eckart, M. R. & Bussineau, C. M. Quality and authenticity of heterologous proteins synthesized in yeast. *Current Opinion in Biotechnology* 7, 525–530 (1996).
4. Riggs, A. D. Making, Cloning, and the Expression of Human Insulin Genes in Bacteria: The Path to Humulin. *Endocrine Reviews* 42, 374–380 (2021).
5. Köhler, S., Schmid, F. & Settanni, G. The Internal Dynamics of Fibrinogen and Its Implications for Coagulation and Adsorption. *PLoS computational biology* 11, e1004346 (2015).
6. Silverthorn, D. U. *Human Physiology: An Integrated Approach*. (2019).
7. Scott-Robinson, S. *Saccharomyces cerevisiae*. <http://www.microplia.nl/en/discover/microbiology/saccharomyces-cerevisiae/>.
8. Murray, A. W. & Szostak, J. W. Construction of artificial chromosomes in yeast. *Nature* 305, 189–193 (1983).

7. CALCULATION OF EXAM RESULTS

7.1 NORMALISING RAW STUDENT EXAM SCORES AND CALCULATION OF FINAL STUDENT SCORE

The way the IBO 2022 organizing committee calculated the final scores of each student is described below. It follows the procedure applied at IBO 2015 and IBO 2013. In Figure X1, the IBO 2022 organizing committee shows the normalization of the raw scores for the four practical exams.

In Figure 6.4, 'Rank' gives each student final rank among all **237** students. The normalized scores for each Practical exam are obtained according to the formula:

$$NS_{i,e} = \frac{(S_{i,e} - \underline{S}_e)}{SD_e}$$

where NS_i is the normalized score student i earned exam e , $S_{i,e}$ is the raw score student i earned exam e , \underline{S}_e is the mean of scores in exam e , and SD_e is the standard deviation of scores in exam e .

Theoretical exam scores are normalized in the same way after summing the students' scores for the two exams (it is labeled as **Theroy_total_normalized** in the Figure X1).

The normalized scores of the practical exams are then summed (labeled as **practical_total** in Figure X1). Followingly the same normalization procedure is applied to the **practical_total** score to obtain the final normalized practical score (labeled as **practical_total_normalized** Figure X1). This second normalization is needed because the IBO 2022 organizing committee attempts to make the practical exams different to test a variety of student skills (which is not the case of the two theoretical exams). The second normalization was introduced in Bern 2013.

The final normalized score is calculated by summing **Theroy_total_normalized** and **practical_total_normalized**. Lastly, the final score is calculated by scaling the final normalized score according to the following formula:

$$FS = FNS * 10 + 50$$

where **FS** is the final score, **FNS** is the final normalized score.

The last transformation is used to make the score more student-friendly.

Rank	student_code	Name	Bioinformatics	Biochemistry	Plant_Physiology	Zoology	Bioinformatics_normalized	Biochemistry_normalized	Plant_Physiology_normalized	Zoology_normalized	practical_total	practical_total_normalized
x1	y1	z1	68	49	77.15	34	0.981	0.602	1.723	0.273	3.578	1.164
x2	y2	z2	85	18.5	77.8	23.75	2.099	-0.952	1.761	-0.328	2.580	0.839
x3	y3	z3	57.4	64	57.35	43.25	0.284	1.366	0.543	0.815	3.008	0.978
x4	y4	z4	54.2	62.5	55.5	27.25	0.073	1.290	0.433	-0.123	1.673	0.544
...												
Mean			53.08	37.18	48.23	29.35	0.00	0.00	0.00	0.00	0.00	0.00
SD			15.21	19.63	16.79	17.06	1.00	1.00	1.00	1.00	3.08	1.00

Figure X1. Score calculations

Rank	student_code	Name	Bioinformatics	Biochemistry	Plant_Physiology	Zoology	Bioinformatics_normalized	Biochemistry_normalized	Plant_Physiology_normalized	Zoology_normalized	practical_total	practical_total_normalized
x1	y1	z1	68	49	77.15	34	0.981	0.602	1.723	0.273	3.578	1.164
x2	y2	z2	85	18.5	77.8	23.75	2.099	-0.952	1.761	-0.328	2.580	0.839
x3	y3	z3	57.4	64	57.35	43.25	0.284	1.366	0.543	0.815	3.008	0.978
x4	y4	z4	54.2	62.5	55.5	27.25	0.073	1.290	0.433	-0.123	1.673	0.544
...												
Mean			53.08	37.18	48.23	29.35	0.00	0.00	0.00	0.00	0.00	0.00
SD			15.21	19.63	16.79	17.06	1.00	1.00	1.00	1.00	3.08	1.00

Rank	student_code	Name	Theory_a	Theory_b	Theory_total	Theory_total_normalized
x1	y1	z1	34.8	36	70.8	1.211
x2	y2	z2	38.8	35	73.8	1.503
x3	y3	z3	36.8	35	71.8	1.308
x4	y4	z4	36.4	39.4	75.8	1.698
...						
Mean			29.34	29.05	58.39	0.00
SD			5.25	5.52	10.25	1.00

Rank	student_code	Name	final_normalized_score	final_score	Gap	Award
x1	y1	z1	2.374	73.742	0.319	Silver
x2	y2	z2	2.342	73.423	0.559	Silver
x3	y3	z3	2.286	72.864	0.440	Silver
x4	y4	z4	2.242	72.424	0.370	Silver
...						
Mean			0.00	50.00	0.39	
SD			1.88	18.79	0.71	

7.2 SUMMARY STATISTICS OF STUDENT SCORES AT THE EXAMS

The scores of the students at the six exams are summarized with box plots in Figure X2. Non-parametric Wilcoxon test was used to test for difference between the theory scores and among the practical exam scores. There was no significant difference detected between the theory scores which indicates that the two exams were uniform. On the other hand, all practical exams were significantly different from each other, which is expected since the IBO 2022 is testing a different set of skills in each exam. This is in agreement with results of statistical analysis of previous IBOs and is the reason the IBO 2022 organizing committee normalizes the scores.

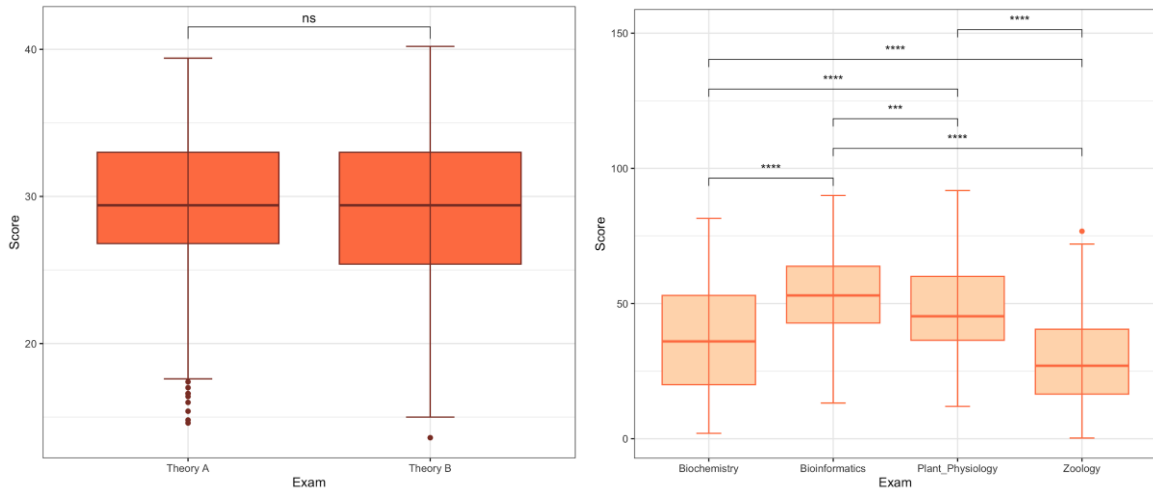
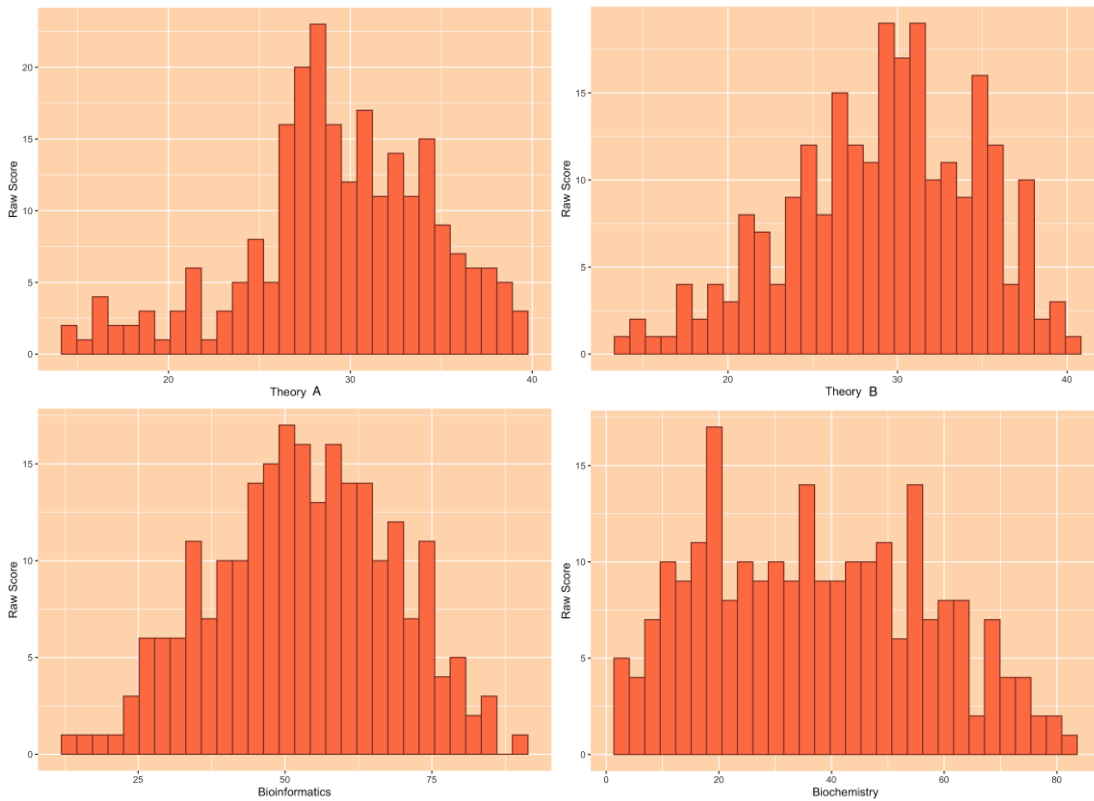


Figure X2. Box plots of the results of theoretical and practical exams. ns=non-significant, *** = $P < 0.001$, **** = $P < 0.0001$.

Histograms illustrating score distributions of the six exams are given in Figure X3.



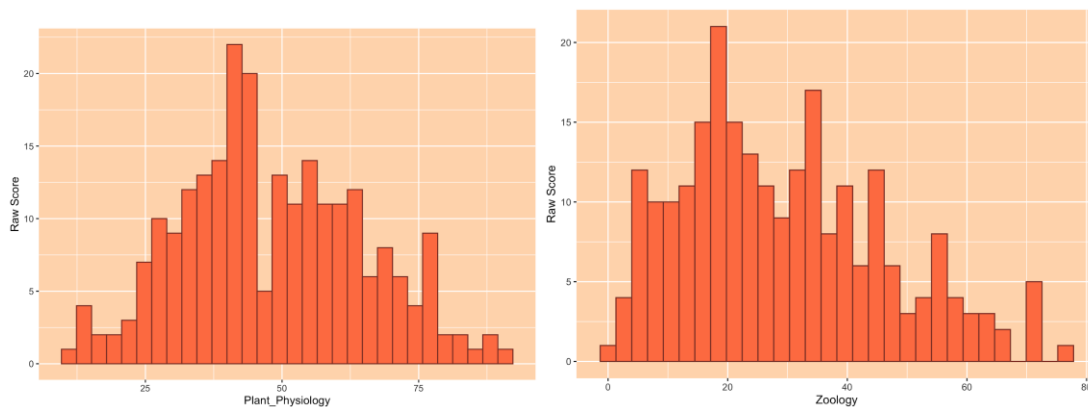
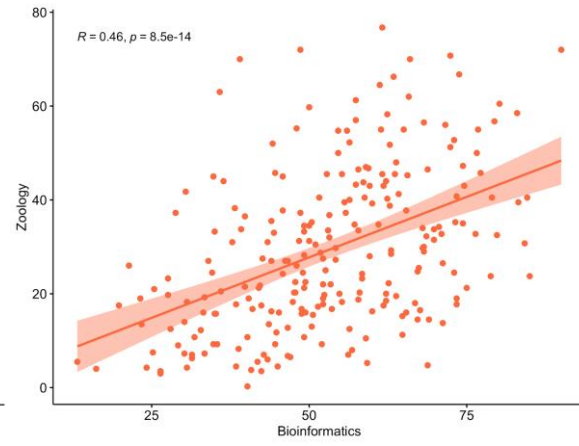
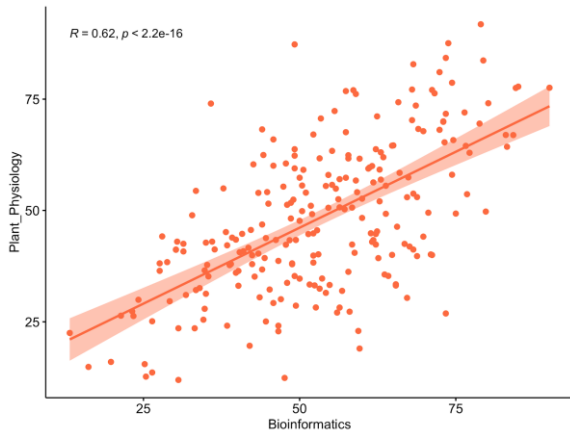
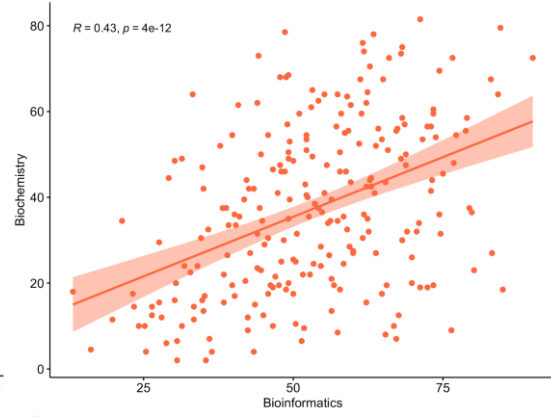
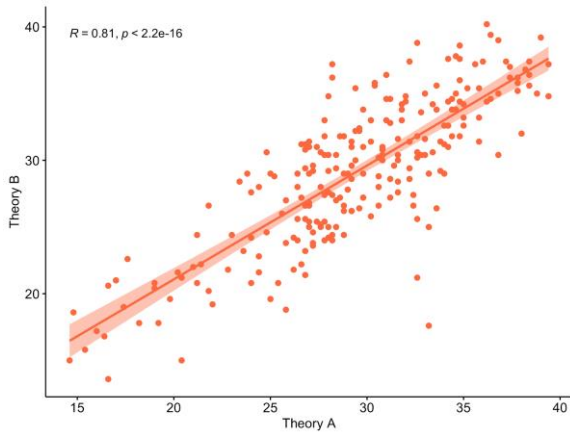


Figure X3. Histograms of student scores in the exams.

7.3 RELATIONSHIPS BETWEEN STUDENT PERFORMANCE IN THE DIFFERENT EXAMS

The two theoretical exams are regarded as replicates. Therefore, the IBO 2022 organizing committee expects individual students to perform similarly in both. This was tested by a simple correlation analysis (Figure X4). R score and P value are measured. R is a correlation coefficient that measures the strength of the relationship between two variables, as well as the direction on a scatter plot.

The individual student scores from the two theoretical exams were highly correlated with $R=0.81$ and $P<2.2e-16$. On the other hand, the four practical exams should certainly not be replicated since they test different practical skills of the students. Therefore, the IBO 2022 organizing committee expected weaker correlations. The possible six correlations between pairs of practical exams are shown in Figure X4 (**R** value on the up-left corner of each plot).



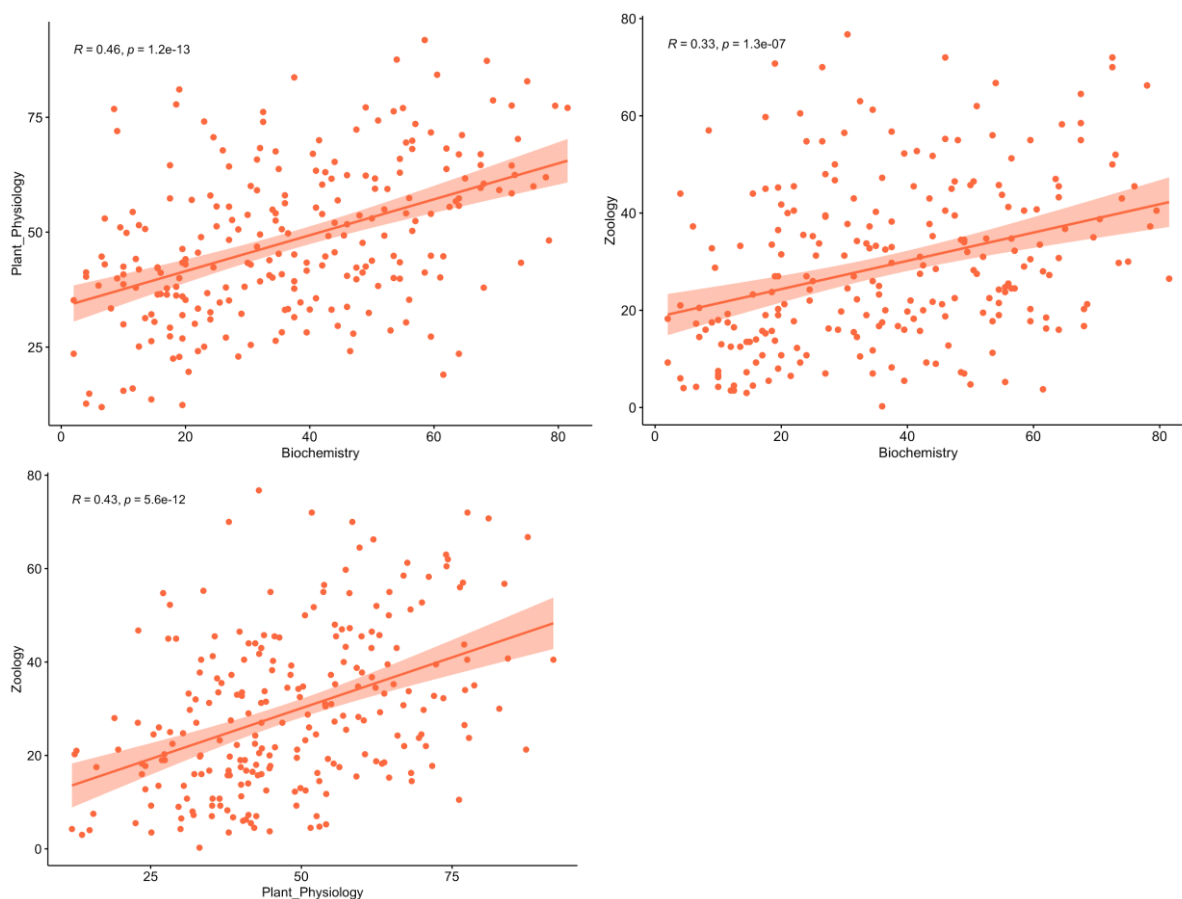


Figure X4. Correlation between raw scores in the four practical exams, and between the two theoretical exams.

The individual student scores from the four practical exams are correlated with R varying from 0.33 to 0.62, which is still high values but the correlation is significantly less strong than in between the theoretical exams. If a student is strong in one practical discipline, they generally perform well in the other practical exams as well, but there is still much differentiation in the skillsets. The IBO 2022 organizing committee has obtained the strongest correlation between Plant Physiology and Bioinformatics, while the weakest correlation is between Zoology and Biochemistry. For comparison, corresponding values for the IBO 2013 practical exams ranged from 0.18 to 0.55, and for IBO 2015 from 0.17 to 0.39.

7.4 FINAL SCORES AND MEDAL DECISION

The normalized scores **Theroy_total_normalized** and **practical_total_normalized** for the exams were strongly correlated ($R = 0.77^{****}$, Figure X5). The distribution of the final scores of the students is given in Figure X6.

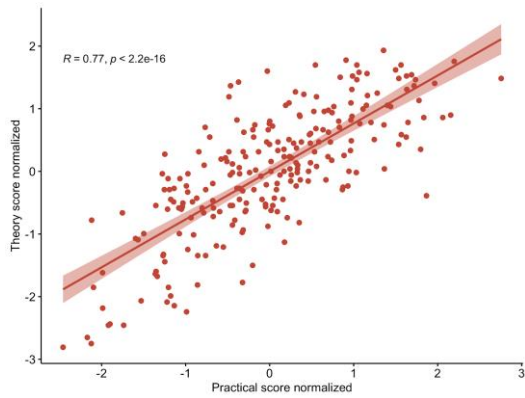


Figure X5. Correlation between the normalized scores for the two kinds of exams

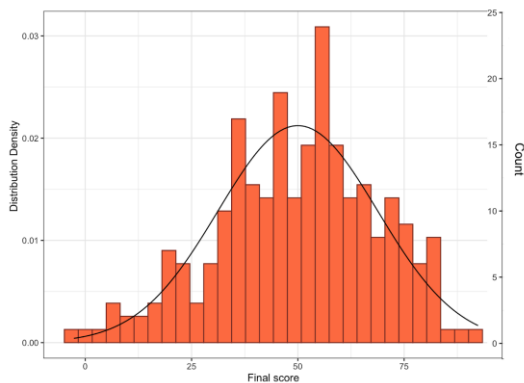


Figure X6. Frequency distribution of the final scores for the students. A normal distribution density function is fitted on the histogram.

Based on the final scores out 237 participants, 26 students have been awarded gold medals (11%), 46 students have been awarded Silver medals (19.4%), 71 students have been awarded Bronze medals (30%), and 25 students have been awarded Merit Certificates (10.5%) (with a 10%-20%-30%-10%-30% distribution being the ideal required by IBO).

The ranking table is presented below.

Rank	Student Code	Country	Name	Theory_a	Theory_b	Theory总分	实验总分	理论总分	生物化学	植物生理	动物学	生物形态学得分	生物化学得分	植物生理得分	动物学得分	实验总分	实验总分/标准化	最终得分	最终得分	Award
1	I002	Independent Olympiad Delegation	YAKOV Dmitrievich KOROBITSYN	37.4	36.2	73.6	1.484	90	72.5	77.55	72	2.427	1.799	1.747	2.500	8.473	2.755	4.239	92.392	Gold
2	BGR1	Bulgaria	Petar Stoilov Zhotev	36.2	40.2	76.4	1.757	73.8	54	87.55	66.75	1.362	0.857	2.342	2.193	6.754	2.196	3.953	89.531	Gold
3	THA3	Thailand	Natchapoi Vongtanakiat	35.6	37.2	72.8	1.406	79	58.5	91.8	40.5	1.704	1.086	2.595	0.654	6.039	1.964	3.370	83.696	Gold
4	IDN2	Indonesia	Gregorius Tendi	39	39.2	78.2	1.932	68	73.5	70.275	29.75	0.981	1.850	1.313	0.023	4.167	1.355	3.288	82.876	Gold
5	CZE3	Czech Republic	Marek Pavlica	38.4	37.4	75.8	1.698	65	67.5	64.6	55	0.784	1.544	0.975	1.504	4.807	1.563	3.261	82.614	Gold
6	I003	Independent Olympiad Delegation	NAZIM Rafievich MUSTAFIN	39.4	34.8	74.2	1.542	74.4	69.5	78.675	35	1.402	1.646	1.814	0.331	5.193	1.689	3.231	82.309	Gold
7	IRN1	Iran	Mahdi - AFSHARI ESFIDVAJANI	34.8	38.6	73.4	1.464	73.4	60.5	84.25	40.75	1.336	1.188	1.468	0.668	5.338	1.736	3.200	82.000	Gold
8	TWN1	Chinese Taipei (Taiwan)	YU-CHEN HUANG	38.4	35.6	74	1.523	65.8	51	74.3	62	0.836	0.704	1.553	1.914	5.007	1.628	3.151	81.510	Gold
9	JPN1	Japan	Taiga Mitamura	38.2	36.8	75	1.620	84.2	64	66.925	30.75	2.046	1.366	1.114	0.082	4.608	1.498	3.119	81.810	Gold
10	TWN3	Chinese Taipei (Taiwan)	CHEN-AN - LIU	34.8	37.6	72.4	1.367	71.6	53.5	76.3	56	1.217	0.831	1.672	1.562	5.283	1.718	3.085	80.848	Gold
11	I004	Independent Olympiad Delegation	SEMEN Sergeevich SHMAKOV	35	32.6	67.6	0.899	84.6	79.5	77.5	40.5	2.072	2.156	1.744	0.654	6.625	2.154	3.053	80.529	Gold
12	I0D1	Independent Olympiad Delegation	KARINA Markovna KARIMOVA	37.8	35.8	73.6	1.484	72.4	19	81.05	70.75	1.270	-0.926	1.955	2.427	4.726	1.537	3.021	80.207	Gold
13	IRN4	Iran	Amireza - ZENALI	34.2	37.6	71.8	1.308	68.2	75	82.825	30	0.994	1.926	2.061	0.038	5.019	1.632	2.940	79.404	Gold
14	TUR4	Türkiye	Tolga Atlar	35.8	31.4	67.2	0.860	83	67.5	66.95	58.5	1.967	1.544	1.115	1.709	6.335	2.060	2.920	79.197	Gold
15	SGP4	Singapore	Owen JunHeng Ong	38	32	70	1.133	79.4	37.5	83.675	56.75	1.730	0.016	2.111	1.606	5.464	1.777	3.199	79.096	Gold
16	IRN3	Iran	Mohammad Amin - KIANI	36.8	39	75.8	1.698	73.4	59.5	71.7	17.75	1.336	1.137	1.398	-0.680	3.191	1.038	2.736	77.350	Gold
17	TWN4	Chinese Taipei (Taiwan)	LIANG-SHIN HUANG	37.4	37	74.4	1.562	78.8	55.5	69.5	23.75	1.691	0.933	1.287	-0.328	3.563	1.159	2.727	77.203	Gold
18	THA4	Thailand	Yannaruk Thawomrungrit	36.8	30.4	67.2	0.860	66	72.5	58.45	70	0.849	1.799	0.609	2.383	5.640	1.834	2.694	76.936	Gold
19	TUR3	Türkiye	Latif Hatipoğlu	39.4	37.2	76.6	1.776	57.8	50.5	61.675	46.5	0.310	0.678	0.801	1.005	2.795	0.909	2.685	76.852	Gold
20	POL2	Poland	JAGIENKA MADRZAK	37.2	37.4	74.6	1.581	59	63.5	56.725	47	0.389	1.341	0.508	1.035	3.270	1.063	2.845	76.448	Gold
21	HUN3	Hungary	Anna Barina-Lazar	35.8	35.4	71.2	1.250	76.8	44	53.65	55	1.559	0.551	1.304	0.937	2.920	1.263	2.530	75.299	Gold
22	IDN1	Indonesia	Michael Purnama	37.8	36.2	74	1.523	73.2	44	65.3	35.25	1.323	0.347	1.017	0.346	3.033	0.986	2.509	75.090	Gold
23	IRN2	Iran	Mohammad Mehdì - RAHMPOUR	36	37.4	73.4	1.464	49.2	68.5	87.275	21.25	-0.255	1.595	2.328	-0.475	3.191	1.038	2.502	75.019	Gold
24	DEU1	Germany	Kasimir Reich	35.8	33.2	69	1.035	80.2	23	74.075	60.5	1.783	-0.722	1.540	1.826	4.426	1.439	2.474	74.745	Gold
25	IND2	India	Mayank Pandhari	34.8	34.4	69.2	1.055	77.2	54.5	62.95	45.75	1.586	0.882	0.877	0.961	4.306	1.400	2.455	74.549	Gold
26	SGP3	Singapore	Min Seo Koo	32.8	33.6	66.4	0.781	62.4	64.5	71.125	58.25	0.613	1.392	1.364	1.694	5.062	1.646	2.428	74.276	Gold
27	THA1	Thailand	ARIN INTARATAT	34.8	36	70.8	1.211	68	49	77.15	34	0.981	0.602	1.723	0.273	3.578	1.164	2.374	73.742	Silver
28	KOR4	South Korea	Joo Hyun Hamm	38.8	35	73.8	1.503	65	18.5	77.8	23.75	2.099	-0.952	1.761	-0.328	5.880	2.589	3.342	73.423	Silver
29	BGR2	Bulgaria	Borislav Valentinov Stoyanov	36.8	35	71.8	1.308	57.4	64	57.35	43.25	0.284	1.366	0.543	0.815	3.008	0.978	2.286	72.864	Silver
30	NZL4	New Zealand	Junzhe Li	36.4	39.4	75.8	1.698	54.2	62.5	55.5	27.25	0.073	1.290	0.433	-0.123	1.673	0.544	2.242	72.424	Silver
31	SAU2	Saudi Arabia	YAZAN ALMOGHRABI	33.6	35.6	69.2	1.055	62.8	70.5	59.175	38.75	0.639	1.697	0.652	0.551	3.539	1.151	2.205	72.054	Silver
32	POL3	Poland	ALEKSANDRA WERONIKA KOWALCZYK	31	33	64	0.547	71.2	81.5	77.05	26.5	1.191	2.257	1.717	-0.167	4.998	1.625	2.173	71.728	Silver
33	ITA2	Italy	Leonardo Morotti	28.2	36.2	64.4	0.586	61.2	67.5	59.65	64.5	0.534	1.544	0.680	2.061	4.819	1.567	2.153	71.534	Silver
34	SVK2	Slovakia	Ján Plachý	29.6	32.4	62	0.352	76.6	62.5	64.5	50	1.546	1.799	0.969	1.211	5.525	1.797	2.149	71.489	Silver
35	JPN3	Japan	Satsu Shimada	34.2	34.4	68.6	0.996	44.2	73	62.45	52	-0.584	1.824	0.847	1.328	3.415	1.111	2.107	71.067	Silver
36	DEU3	Germany	Martha Genzer	31.8	34.6	66	0.742	61.6	76	59.975	45.5	0.560	1.977	0.700	0.947	4.184	1.360	2.103	71.021	Silver
37	POL1	Poland	SZYMON STANISLAW BANDER	32.2	37.4	69.6	1.094	74.4	36	58.025	47.25	1.402	-0.060	0.583	1.049	2.974	0.967	2.061	70.608	Silver
38	NZL2	New Zealand	Shuux Janet Guo	32	34.4	66.4	0.781	68.6	57	73.55	32.25	1.020	1.009	1.508	1.170	3.708	1.206	1.987	69.873	Silver
39	SGP2	Singapore	George Lee	28	34.8	62.8	0.430	72.4	56.5	68.1	51.25	1.270	0.984	1.184	1.284	4.722	1.535	1.966	69.657	Silver
40	TUR1	Türkiye	Abdullah Akif Çelikçaya	33.6	33.8	67.4	0.879	83.2	27	64.3	39.5	1.980	-0.519	0.957	0.594	3.014	0.980	1.859	68.591	Silver
41	DEU2	Germany	Konrad Jannes Köhler	30.4	35.8	66.2	0.762	73	56.5	69.9	24.5	1.310	0.984	1.291	-0.284	3.300	1.073	1.835	68.351	Silver
42	POL4	Poland	ZUZANNA ZYRA	34.4	34.6	69	1.035	59.6	63.5	61.625	43	0.429	0.322	0.798	0.800	2.348	0.764	1.799	67.988	Silver
43	GBR4	United Kingdom	Si Nivasan Loganathan	34.2	32.6	66.8	0.821	74.6	31.5	65.8	43	1.415	-0.289	1.047	0.800	2.972	0.966	1.787	67.870	Silver
44	HUN2	Hungary	Tamas Soma Szalay	29.8	33.8	63.6	0.508	58.6	55	77	43.75	0.363	0.908	1.714	0.844	3.828	1.245	1.753	67.533	Silver
45	KAZ1	Kazakhstan	Yerassy Temirkobov	36.2	34.4	70.6	1.191	76.4	9	72	32.75	1.533	-1.435	1.416	0.199	1.713	0.557	1.748	67.482	Silver
46	TWN2	Chinese Taipei (Taiwan)	KAI-JIE HU	33	35	68	0.938	61	52.5	59.4	34.75	0.521	1.730	0.665	0.137	2.283	0.742	1.680	66.798	Silver
47	IND4	India	Rohit Panda	34.6	33.8	68.4	0.977	57.4	8.5	76.8	57	0.284	-1.461	1.702	1.621	2.146	0.698	1.674	66.744	Silver
48	KAZ2	Kazakhstan	Alkhan Zhumagalayev	36.4	34.6	71	1.230	70.6	32	49.5	34.25	1.152	-0.264	0.075	0.287	1.251	0.407	1.637	66.368	Silver
49	ARG3	Argentina	Donato Elias Pellegrini	34	32.6	66.6	0.801	62.8	44	52.05	51.75	0.639	0.347	0.227	1.133	2.527	0.822	1.623	66.227	Silver
50	THA2	Thailand	Archawin Kittirattanapaboon	34.4	33.8	68.2	0.957	79.8	36.5	49.75	32.5	1.757	-0.035	0.090	1.855	1.997	0.649	1.606	66.066	Silver
51	NLD2	Netherlands	Sebastian Jacob Krikke	32.6	38.8	77.4	1.269	63.8	52	49.25	19.5	0.705	0.755	0.061	-0.577	0.943	0.307	1.576	65.757	Silver
52	IND1	India	Amritansh Nigam	38.4	36.4	74.8	1.601	64.8	17.5	64.55	15.25	0.770	-1.002	0.972	-0.827	0.907	-0.027	1.835	65.726	Silver
53	ISR1	Israel	Nadav Ovit	31	34.6	65.6	0.703	68.2	30	53.775	56.5	0.994	-0.366	0.330	1.592	2.550	0.829	1.533	65.327	Silver
54	LTU3	Lithuania	Povilas Šaučiūnas	35	33.2	66.2	0.957	64.2	56	35.3	41.25	0.731	0.959	-0.770	0.698	1.617	0.528	1.483	64.828	Silver
55	NLD3	Netherlands	Allie Heyue Zong	26.4	28	54.4	-0.389	63.4	78	61.95	66.25	0.678	2.079	0.817	2.163	5.738	1.866	1.477	64.769	Silver
56	LVA2	Latvia	Nauris Priksans	33	30.4	63.4	0.489	61.4	59.5	44.875	55									

95	PHL3	Philippines	Chlara Bernadette Zhang Tan-Gatue	29.8	27.2	57	-0.135	68.8	47.5	39.75	46.5	1.033	0.526	-0.505	1.005	2.059	0.670	0.534	55.342	Bronze
96	NZL1	New Zealand	Sarah Jane Ellis	31.6	30.4	62	0.352	60	27	48.325	39.25	0.455	-0.519	0.005	0.580	0.522	0.170	0.522	55.221	Bronze
97	VNM3	Vietnam	NGUYEN TRONG PHUOC DO	28.8	31.8	60.6	0.216	52.2	40.5	67.05	22	-0.058	0.169	1.121	-0.431	0.801	0.260	0.476	54.762	Bronze
98	BRA3	Brazil	José Eduardo Pascualho Bertozzi	29.8	31	60.8	0.235	71	34	40.125	32.75	1.178	-0.162	-0.483	0.199	0.732	0.238	0.473	54.734	Bronze
99	SWE4	Sweden	Ivar Avelin	32.2	28.6	60.8	0.235	65.4	43.5	33.15	37.75	0.810	0.322	-0.899	0.492	0.726	0.236	0.471	54.712	Bronze
100	NLD1	Netherlands	Tristan van der Beek	33.8	31.4	65.2	0.664	50.6	31.5	59.125	15.5	-0.163	-0.289	-0.849	-0.812	-0.616	-0.200	0.464	54.642	Bronze
101	DNK4	Denmark	Albert Rumlé Eriksen	27.4	31	58.4	0.001	47.8	68	60.55	20.25	-0.347	1.570	0.734	-0.534	1.423	0.463	0.464	54.638	Bronze
102	FIN4	Finland	Emilia Maja Elisabet Jaakkola	32.4	27.4	59.8	0.138	62.4	35	45.3	40.25	0.613	-0.111	-0.175	0.639	0.966	0.314	0.452	54.518	Bronze
103	ROU2	Romania	DAVID-ANDREI VLAD	31.6	31.6	63.2	0.469	52.2	53.5	44.85	17.75	-0.058	0.831	-0.202	-0.680	-1.108	-0.035	0.434	54.341	Bronze
104	HUN4	Hungary	Otto Tatali	30.6	28.8	59.4	0.099	49.2	50.5	59.45	28.25	-0.255	0.678	0.668	-0.065	1.027	0.334	0.433	54.326	Bronze
105	SGP1	Singapore	Aravindh Velmurugan Kuppusamy	32	34.8	66.8	0.821	67.2	7	52.975	14.5	0.928	-1.537	0.282	-0.871	-1.197	-0.389	0.431	54.312	Bronze
106	HUN1	Hungary	Petra Nneka Oparaugo	29.6	32.2	61.8	0.333	61.8	36	56.3	17.5	0.573	-0.060	0.481	-0.695	0.299	0.097	0.430	54.300	Bronze
107	ARG1	Argentina	Gregorio Jaca	32.6	30.2	62.8	0.430	52.8	22	45.55	45.5	-0.019	-0.773	-0.160	0.947	-0.005	-0.002	0.429	54.287	Bronze
108	TUR2	Turkey	Sude Filiz Diren	27.8	33	60.8	0.235	68.8	50	53	4.75	1.033	0.653	0.284	-1.442	0.528	0.172	0.407	54.070	Bronze
109	LUX4	Luxembourg	Nina Hélène Gaëlle Bemier	28.4	30.4	58.8	0.040	58.8	46	40.5	40.5	0.376	0.449	-0.461	0.654	1.018	0.331	0.371	53.712	Bronze
110	LTU2	Lithuania	Paulius Mikaluskas	33.4	30.6	64	0.547	62.6	32	39.3	22.25	0.626	-0.264	-0.532	-0.416	1.616	-0.191	0.357	53.566	Bronze
111	KOR2	South Korea	Seoyeon Jeon	31.8	33	64.8	0.625	58.4	24.5	42.35	24.25	0.350	-0.646	-0.350	-0.299	-0.946	-0.308	0.318	53.178	Bronze
112	PHL2	Philippines	Raven Glorianne Herrera Foronda	33.2	25	58.2	-0.018	54.8	28.5	50.6	9	0.100	-0.442	0.141	1.211	1.009	0.328	0.310	53.098	Bronze
113	JPN4	Japan	Kohel Kawakami	27.2	29.6	56.8	-0.155	51	59.5	54	30.5	-0.137	1.137	0.344	0.067	1.411	0.459	0.304	53.039	Bronze
114	NZL3	New Zealand	Jacob Liam Miller	29.8	29	58.8	0.040	65.6	19.5	46.35	45.25	0.823	-0.901	-0.112	0.932	0.742	0.421	0.282	52.816	Bronze
115	MNG2	Mongolia	Jergalin Chibat	29.8	27.2	57	-0.135	50	17.5	57.35	59.75	-0.203	-1.002	0.543	1.782	1.120	0.364	0.229	52.289	Bronze
116	CHE2	Switzerland	Domink Rožman	26.6	31.2	57.8	-0.057	44.6	50	43.8	45.75	-0.558	0.653	-0.264	0.961	0.793	0.258	0.200	52.004	Bronze
117	IDN3	Indonesia	Jefferson Filbert Tjoenardi	28.8	29	57.8	-0.057	49.2	35	63.75	32.25	-0.255	-0.111	0.924	0.229	0.787	0.256	0.198	51.984	Bronze
118	LKA2	Sri Lanka	Harshan Arulmolli	30.2	31.4	61.6	0.313	47.4	41	55.35	18.25	-0.374	0.195	0.424	-0.061	-0.406	-0.132	0.181	51.813	Bronze
119	ROU3	Romania	ȘTEFAN IONEL DUMITRESCU	31.6	28.4	60	0.157	64.8	53.5	40.625	11.25	0.770	0.831	-0.489	-1.061	0.515	0.017	0.174	51.740	Bronze
120	CHE3	Switzerland	Zora Frieda Althaus	27	31.4	58.4	0.001	67.2	55.5	30.375	24.75	0.928	0.933	-1.064	-0.270	0.528	0.172	0.173	51.728	Bronze
121	LTU4	Lithuania	Mindaugas Smetaninas	29	27.8	56.8	-0.155	48	46	33.75	55.25	-0.334	0.449	-0.863	1.518	0.771	0.251	0.096	50.957	Bronze
122	BGR4	Bulgaria	Yana Aleksandrova Atanasova	29.6	26.4	56	-0.233	53	61	40.15	33.5	-0.005	1.213	-0.482	0.243	0.970	0.315	0.082	50.823	Bronze
123	EST1	Estonia	Vesta Selg	29.2	28.6	57.8	-0.057	45.8	30.5	60.05	37.75	-0.479	-0.340	0.704	0.947	0.377	0.123	0.065	50.653	Bronze
124	HRV3	Croatia	Mislav Mihajević	28	30.4	58.4	0.001	43.4	42	53.95	31	-0.637	0.245	0.341	0.097	0.046	0.015	0.016	50.161	Bronze
125	LVA1	Latvia	Markuss Gustavs Kenins	32.2	29.4	61.6	0.313	48	25	51.275	26	-0.334	-0.620	-0.116	-1.196	-0.970	-0.315	-0.002	49.979	Bronze
126	SVK1	Slovakia	Tomáš Kompiš	30.8	30	60.8	0.235	54.2	37.5	31.5	29.75	0.073	0.016	-0.997	0.023	-0.884	-0.287	-0.052	49.479	Bronze
127	DNK2	Denmark	Alexander Levanius Ardlise	31.8	33.8	65.6	0.703	46.6	46.5	24.125	12.75	-0.426	0.475	-1.436	-0.973	-2.361	-0.768	-0.064	49.357	Bronze
128	BGD4	Bangladesh	Khundiker Ishtaq Hammad	27.2	29.2	56.4	-0.194	59.2	55.5	54.1	5.25	0.402	0.933	0.350	-1.413	0.272	0.068	-0.106	48.945	Bronze
129	KAZ4	Kazakhstan	Bakdaulet Yernazarov	30.6	28	58.6	0.021	59.4	28.5	22.95	46.75	0.415	-0.442	-1.506	1.020	-0.513	-0.167	-0.146	48.539	Bronze
130	SVN4	Slovenia	Emu Šuligoj	31.2	32.8	64	0.547	33.2	64	23.55	16	-1.307	1.366	-1.470	-0.783	-2.194	-0.714	-0.166	48.338	Bronze
131	BGD2	Bangladesh	Fayyad Ahmed	31.6	30	61.6	0.313	50	25.5	34.7	31.25	-0.203	-0.595	-0.806	-1.111	-1.493	-0.845	-0.172	48.279	Bronze
132	BGD3	Bangladesh	Tahseen Shaan Leon	26.8	30.8	57.6	-0.077	58	59.5	27.275	20.25	0.323	1.137	-1.249	0.534	-0.322	1.105	-0.182	48.184	Bronze
133	PRT3	Portugal	André Daniel Malta Aires Melo da Cruz	28.8	26.6	55.4	-0.291	37.8	52	54.95	31	-1.005	0.755	0.400	-0.937	-0.247	0.080	-0.211	47.888	Bronze
134	PHL4	Philippines	Yosef Alexander Oliveros Segotter	26.8	29.4	56.2	-0.213	56	26.5	27.075	54.75	0.192	-0.544	-1.260	1.489	-0.124	-0.040	-0.254	47.464	Bronze
135	FIN1	Finland	Nina Seidi Sofia Seppälä	27.8	30.4	58.2	-0.018	39.8	54.5	43.45	21.5	-0.873	0.882	-0.285	-0.460	-0.736	-0.239	-0.258	47.422	Bronze
136	ARM4	Armenia	Arman Hayrapetyan	27	26.8	53.8	-0.448	56.4	39.5	28.2	52.25	0.218	1.118	-1.193	1.343	0.485	1.158	-0.290	47.103	Bronze
137	ROU4	Romania	IUSTINA ROSU	32.4	26.6	59	0.060	57.8	18.5	36.225	33.5	0.310	-0.952	-0.715	2.243	-1.113	-0.362	-0.302	46.976	Bronze
138	BGD1	Bangladesh	Rayan Rahman	29.2	31.4	60.6	0.216	44	23.5	36.75	35.5	-0.597	-0.697	-0.684	0.361	-1.618	-0.526	-0.310	46.897	Bronze
139	EST2	Estonia	Karl Valter Oja	27.8	31.8	59.6	0.118	54.8	36.5	33.275	20	0.113	-0.035	-0.891	-1.361	-0.443	-0.324	-0.456	46.576	Bronze
140	SWE2	Sweden	Tekla Nilsson	33.6	26.4	60	0.157	52.6	35.5	28.225	25	-0.032	-0.086	-1.192	-0.255	-1.564	-0.509	-0.351	46.485	Bronze
141	KGZ2	Kyrgyzstan	Daniyar Iskenderovich Gaipov	25.2	28.8	54	-0.428	42.6	42	60.35	27.5	-0.689	0.245	0.722	-0.108	0.170	0.055	-0.373	46.271	Bronze
142	PRT1	Portugal	Tiago Miguel Gomes de Sousa	28.6	31.8	60.4	0.196	46.2	19.5	43.375	27.5	-0.453	-0.901	-0.289	-0.138	-1.780	-0.579	-0.383	46.173	Bronze
143	FIN2	Finland	Jenni Orvolki Ruokkolainen	26.8	31.2	58	-0.038	39.2	33.5	43.9	33.75	-0.913	-0.188	-0.258	-1.100	-0.358	-0.396	-0.403	46.040	Bronze
144	ITA3	Italy	Francesco Petrone	27.6	30.6	58.2	-0.018	52.4	40	33.175	19.75	-0.045	0.144	-0.897	-0.563	-1.361	-0.443	-0.461	45.939	Merit
145	CYP4	Cyprus	Loukas Iakovou	26.8	23.2	50	-0.818	63.6	41	35.625	45.5	0.691	0.195	-0.751	0.947	1.082	0.352	-0.466	45.336	Merit
146	BEL2	Belgium	Loïc Lucas ROCHET	26.4	29	55.4	-0.291	47.8	47.5	42.3	22.5	-0.347	0.526	-0.353	-0.402	-0.577	-0.188	-0.479	45.210	Merit
147	LIE1	Liechtenstein	Seraphim Jollat	23.8	29	52.8	-0.545	62.2	42.5	44.725	20	0.599	0.271	-0.209	-0.548	-1.113	0.037	-0.508	44.917	Merit
148	SYR4	Syria	LAWAND MOHAMED BAIRAM	28.4	29.4	57.8	-0.057	73.4	19.5	26.875	19	1.336	-0.901	-1.272	-0.648	-0.444	0.470	-0.527	44.731	Merit
149	GBR2	United Kingdom	Kez Matthew Ward	30.8	30.8	61.6	0.313	51.4	6.5	44.7	17.25	-0.111	-1.563	-0.210	-0.709	-2.593	-0.843	-0.530	44.700	Merit
150	JPN2	Japan	Yasunao Inoue	33.2	17.6	50.8	-0.740	50	48.5	47.675	34.5	-0.203	0.577	-0.033	0.302	0.643	0.209	0.531	44.688	Merit
151	BRA4	Brazil	Nilton Gama de Castro	32.6	21.2	53.8	-0.448	52.2	54.5	39.875	19	-0.058	0.882	-0.498	-0.607	-0.281	-0.091	-0.539	44.612	Merit
152	ISR2	Israel	Amir Gasul	23.4	28.4	51.8	-0.643	53.4	24.5	70.65	22	0.021	-0.646	1.335	-0.431	0.279	0.091	-0.552	44.483	Merit
153	SVK4	Slovakia	Simon Kriňak	28	25	53	-0.526	59.6	61.5	19	28	0.429	1.239	-1.742	-0.079	-0.153	-0.500	-0.575	44.245	Merit
154	GRE3	Greece	Akaterini Karpouzi	26.4	25.6	52	-0.623	58.4	35.5	50.65	23.25	0.350	-0.086	0.144	-0.358	0.050	0.016	-0.607	43.932	Merit
155	EST3	Estonia	Liisa Pata	28.2	24.4	52.6	-0.565	53.2	49.5	32.45	32	0.008	0.627	-0.940	0.155	-0.150	-0.049	-0.613	43.867	Merit
156	PHL1	Philippines	Liam Audrey Albos Aleda	27.6	28	56.6	-0.272	51.6	22	33.375	40.5	-0.097	-0.773	-0.885	0.654	-1.102	-0.358	-0.630	43.696	Merit
157	ESP3	Spain	Pablo Gómez García	27.8	27.4	55.2	-0.311	56.2	34.											

198	SYR3	Syria	ADNAN RIHAWI	27.2	23.6	50.8	-0.740	56.8	19.5	31.95	8	0.244	-0.901	-0.970	-1.252	-2.878	-0.936	-1.676	33.240
199	DNK1	Denmark	Celine Xie	21	22	43	-1.501	38.2	37.5	45.15	38.25	-0.979	0.016	-0.184	0.522	-0.624	-0.203	-1.704	32.960
200	MNG1	Mongolia	Nomin Amartuvshin	24.4	21.6	46	-1.208	45.8	17.5	29.225	45	-0.479	-1.002	-1.132	0.917	-1.696	-0.552	-1.760	32.400
201	NOR3	Norway	Las Hardy	28	24.2	52.2	-0.604	43.6	15	30.5	13.5	-0.623	-1.130	-1.056	-0.929	-3.739	-1.216	-1.819	31.805
202	ARM3	Armenia	Mane Kurghinyan	25.4	20.8	46.2	-1.189	30.4	20	43	41.75	-1.491	-0.875	-0.312	0.727	-1.951	-0.635	-1.823	31.766
203	GEO1	Georgia	Giorgi Nebulishvili	27.4	25.4	52.8	-0.545	43.4	4	40.325	6	-0.637	-1.690	-0.471	-1.369	-4.167	-1.355	-1.900	30.999
204	KGZ3	Kyrgyzstan	Nurislam Abdislamov	26.2	21.8	48	-1.013	38.8	37.5	37.725	8.25	-0.939	0.016	-0.626	-1.237	-2.786	-0.906	-1.919	30.808
205	BEL4	Belgium	Thomas Lieven Buysse	24	24.2	48.2	-0.994	28.8	6	38.4	37.25	-1.597	-1.588	-0.586	0.463	-3.307	-1.076	-2.069	29.307
206	ARM2	Armenia	Yana Mkrtchyan	17.6	22.6	40.2	-1.774	34.8	47	27.925	45	-1.202	0.500	-1.210	0.917	-0.994	-0.323	-2.097	29.026
207	ZAF3	South Africa	DANIEL VAN DEN HEEVER	25.8	18.8	44.6	-1.345	36.4	4	41.25	44	-1.097	-1.690	-0.416	0.859	-2.344	-0.762	-2.107	28.928
208	ZAF2	South Africa	TARIKA HARILAL	22.8	21.8	44.6	-1.345	48.8	18.5	38.125	15.75	-0.282	-0.952	-0.602	-0.797	-2.633	-0.856	-2.201	27.990
209	KGZ1	Kyrgyzstan	Alai Almazovich Almazov	21.2	24.4	45.6	-1.247	34	24	32.575	27	-1.255	-0.671	-0.933	-0.138	-2.997	-0.974	-2.222	27.781
210	LKA3	Sri Lanka	Praveen Charuka Thennakoon	24	27.6	51.6	-0.662	30.6	2	23.55	18.25	-1.478	-1.792	-1.470	-0.651	-5.391	-1.753	-2.415	25.846
211	NGA1	Nigeria	Paul Chinazekpere Ugwu	26.8	21.4	48.2	-0.994	31.4	10	40.8	6.25	-1.426	-1.385	-0.443	-1.354	-4.607	-1.498	-2.492	25.080
212	SAU4	Saudi Arabia	ALEEN OMAR BAHARAN	24	20.8	44.8	-1.325	38.4	15.5	42.175	4.5	-0.965	-1.104	-0.361	-1.457	-3.888	-1.264	-2.590	24.104
213	MDA1	Moldova	Francesca Alexandrina Talmaci	25	19.6	44.6	-1.345	30.2	16	41.175	14	-1.505	-1.079	-0.420	-0.900	-3.904	-1.269	-2.614	23.856
214	PAK2	Pakistan	Tabinda Javeed	24.4	22.8	47.2	-1.091	23.2	17.5	27.35	19	-1.965	-1.002	-1.244	-0.607	-4.818	-1.567	-2.658	23.419
215	TJK1	Tajikistan	MUNAVVARKHON VALIEV	23	24.4	47.4	-1.072	35.4	2	35.2	9.25	-1.163	-1.792	-0.776	-1.178	-4.909	-1.596	-2.668	23.317
216	QAT3	Qatar	Alghalya ABDULAZIZ Ahajri	19	20.8	39.8	-1.813	30.2	48.5	41.225	7.25	-1.505	0.577	-0.418	-1.296	-2.641	-0.859	-2.672	23.280
217	MNE1	Montenegro	Anel Memic	21.4	22.2	43.6	-1.442	27.6	15.5	36.45	23.25	-1.675	-1.104	-0.702	-0.358	-3.839	-1.249	-2.691	23.090
218	NGA2	Nigeria	Alqodus William Lawal	26.4	24	50.4	-0.779	28.4	14.5	13.625	3	-1.754	-1.155	-2.062	-1.545	-6.516	-2.119	-2.898	21.018
219	QAT2	Qatar	Farah Mohamed Aladem	21.2	20.8	42	-1.599	34.8	16	36.55	9.25	-1.202	-1.079	-0.696	-1.178	-4.155	-1.351	-2.950	20.502
220	IRQ2	Iraq	RASTI BAHMAN AHMED AHMED	21.8	20.2	42	-1.599	28	12	44.175	12.5	-1.649	-1.283	-0.242	-0.988	-4.161	-1.353	-2.952	20.482
221	ZAF1	South Africa	MARIETJIE JEANNE CILLIERS	20.4	21.2	41.6	-1.638	31.8	24	31.025	10.75	-1.399	-0.671	-1.025	-1.090	-4.186	-1.361	-2.999	20.011
222	SAU3	Saudi Arabia	ADNAN MOHAMMAD ALSADAH	22	19.2	41.2	-1.677	42.4	12	37.95	3.5	-0.702	-1.283	-0.613	-1.516	-4.113	-1.338	-3.014	19.859
223	MDA4	Moldova	Maxim Varzari	19	20.4	39.4	-1.852	46.6	10	38.675	6.75	-0.426	-1.385	-0.569	-1.325	-3.705	-1.205	-3.057	19.430
224	CYP2	Cyprus	Sotiris Christoforou	17	21	38	-1.989	35.2	17	37.775	15.75	-1.176	-1.028	-0.623	-0.797	-3.624	-1.179	-3.167	18.328
225	GRC4	Greece	Michaels Konstantridou	20.4	15	35.4	-2.242	32.8	22.5	48.925	12.25	-1.334	-0.748	0.041	-1.003	-3.043	-0.989	-3.232	17.682
226	GEO2	Georgia	Archil Japharidze	17.4	19	36.4	-2.145	36	7	43	20.5	-1.123	-1.537	-0.312	-0.519	-3.491	-1.135	-3.280	17.200
227	UZB4	Uzbekistan	Golbjon Gulomjonovich Sharifov	19.2	17.8	37	-2.086	42	20.5	19.625	21.25	-0.729	-0.850	-1.704	-0.475	-3.758	-1.222	-3.308	16.918
228	ARE3	United Arab Emirates	Mozah Saeed Rashed Ali Aldhanhani	16.6	20.6	37.2	-2.067	33.4	14.5	32.125	7.25	-1.294	-1.155	-0.960	-1.296	-4.705	-1.530	-3.597	14.034
229	MNE2	Montenegro	Jelena Sekulic	20.2	21.6	41.8	-1.618	25.4	4	12.7	21	-1.820	-1.690	-2.117	-0.490	-6.117	-1.989	-3.607	13.929
230	ARE1	United Arab Emirates	Hudanz Mushtaq Ahmed Sange	19.8	19.6	39.4	-1.852	25.2	10	15.5	7.5	-1.833	-1.385	-1.950	-1.281	-6.449	-2.097	-3.949	10.508
231	GEO4	Georgia	Nikoloz Arveladze	18.2	17.8	36	-2.184	19.8	11.5	16	17.5	-2.188	-1.308	-1.920	-0.695	-6.111	-1.987	-4.171	8.289
232	TJK3	Tajikistan	DILDORA NAZIRBOBOEVA	16	17.2	33.2	-2.457	23.4	14.5	26.3	13.5	-1.952	-1.155	-1.307	-0.929	-5.343	-1.737	-4.194	8.057
233	ARE2	United Arab Emirates	Sabah Khadija Sheik Abdul Safur	14.8	18.6	33.4	-2.437	24.2	10	29.95	4.25	-1.899	-1.385	-1.089	-1.472	-5.844	-1.900	-4.338	6.621
234	GEO3	Georgia	Davit Giorgadze	16.4	16.8	33.2	-2.457	26.4	12.5	25.125	3.5	-1.754	-1.257	-1.377	-1.516	-5.904	-1.920	-4.377	6.233
235	ARE4	United Arab Emirates	Almaha Saif Ahmed Kameel Albooshi	15.4	15.8	31.2	-2.652	30.6	6.5	11.95	4.25	-1.478	-1.563	-2.162	-1.472	-6.674	-2.170	-4.822	1.777
236	CYP1	Cyprus	Anthia Orfanou	16.6	13.6	30.2	-2.750	13.2	18	22.5	5.5	-2.622	-0.977	-1.533	-1.398	-6.531	-2.124	-4.873	1.268
237	TJK4	Tajikistan	AKMAL PULODOV	14.6	15	29.6	-2.808	16.2	4.5	14.875	4	-2.425	-1.665	-1.987	-1.486	-7.563	-2.459	-5.267	-2.675

IBO 2022 MEDALS



IBO 2022 CERTIFICATES



THE 33rd INTERNATIONAL BIOLOGY OLYMPIAD

CERTIFICATE OF PARTICIPATION

This is to certify that

AHMED OKLAH FARIS

from

Qatar

participated in the 33rd International Biology Olympiad
held in Yerevan, Armenia on July 10-18, 2022

as a
jury member

A handwritten signature in blue ink, appearing to read "Gayane".

Dr. Gayane Ghukasyan
Chairwoman of the IBO 2022



THE 33rd INTERNATIONAL BIOLOGY OLYMPIAD

CERTIFICATE OF PARTICIPATION

This is to certify that

Gaëtan Jougla

from

France

participated in the 33rd International Biology Olympiad
held in Yerevan, Armenia on July 10-18, 2022

as an
observer

A handwritten signature in blue ink, appearing to read "Gayane".

Dr. Gayane Ghukasyan
Chairwoman of the IBO 2022





**THE 33rd INTERNATIONAL
BIOLOGY OLYMPIAD**

CERTIFICATE OF AWARD

This is to certify that

Koo Min Seo

from

Singapore

has been awarded a

Gold Medal

at the 33rd International Biology Olympiad
held in Yerevan, Armenia on July 10-18, 2022

Dr. Gayane Ghukasyan
Chairwoman of the IBO 2022



8. LOGISTICS AND INFRASTRUCTURE

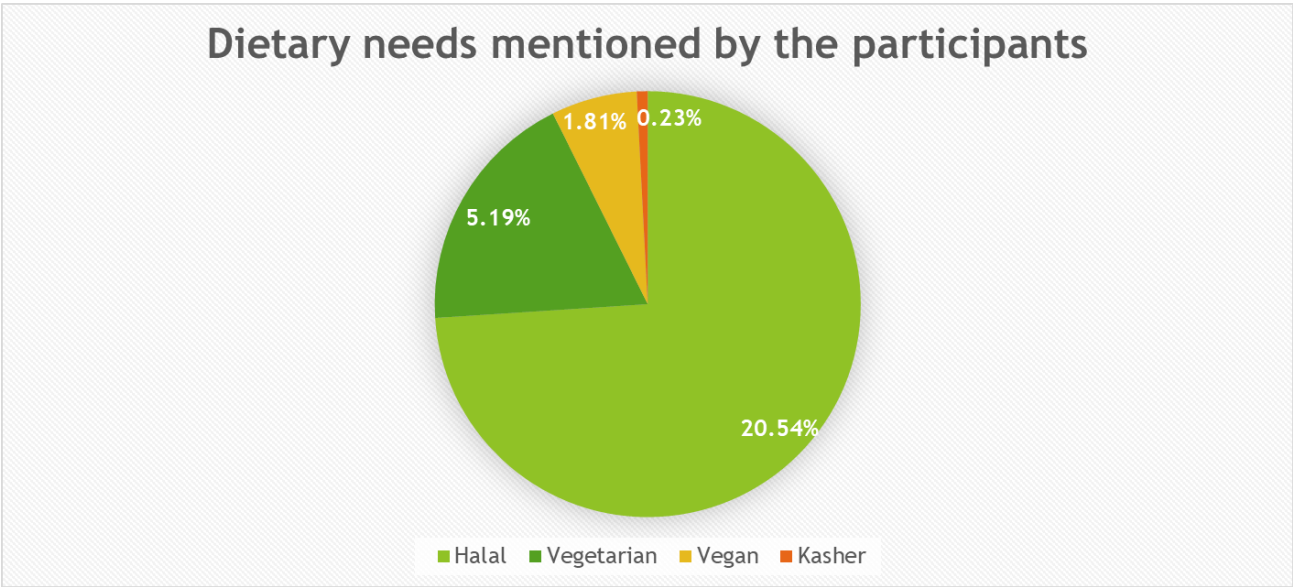
8.1 Accommodation

During the IBO week competitors and team guides were accommodated at Ani Grand Hotel, in Yerevan.

Jury members, observers and international advisors were accommodated at Ani Plaza Hotel in Yerevan. Jury sessions took place at the same hotel. The subgroup also conducted its sessions at Ani Plaza Hotel on July 5-10, 2022.

The jury room was located at the same hotel where the jury members stayed. The jury room was set up with two large screens showing the discussion progress. The seating arrangement of jury delegations was organized according to native languages as accepted in the previous IBOs. Each seat had a power supply for the jury members' laptops. There was a WiFi connection in the jury room available only for the jury members. In the jury room, IT volunteers were present to assist the jury members if needed.

During the IBO week participants experienced a variety of Armenian food and drinks. The food and beverage plan was developed based on the requirements mentioned on the registration form.



8.2 Transport

18 buses were rented to organize the transportation of the participants during the IBO 2022. A free of charge pick-up service from Zvartnots International Airport was offered for all participants even before the official arrival date. IBO 2022 volunteers met the participants at the airport and accompanied them to the hotels. The volunteers were holding a special sign with the IBO 2022 logo to be easily noted. All participating teams were offered to be transferred from the hotels to "Zvartnots" International Airport after the end of the Olympiad.





9. VOLUNTEERS

The IBO 2022 organizing committee started recruiting volunteers since April 2021. Cooperating with the faculties of Yerevan State University as well as through outsourcing, the IBO 2022 organizing committee recruited **147** volunteers. **77** volunteers were located at the students' hotel, among which **61** volunteers were the IBO guides accompanying the students, **23** volunteers were located at the exam venue, **30** volunteers in buses and **17** volunteers at the IT sector of the jury's hotel.









10. MEDIA AND PR

The IBO 2022 was the biggest event held in Armenia in 2022.

TV features, articles, press releases were made about the IBO 2022 before, during and after the Olympiad.

During the IBO week, the official website of Yerevan State University / ysu.am and the official YSU Facebook page published updates regarding the IBO 2022 activities.

The official website of the IBO 2022 / ibo2022.org was created in 2020. The website was used to provide information about Armenia, the IBO 2022 and the participation (accommodation, venues, visa requirements etc.). The information regarding the International group project, visa requirements and Covid requirements, as well as the practical information was sent to the coordinators through email as well, besides being published on the website.

Social media networks were used to keep in touch with the participants and make announcements.

We created Facebook and Twitter pages in 2020 and an Instagram page in 2022.

Informational posters about the Olympiad were placed In Yerevan, on Yerevan State University building, on the Sport and Concert Complex building, on the National Academic Theater of Opera and Ballet building and at the hotels of the Olympiad.

Daily newspapers covering the course of the Olympiad were printed and distributed to the participants.



IBO
33rd 2022
ARMENIA

DAILY

IBO2022.ORG

11.07.2022

THE 33rd INTERNATIONAL BIOLOGY OLYMPIAD



WELCOME



About 500 students from 66 countries of the world arrived in Armenia on July 5 to participate in the 33rd International Biology Olympiad. At the largest airport in Armenia, Zvartnots, the participants were greeted by members of the organizing committee.



For the first time, Armenia is hosting a large number of participants in the International Olympiad (hosted by Yerevan State University) and it is unique in its kind. It was organized with the support of the Ministry of Education, Science, Culture, and Sports of the Republic of Armenia.

Department in organizing the Olympiad is great; in these pages, the information about Armenia and YSU, presented to you, was collected by the staff of the department, and the YSU photojournalist is the author of most of the colorful photos. The Olympics started in Yerevan. It should be noted



that Yerevan has been the capital of the Republic of Armenia since 1918.



THE OPENING CEREMONY OF THE 33rd INTERNATIONAL BIOLOGY OLYMPIAD TOOK PLACE



The opening ceremony of the 33rd International Biology Olympiad took place in the concert hall of the Alexander Spendiaryan National Academic Opera and Ballet Theater. The event started with the presentation of the symbols of the Olympiad, the flag and the cup.

Representatives of the countries participating in the Olympiad entered the concert hall with a parade.

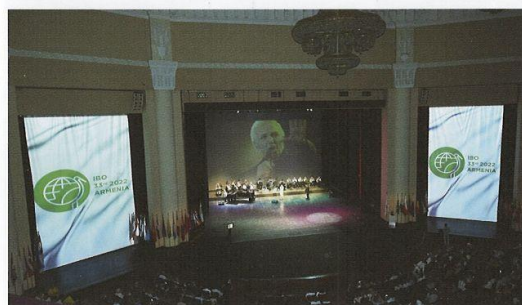
Arayik Harutyunyan, Chief of Staff to the Prime Minister gave the first speech, followed by speeches by Matsuda Ryoichi, Chairman of the International Biology Olympiad Association, Gayane Ghukasyan, Program Manager of the 33rd International Biology Olympiad, Vahram Dumanyan, Minister of Education, Science, Culture and Sports.

The graduates of the International Biology Olympiad also made a speech.



The audience was given the opportunity to "travel" through time through a hologram, greeted future biologists, wished success to the great 12th century great Armenian scientist, doctor, naturalist, philosopher Mkhitar Heratsi.

The solemn swearing-in ceremony of the members and participants of the Olympiad jury took place,



which was followed by a concert program organized by YSU Charles Aznavour Cultural Center (you can learn more about the center in our next issues). The pop-symphony orchestra of the Public Radio and Television of Armenia, whose artistic director is the People's Artist of the Republic of Armenia Yervand Yerznkyan, Sargis Bazhbeuk Melikyan (bass), the "Barekamutyun" dance ensemble with the number "Our Century" performed by the People's Artist Ani Haroyan performed the "Komitas" solo dance.





IBO
33rd 2022
ARMENIA

DAILY

IBO2022.ORG

12.07.2022

THE 33rd INTERNATIONAL BIOLOGY OLYMPIAD



Armenia has been a member of IBO since 2009 (in 2008 Armenia participated as an observer country). Since 2009, 35 Armenian students have participated in the IBO. During the IBO 2018 Tehran Olympiad, the IBO Association decided to confirm that the Republic of Armenia would officially host the 33rd International Biology Olympiad on July 10-18, 2022. Today, the first practical exam took place at the Karen Demirchyan Sports and Concert Complex, participants from 64 countries took part in it. According to the participants, the exam held in Yerevan passed with great discipline and was very



interesting. The anxiety among the participants increased during the break, and at the end of the exam, the students talked happily and joyfully with each other, discussing how they coped with their tasks. IBO participants were excited. Due to the location of the complex, the students had the opportunity to enjoy the beautiful view. They could see Mount Ararat and the Tsitsernakaberd Armenian Genocide Memorial. Before going to their hotel, the students took pictures with each other in that wonderful scene.



IBO
33rd 2022
ARMENIA

DAILY

IBO2022.ORG

13.07.2022

THE 33rd INTERNATIONAL BIOLOGY OLYMPIAD



VISIT TO GARNI TEMPLE AND GEGHARD MONASTERY



The participants visited Garni temple and Geghard monastery. In Garni canyon, they studied stunning geological monuments, represented by columnar basalts, which are the result of lava flows.

They also visited the Garni temple, which towers over a triangular cape, which is the unique surviving example of heathen culture in Armenia. It is a blend of Greco-Roman and Armenian styles. After adopting Christianity in 301 A.D., the pagan temple lost its significance and the fortress of Garni became the summer residence of the kings. Nowadays the ruins of the royal palace and the bathroom with stunning mosaic work can be found near the temple.

Geghard monastery is the unsurpassable masterpiece of 13th-century Armenian architecture. Visitors learned that from the outset the complex was called Ayrivank (cave monastery), later it was renamed Geghard (lance) as the lance, used by the roman soldier to sting Jesus Christ's side, had been kept in this monastery for many centuries. They stated that the complex is rich in subtle sculptural embellishments and many striking khachkars (cross-stones).



EXCURSION IN YEREVAN





IBO
33rd 2022
ARMENIA

DAILY

IBO2022.ORG

14.07.2022

THE 33rd INTERNATIONAL BIOLOGY OLYMPIAD

THE LAST EXAM IS SUCCESSFULLY PASSED

The theoretical test was held at the Karen Demirchyan Sports and Concerts Complex in Yerevan on Thursday. The test was divided into two parts, and it was web-based. The six-hour test started at 9:00 and finished at 17:00. Each part of the theoretical test consisted of 50 questions and was implemented in accordance with the protocol. Each test lasted three hours. According to participants, the exams held in Yerevan are under great discipline.

After the end of the theoretical test, the students talked joyfully and excitedly with each other discussing the test and how they coped with it. Students had got closer compared to the first round of exam (practical) and different teams were in talks. The next step was the After Party at the same Complex in Yerevan. Thanks to the location of the Complex, students got a chance



to enjoy the beautiful view, as it seemed like they could hold the whole city in their hands. As it was a clear evening, they could see the Mount Ararat and Tsitsernakaberd Armenian Genocide Memorial Complex. Before going to their hotel, students took many photos of that sight.

"BIOEXPO" AT YSU



YSU Student Council is a student organization operating at YSU. One of the goals of this is to organize students' free leisure and recreation, to promote their scientific, educational, cultural, creative, and physical development, etc.

In April of this year, on the initiative of the Student Council of YSU Faculty of Biology, a two-day exhibition "BIO EXPO" was held. During the exhibition, the attendees witnessed several scientific experiments and had the opportunity to get acquainted with the research work carried out by the faculty, the latest equipment used in laboratory research, etc.

STUDENTS WITH DIFFERENT BACKGROUNDS AND INTERESTS FOUND A COMMON LANGUAGE



As we already know there were participants from more than 64 countries with different backgrounds, interests, cultural and national features. We managed to talk to some of the students. The first thing they mentioned about the Olympiad was the way it was organized. They appreciated the discipline, the way the exams were held, and the professional behavior of the professors, who introduced and prepared them for the upcoming exams. One of the students mentioned how hard it was to

get selected as a participant in 33rd IBO, but as it is one of the biggest and most recognizable competitions, it was worth it. One of the students from Greece found some similarities between Armenians and Greeks as both nations are hospitable, have delicious cuisine, and have numerous ancient monuments. She pointed to the ancient monuments as she was interested in archeology as well, and in her free time, she was reading about the old countries and their cultural heritages, including Armenia.



IBO
33rd 2022
ARMENIA

DAILY

IBO2022.ORG

15.07.2022

THE 33rd INTERNATIONAL BIOLOGY OLYMPIAD



THE PARTICIPANTS OF THE OLYMPIAD VISITED THE EREBUNI RESERVE-MUSEUM



Today the participants visited the "Erebuni" historical-archaeological reserve museum. Upon entering the museum, the participants of the Olympiad were surprised to see a building replicated in the Urartian palace structures of the Erebuni Museum. Then they toured the entire museum, exploring the museum's large collection. The participants viewed with great interest the archeological objects related to the pre-Urartian, Urartian, Achaemenid, Hellenistic, and early Armenian periods from the Arin Berd, Karmir Blur, Shengavit sites, as well as from the excavations in different regions of Armenia. Erebuni Museum was established in 1968. The opening of the museum was timed to coincide with the 2750th anniversary of Yerevan. The Museum stands at the foot of the Arin Berd hill, on top of which the Urartian Fortress Erebouni has stood since 782 BC.

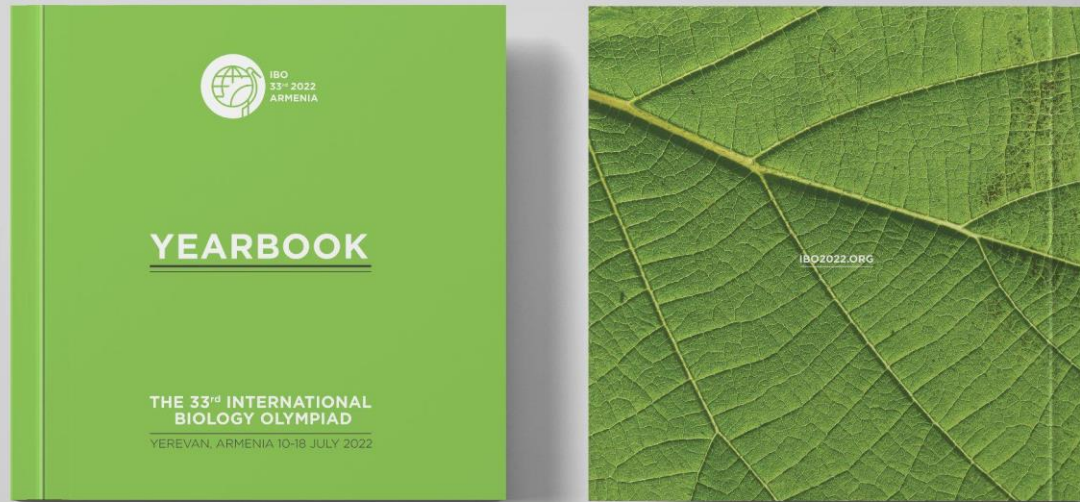
The building of the Museum which houses 12,235 exhibits was constructed by architects Baghdasar Arzoumanian and Shmavon Azatian and sculptor A. Harutiunian. It has two branches in Shengavit and



Karmir Blur with 5,288 and 1,620 exhibits respectively in stock. The sculptural design of the museum is the history of the ancient state of Urartu, represented by plastic means of expression.

Geghard monastery is the unsurpassable masterpiece of 13th-century Armenian architecture. Visitors learned that from the outset the complex was called Ayrivank (cave monastery), later it was renamed Geghard (lance) as the lance, used by the roman soldier to sting Jesus Christ's side, had been kept in this monastery for many centuries. They stated that the complex is rich in subtle sculptural embellishments and many striking khachkars (cross-stones).

IBO 2022 YEARBOOKS



11. RISK MANAGEMENT

During the implementation of the Olympiad the IBO 2022 organizing committee faced the following risks:

1. Financial risk

The Armenian Ministry of Education, Science, Culture and Sports secured 800.000 USD in the beginning of the program.

2. Time scarcity risk

The participation fee is transferred to the host country only months before the Olympiad as accepted in the IBOs. To acquire all the necessary equipment, accessories, chemicals etc. the IBO 2022 organizing committee ordered everything required beforehand, relying on the money secured by the Ministry.

3. Pandemic risk

Considering the pandemic situation in the world, the IBO 2022 organizing committee understood the risk of an outbreak of the pandemic during the Olympiad. To minimize the risk of virus spread during the Olympiad, the organizing committee applied to the Armenian Ministry of Health asking for help to prevent the outbreak.

A related-information was sent to the team leader through email, was published on the website and flyers with this information were distributed among the participants during the Olympiad.



THE 33rd INTERNATIONAL BIOLOGY OLYMPIAD

10-18 JULY 2022

COVID-RELATED INFORMATION FOR PARTICIPANTS

During the International Biology Olympiad 2022, COVID-related measures are as follows:

- The medical ambulance is on duty every day.
- There are masks and alcohol in the jury's working hall and students' exam venue.
- Please, keep social distance in your turn.
- In case of feeling unwell, students should inform their guides, who will immediately inform the IBO 2022 Organizing Committee.
- In case of feeling unwell, jury members should inform the IBO 2022 Organizing Committee directly.
- Testing will be conducted upon request and free of charge.
- If a participant tests positive during the Olympiad, necessary supervision will be established by the medical health care organization closest to the jury's place of residence (Ani Plaza Hotel) and students' place of residence (Ani Grand Hotel).
- Infected participants will be isolated at the hotel.
In case of complete vaccination, 7 days of self-isolation is required under medical supervision, in case of unvaccination, 10 days of self-isolation is required under medical supervision. During the period of self-isolation, on the 7th day after being tested positive for COVID-19, the unvaccinated participants may undergo, on their own initiative, a PCR test and in case of a negative result, get out of self-isolation.
- Infected participants will be treated free of charge.
- If the participants have to stay in Armenia due to COVID infection after the Olympiad, the host country covers the expenses **ONLY IN CASE OF HOSPITALIZATION.**

In spite of the prevention measures:

- 5 students out of **237** were infected during the Olympiad (2%).
- However, all the students managed to participate in the practical exam
- Only 1 student took the theoretical test at the hospital

4. Safety risk

To ensure the safety of all students, the organizing committee cooperated with the police, and during the exams, a group of policemen and ambulance were on duty.

- In general, there were about 20 ambulance calls. Besides the Covid cases, there were also cases of diarrhea caused by drinking too much water and eating lots of apricots.
- And finally, a Hungarian student had to undergo an urgent surgery of a hernia and returned back to her country in a good state of health.

Students With Special Health Requirements

- 1 color blinded participant was assisted by a volunteer
- 1 autistic participant was provided by psychological help
- 1 participant with broken arm was provided by a pillow for comfort

AFTER THE OLYMPIAD

- Post-Olympiad survey was done among volunteers to identify all organizational and health related problems.
- Certificates and yearbooks were sent to the team leaders.
- A final report was prepared.
- An after movie was created and uploaded on the IBO 2022 website (<https://www.ibo2022.org/en/mediabox/video-gallery>).

IBO 2022 ARMENIA
FINAL REPORT

2023 Yerevan, Armenia